Dynamic Load Models for Power Systems - Estimation of Time-Varying Parameters During Normal Operation

Romero, Ines

2002

Dynamic Load Models
for Power Systems

Estimation of Time-Varying Parameters
During Normal Operation

Inés Romero Navarro

LUND UNIVERSITY
Licentiate Thesis
Department of Industrial Electrical Engineering
and Automation

i

Abstract

Economic and environmental concerns will slow down the expansion of the transmission system in many countries. The addition of new transmission lines will be few and far between. The de-regulation of the power supply will introduce new power flow patterns on the bulk transmission systems. The net result is that the power systems will operate much closer to their transfer limits and operate there much longer time than has been necessary.

The risk for voltage collapse determines the transfer limits in many bulk transmission systems. The accurate determination of the transfer limits will be an increasingly important task to maintain the operational security and economic operation of the power system. Many studies have shown the importance of the load representation in voltage stability analysis. Static load models are not accurate enough for capturing the dynamics of the network. Therefore dynamic load models are needed even if voltage collapse, in many cases, is a slow phenomenon.

Due to the large amount of electric heating loads in Sweden and its effect on voltage stability, Hill and Karlsson have proposed a load model with exponential recovery. The model is expressed as a set of nonlinear differential equations, where the real and reactive load powers have a nonlinear dependency with voltage. The standard dynamic active load model is characterized by three parameters, steady state load-voltage dependence, transient load-voltage dependence and a load-recovery time constant. The same applies to reactive load. As an extension of the mentioned work, the present author proposes an automatic method for the determination of parameters in standard dynamic load models. The dynamic set of nonlinear equations has been linearised and the problem has been reduced to a linear identification problem. The Least Squares criterion is used for minimizing the error function between measured and simulated data.

Field measurements from continuous normal operation at the 20 kV and 50 kV-level from a substation in the South East of Sweden have provided over 1 GByte of data covering all seasons during the time period July 2001-June 2002. The determination of the load parameters based on this data has resulted in valuable information. The parameters' time-varying characteristic and their dependency with weather and season of the year have been studied; there is correlation between the active and reactive recovery time constants, and between them and the corresponding steady-state characteristic of the load. Strong dependency of the transient active and reactive characteristic of the load with the temperature has been found.

Furthermore, some unexpected deviations in the reactive load parameters have led to a new representation of the reactive load. The reactive power level, which was previously used as normalization factor, is inappropriate. If instead apparent power level is used, the variability in the parameters that describe the reactive load response is drastically reduced.

Keywords

iv

Acknowledgements

Firstly, I would like to thank Prof. Gustaf Olsson, Dr. Mats Larsson and Dr. Olof Samuelsson from IEA, and in general the people who made it possible the beginning of my PhD studies in Sweden. I am really grateful to all you, for your enthusiasm with me and your unconditional trusting.

I would like to thank my supervisors Prof. Gustaf Olsson, Dr. Olof Samuelsson and Prof. Sture Lindahl for the encouragement and help. I want to give special thanks to Dr. Olof Samuelsson for his constant guidance and support with the development of my work and for his unlimited help with the field measurements in Tomelilla. His support, knowledge and contacts have given me many ideas and opportunities. Olof, I am really grateful for all the proof reading, and for your daily endless patience with my Swedish. I am completely sure you are now well trained to teach your little son Filip. Prof. Sture Lindahl has been the co-supervisor of my thesis, and an essential source of inspiration during the whole time. He has come up with many ideas, and participated with many interesting discussions on load modeling and voltage stability. I am thankful for his faith in me and my work, and for his efforts to make the best of my PhD studies. Prof. Gustaf Olsson has been always a source of encouragement and optimism.

I would also like to thank my project steering committee, Bo Eliasson, Lars Gertmar, Sture Lindahl, Daniel Karlsson, György Sárosi, Kenneth Walve and Jan Rønne-Hansen, for their support. I want to give special thanks to Dr. Daniel Karlsson. He has been a great asset during this time and has provided many useful comments for the development of this thesis. His PhD thesis has been the origin of the work I am presenting today. I also wish to thank Chalmers University of Technology, and especially Gunilla Le Dous for their interest in this project and the data they have shared with me.

I am grateful to my colleges at the department IEA, for being friendly and having contributed to a good working environment. I especially would like to thank the following: Tomas Alexandersson for his help when I had problems with Macintosh computers, Getachew Darge for the time he has spent with me in the lab, Anita for keeping our spirits up and providing a fantastic atmosphere in the department, Olof Strömstedt for his great optimism and warm heart, Dalius, Christian, Per, David, and many others for making me smile every day even though it was Monday.

I also wish to thank to all my friends, those who are in Sweden but also around the world. Thank you Ana for being every day an email away, discussing about technical stuff but also about having a life away from home. Thank you David, Calamarc and Alexis for all the good moments in Lund.

Finally, I want to thank my parents, my brother and my boyfriend for their love, support and patience every day. This thesis is dedicated to you.

Lund, September 10, 2002

Inés Romero Navarro

vi

Contents

viii

Chapter 1

Introduction

The on-going situation of today's world and the impact of the fast development of technology and communications in our society have resulted in a new Era, "The Era of Globalization", which is strongly affecting peoples' way of living and thinking. People around the world are more connected to each other than ever before, and information, as well as goods and services produced in one part of the world, are available on the other side of the planet. The demands of our societies are rapidly increasing, the technology has to move faster than ever in order to satisfy the new changes, and the overall situation is making the day-to-day world economical situation more and more vulnerable. The increasing disparity between demand of energy and supply leads to a number of concerns in relation to the present and future availability of energy sources in the world, the environmental costs that will be associated with this growth in energy demand and about how less developed countries will be able to meet the energy needs of their growing populations [Bearden, 2000]. The electricity requirements in the next years will thus depend on the future industry growth rate and the use of the existing capacity in the most effective way. Therefore current challenges in power engineering includes optimizing the use of the available resources, keeping high reliability for operating conditions that will include narrow stability and security margins during peak loads in day-to-day operation.

Chapter 1 is structure as follows: Section 1.1 gives an overview of the current trends within the electricity industry, emphasizing the importance in optimizing the use of available resources, the integration of new

1

technologies and the application of real-time monitoring and control. Sections 1.2 and 1.3 describe the origin, motivation and objectives of the thesis, and which contributions have been achieved during the work. Section 1.4 and 1.5 present an outline of the thesis and the main publications of the author.

1.1   New challenges

In order to match the increasing demand in the load areas, optimizing the available resources while making environmental consideration, and ensuring high reliability in the system operation, changes of the power system at the generation and transmission levels are necessary. The available production margins will almost surely shrink in comparison with the traditional power systems. Some of the changes can be characterized as follows:

- The system planning must ensure controllable generation for regulating both frequency (by controlling the output of the active power) and voltage (by controlling the output of reactive power), and must control the costs and ability to operate as spinning reserves when needed. An optimization and coordination of the available resources, as well as the construction of new generation plants will thus be necessary.

- The transmission system expansion must be adequate to place new generating units and to support load demand variations. This will involve the optimization in the use of the existing transmission system but also its expansion.

- The integration of distributed generation and storage of energy will make it possible to support the reliability of the system in emergency situations.

- The use of advanced technologies will transform the static grid to an intelligent network, with available real-time control and monitoring of the system.

- The general deregulation will also add new economic and organizational problems. The operational margins will almost surely be decreasing. At the same time the electricity from several producers has to be satisfactorily distributed in the available network, which will require a significant control and operation effort.

Distributed Generation of power (DG), especially those facilities based on emerging technologies (solar panels, wind power, fuel cells, micro gas turbines, etc.) or hybrid systems will play a key role in the future, supporting the available capacity to meet peak power demands. DG provides, among other many potential advantages, an improved user power quality and reliability (voltage support, source of reactive power), low-cost energy in co-generation applications (combined uses of heat and power), elimination of transmission and distribution line losses, and a cost-effective source of peak demand power.

As mentioned above, the use of advanced technologies will transform the system to an intelligent system where a real-time feedback of information will be required in order to be competitive and successful in the new deregulated market. In a near future, the power control centers will become information technology centers, where the continuous monitoring and control of different signals and components will result in powerful diagnosis of the system [IEEEStability, 2002], and therefore in high reliability of the substations. Information is needed about the industrial as well as other types of customers, i.e. computerized load forecast, and complex metering system bulk trading and energy management.

Moreover, environmental issues in relation to the emissions and the location of new generation areas will limit the construction of new plants and the expansion of the transmission network.

1.2   Motivation

The transfer limits or the maximum power flows that are allowed across certain sections of the power system, depends on the operating conditions of the power system, and therefore on a large number of factors, such as

network topology, loading and generating conditions, which lead to different power flows. In order to simplify these calculations, a number of approximations are used, which introduce high or low uncertainty in the obtained transfer limits, according to the used assumptions [Taylor, 1994]. An optimistic approach may lead the system to unacceptable values under severe conditions and therefore compromise the security of the system. A pessimistic approach will avoid risks in the delivery by introducing larger security margins, but on the other hand it will lead to a poor utilization of the resources. As mentioned in the previous section the continuous changes in the electricity industry are forcing changes in the transmission system. To avoid an unnecessary expansion it would be optimal to use the existing lines and transformers to their full capacity. The accurate determination of the transfer limits will play an important role in maintaining the secure and economic operation of the power system.

Accurate power system models are necessary in order to reduce power system operational uncertainty. Accurate models of different complexity for generators, lines and transformers are available today, whereas load models are usually simplified. Different studies, [Taylor, 1994] and [IEEELoad, 1993], have shown the importance of the load representation in voltage stability analysis. Static load models are not accurate enough for capturing the dynamics of the network. Therefore dynamic load models are needed even if voltage collapse, in many cases, is a slow phenomenon. This situation is particularly critical in Sweden, [Johansson and Sjögren, 1995], [Arnborg, 1997], where the limiting factor is often voltage stability and where load dynamics due to the large percent of electric heating and tap changer operations, are the main issues.

The work presented here is motivated by the need of finding more accurate dynamic load models. The result will provide a better understanding of the load dynamics and its representation, making it possible to decrease uncertainty margins, and therefore optimizing both, the economy and reliability of the system operation. By the use of a continuous acquisition of data from normal operation, the behavior of the load, which immediately provides information about operating conditions, will be recorded. A real-time application will track the time varying characteristic of the load, as well as possible deviations from normal operation, and the resulting information might be utilized for on-line security assessment.

1.3   Objectives and Contributions

The thesis mainly deals with modeling and description of the dynamic load characteristic of the long-term voltage stability studies. The focus is on the identification and interpretation of the parameters that describe the standard active and reactive dynamic load models. The main objective is thus the selection of an appropriate load model structure, and the design of an automatic process for the identification of the parameters that describe that model using continuously recorded data from normal operation. A second objective is to investigate the results obtained from the identification procedure. The exploration will make it possible to track seasonal and daily variations, but also to describe deviations from normal operation.

This work is motivated by the critical effect that load representation has on voltage stability studies. It can be shown that under the same operating conditions, transfer capacity depends on the load characteristic. Furthermore, a system that is theoretically stable may behave unstable, resulting in voltage collapse under extreme conditions. This investigation evidences the importance of finding more accurate load models in order to obtain a better representation of the load, and therefore an improved reliability of the system by decreasing uncertainty security margins.

The next step was the selection of a suitable load model for the representation of an area mainly characterized by electric heating. High complexity models, defined by a large number of parameters are not flexible for general applications, i.e. they may represent the load accurately for specific situations, but the parameters may not be appropriate for other different conditions. A more simplified model defined by less parameters, provides a general description of the problem and high flexibility in the use. A non-linear dynamic load model with exponential recovery was selected [Karlsson and Hill, 1994]. The model was reduced to a linear system. Simulations have verified that both models, linearised and non-linear, agree with each other, and therefore it has been proven that the non-linear parameters can be calculated straightforward from the linear identification results. At this point the thesis aimed at an automatic determination of the parameters in the mentioned dynamic load model based on normal operation data. An automatic procedure for acquisition of data, detection of voltage variations and determination of parameters has been defined and applied to a long sequence of data from normal operation. Continuous data

from normal operation have provided valuable information related to load dynamics for the realization of this study. The identification conditions for this procedure have thus been studied and specified.

Since the main goal of this work was the determination of an appropriate representation of the load to decrease uncertainty margins, the main contribution of the thesis is the analysis and interpretation of the identified parameters obtained from the procedure described above.

Unexpected deviations in the reactive load parameters have led to a new representation of the reactive load, where the used normalization factor for the model, corresponds to the active power level Po, or apparent power level So, instead of the previously suggested reactive power level Qo. Furthermore, a description of the time varying characteristic of the load parameters, and its dependency with temperature is presented.

1.4   Outline of the Thesis

Introduction (Chapter 1)

- Introduction to load modeling and description of the facts that have motivated the realization of the work held in this thesis

Voltage and Load Stability (Chapter 2)

- Introduction to voltage stability phenomena, transfer limits and maximum transfer capacity of a power system

- Voltage and load stability. Influence of the load characteristic in the determination of the maximum transfer capacity of a system, and effect of power system loads in the long-term voltage stability studies

Load Modeling (Chapter 3)

- Introduction to basic principles in modeling and characterization of the load depending on load type, classes and composition

- Outline of standard load models, including static and dynamic types

Field Measurements (Chapter 4)

- Description of field measurements, from staged tests and from normal operation, in the South of Sweden

- Analysis of normal operation data

Determination of Parameters in Dynamic Load Models (Chapter 5)

- A method for determination of parameters in dynamic load models is proposed and tested using field test data

Automatic Determination of Parameters (Chapter 6)

- Analysis of suitable conditions for an automatic determination of parameters in dynamic load models. Determination of window length for the identification

- Effect of normalization in dynamic reactive load models

Analysis of Experimental Results (Chapter 7)

- Simulation results based on field measurements from normal operation data during the period July 2001-June 2002

- Determination of monthly and daily variations of the identified dynamic load parameters, and study of the load dependency with time, season and weather conditions

Conclusions (Chapter 8)

- Main conclusions and suggestions for future work

1.5   Publications

Some results of this thesis have already been published in the publications below. Chapters 5 and 6 are describing the content of [2]. The results in [3] are discussed in Chapter 6. The main results in Chapter 7 are described in [4] and the influence of load representation in voltage stability studies [5] is included in Chapter 2.

- I. Romero Navarro, M. Larsson, G. Olsson. 'Object-Oriented Modeling and Simulating of Power Systems using MODELICA'. *IEEE Winter Meeting, Singapore. January 2000.*

- I. Romero Navarro, and O. Samuelsson. 'Analysis Window for Determination of Parameters in Dynamic Load Models'. Reglermötet, Högskolan i Linköping (*National Swedish Symposium on Control 2002*), May 28-30.

- I. Romero Navarro, O. Samuelsson and S. Lindahl. 'Influence of Normalization in Dynamic Reactive Load Models'. *Submitted and reviewed for publication in IEEE Power System letters (2003).*

- I. Romero Navarro, O. Samuelsson and S. Lindahl. 'Automatic Determination of Parameters in Dynamic Load Models from Normal Operation Data'. *Submitted and accepted for Panel session on load modeling at IEEE Power Engineering Society meeting in July 2003, Toronto.*

- I. Romero Navarro, O. Samuelsson. 'Influence of the Load Characteristic in Voltage Stability Analysis'. *Submitted to IASTED International Conferences. Power and energy systems, PES 2003. February 2003, California.*

Internal Reports

I. Romero Navarro, (2000). 'Cold Load Pick Up using MODELICA'. *Technical Report, CODEN:LUTEDX/(TEIE-7148). 2000 IEA, Lund, Sweden.*

I. Romero Navarro, (2001). 'Analysis and Identification of Load Responses in the Österlen Test System using MODELICA-MATLAB'. *Technical Report, CODEN: LUTEDX/(TEIE-7149). 2001 IEA, Lund, Sweden.*

I. Romero Navarro, (2001). 'Recording of Voltage, Active and Reactive Power at Tomelilla. TOMELILLA I'. *Technical Report, CODEN: LUTEDX/(TEIE-7150). 2001 IEA, Lund, Sweden*.

I. Romero Navarro, (2001). 'Recording of Voltage, Active and Reactive Power at Tomelilla. TOMELILLA II'. *Technical Report, CODEN: LUTEDX/(TEIE-7151). 2001 IEA, Lund, Sweden*.

I. Romero Navarro, (2002). 'Automatic Determination of Parameters in Dynamic Load Models'. *Technical Report, CODEN: LUTEDX/(TEIE-7188). 2002, IEA, Lund, Sweden.*

Chapter 2

Voltage and Load Stability

The on-going changes in the electricity industry are resulting in new features of the power systems, which are characterized by complex interconnections, and the utilization of a large variety of controllers for optimizing the system operation and the use of the available sources. Moreover, with the deregulation process of the power supply utilities, the power networks are understood to be channels for the transfer of electricity from points of production to points of consumption, depending on a competitive system based on time varying prices. The complexity of the system, the nature of the dynamics that affect it and the external factors interacting simultaneously require special attention, in order to provide a properly operated and designed power system.

The system must provide high supply reliability at minimum cost and ensure the minimum impact on the natural environment. In order to avoid inconvenience to the customers and severe technical problems which will lead to expensive costs, the system must be able to meet the frequent variations in active and reactive load. High level of system security, availability of 'spinning' reserve of active and reactive power, high quality in the design of the system components and availability of different paths for the delivery of the energy to the customers are some of the factors that can help to ensure this reliability [Machowski, et al., 1997]. At last, high quality in the delivered power must be guaranteed according to minimum standards related to constant frequency, constant voltage, and low harmonic content.

The voltage stability phenomena and the impact of the load representation in stability studies, is described throughout this chapter. Section 2.1 introduces the Swedish power system as an integrated part of the Nordel system. A general classification of power system stability is introduced in Section 2.2. Definitions of voltage stability and instability are also included. Throughout Section 2.3 the transfer capacity of the system and the transfer limiting factors are studied. P-V curves are introduced for the determination of the maximum transfer power of the system. The influence of the load characteristic in voltage stability is described and the use of dynamic models for the representation of the load is motivated.

2.1   The Swedish Power System

The Swedish power system is integrated into a more complex system, denominated Nordel [Nordel, 2001], that comprises the interconnected power systems of Norway, Sweden, Finland, Iceland and parts of Denmark (see Figure 2.1).

Denmark is divided in two separate grid areas. Jylland/Fyn is connected to the Continental grid, and Zealand to the Nordic grid. Both areas joined to the open Nordic market in 2000.

The Nordel organization was created in 1963 and it constitutes a union for electricity cooperation in the Scandinavian countries. Several AC connections exchange energy between Sweden, Norway, Finland and Zealand (East part of Denmark), while the West part of Denmark and the Polish and German networks are connected to the system through HVDC links. Even though there are common regulations between these countries, every single system is characterized by structural differences. The main purpose of the system is the design and development of a power system operation where a high reliability in the supply is guaranteed at a low cost. Moreover, the system is responsible for the control and regulation of the available transfer capacity, power balance in each country, and the possibility of exchange included in that balance.

The Swedish system is characterized by a concentration of consumption in the southern part of the country, while the generation area is in the North.

Even though the use of renewable energies such as wind power has gained interest in the recent years, still most of the generation is hydro and nuclear power. Oil and gas power plants provide the remaining parts, and are in use during peak load conditions. The transmission system is extended across the country from North to South, connecting the generation and load areas though a meshed system with voltage levels of 400 kV, 220 kV and 130 kV, to deliver the electricity to the consumption areas. The distribution system topography is typically radial with voltage values of 50 kV and 20 kV. A factor limiting the N-S transfers is voltage stability.
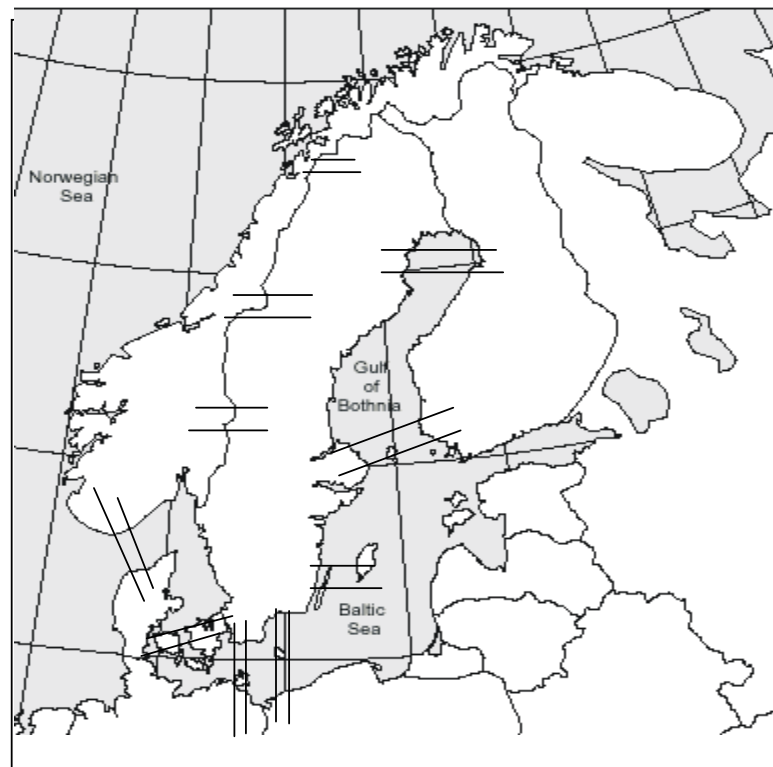
Figure 2.1: Outline of the Nordel Power System.

2.2   Voltage and Load Stability

Voltage stability can be defined according to [Kundur, 1994]: *'The voltage stability is the ability of a power system to maintain steady acceptable voltage at all buses in the system at normal operating conditions, and after being subjected to a disturbance'*. It is thus a characteristic of the power system to remain in equilibrium under normal conditions, and to react, restoring the status of the system to acceptable conditions after a disturbance, i.e. the voltage after a disturbance is restored to a value close to the pre-disturbance situation. When the voltage in the system is uncontrollable and continuously decreases due to failures in the design, external factors, variations in load or inappropriate voltage control devices, the system becomes unstable and enters in the stage of voltage instability.

According to CIGRE definitions [CIGRE, 1993], '*voltage instability is the absence of voltage stability, and results in progressive voltage collapse (or increase)*'. The main reason to lead a power system to an unstable situation and therefore to instability, is the incapacity of satisfying the reactive load demand under heavily stressed conditions, to keep voltage at acceptable levels. Voltage collapse follows voltage instability, and it is often the result of the action of voltage control devices, load tap changers, the voltage dependence characteristic of the load, the generator reactive power limits or the combination of several of them. Voltage collapse leads the system to low-voltage values in a large part of the power system, and therefore to partial or total collapse. According to IEEE definitions [IEEE, 1990], '*voltage collapse is the process by which voltage instability leads to loss of voltage in a significant part of the system'*.

Voltage stability is often denominated load stability; the load characteristic and its dynamics indicate the dependency between the load and the voltage, and therefore the close coupling with the voltage stability phenomenon. A voltage drop will initially result in decay in load, but after few seconds, a load restoration process will start. The restoration can lead to heavily loaded conditions, and to voltage instability and voltage collapse if under those conditions, appropriate control decisions are not taken, and/or the system is not able to meet the reactive load demand.

Power system stability can be basically classified into angle stability and voltage stability as described the Figure 2.2 [Kundur, 1994].
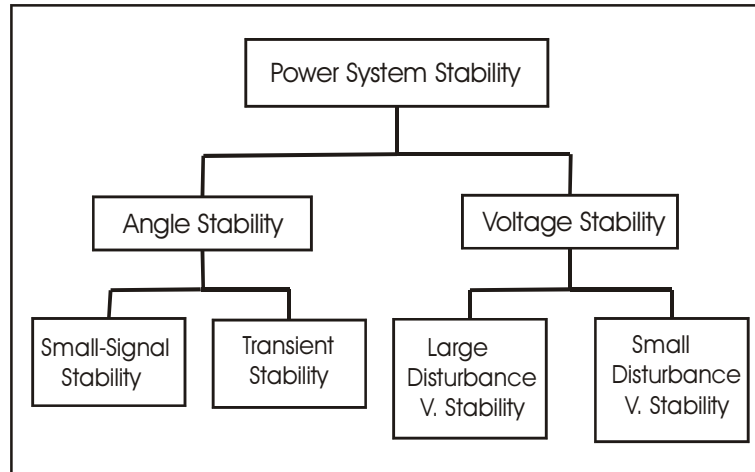
Figure 2.2: Classification of power system stability dynamics.

The capability of the system to keep synchronism in interconnected machines is defined as angle stability. Small disturbances, '*small-signal stability*', result in undamped electromechanical oscillations due to insufficient damping torque, while larger disturbances, '*transient-signal stability*', may lead to lack of synchronizing torque. The time frame for angle stability is denominated short-term time scale and it is approximately in the order of few seconds. Voltage stability can be classified into short and long-term voltage stability. The '*short-term*' corresponds to a time frame of about a few seconds, and describes the dynamics of components such as induction motors, static var compensators and excitation of synchronous generators. When the dynamics of the system corresponds to slower time frames, around several minutes, '*long-term stability*', two kinds of stability problems can occur; frequency and voltage problems. '*Frequency stability*' problems are the result of power imbalance between generators and loads after a large disturbance, and can result in system islanding. '*Long-term voltage stability*' acts on a time frame scale in the order of several minutes and includes phenomena such as dynamic recovery of the load in electric heating often due to the action of on-load tap changers, current limiter control in generators, corrective control actions such as reactive compensation and load shedding, operator control actions, etc.

2.3   Transfer Limits

In this section we will discuss voltage stability and particularly the limits for voltage collapse. The so-called nose curve is defined. It is also shown that the load representation will have a significant influence on the voltage stability computations.

2.3.1 Introduction

Based on the description in Section 2.1, the Swedish power system is integrated into a more complex interconnected system denominated Nordel. A system of these characteristics is often subjected to risk from many disturbances that may lead it to heavily loaded conditions, and consequently closer to its transfer capacity limits. It is a challenge for the system operation to increase that transfer capacity which is very much related to congestion management and power transfer limits.

As an example, Figure 2.3 shows a problem concerning stability limits. These limits are generally difficult to determine with sufficient accuracy and reliability due to the high uncertainty related to internal and external factors, and therefore conservative criteria are often used for their determination resulting in smaller secure operation areas.
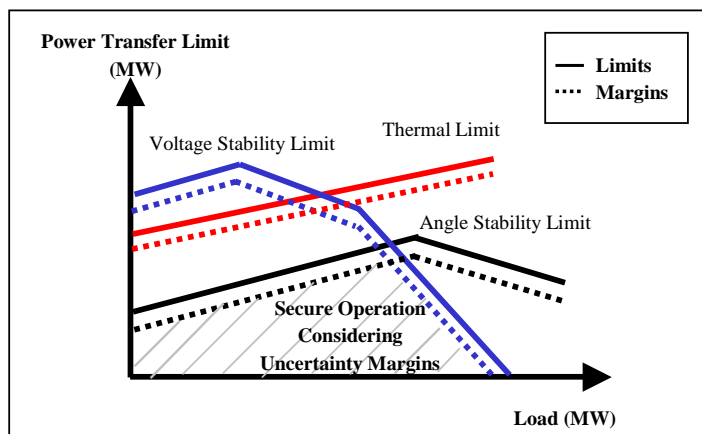
Figure 2.3: Power Transfer Limits operation with uncertainty margins.

Thermal capacity limits, voltage stability, transient stability and small signal stability limits, restrict the amount of power that can be transferred between different parts of the power system. The secure operation area is defined by these limits. A typical situation is that the thermal capacity limit is fairly constant, while the voltage stability limit is strongly dependent on system loading and reactive reserves. The angle stability limits may take different forms, but a loading limit will always exist.

2.3.2 Static aspect of voltage stability

The determination of the maximum amount of power that a system can supply to a load will make it possible to define the voltage stability margins of the system, and how they can be affected by for example connection and disconnection of loads, or as a result of dynamic events. The P-V or nose curve, [Taylor, 1994], corresponds to the graphical representation of the power-voltage function at the load bus, (see Figure 2.4).
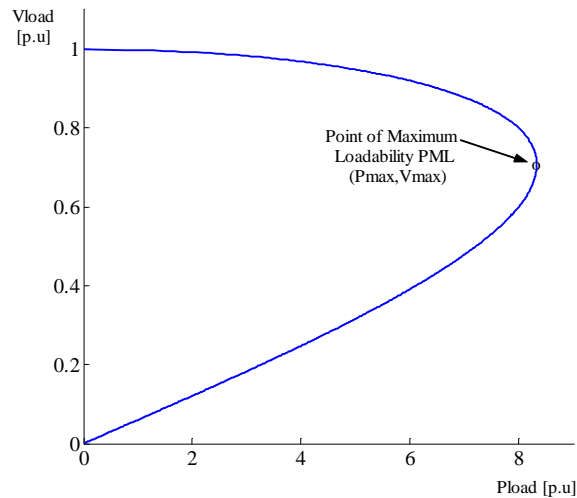
Figure 2.4: Nose curve. Representation of the Power-voltage function for the system in Figure 2.5.

The P-V curves are characterized by a parabolic shape, which describes how a specific power can be transmitted at two different voltage levels, high

and low voltage. The desired working points are those at high voltage, in order to minimize power transmission losses due to high currents at low voltages. The vertex of the parabola determines the maximum power that can be transmitted by the system and it is often called the point of maximum loadability or point of collapse.

The simplified system in Figure 2.5 has been used to determine the analytical expression for the load-voltage function, and its P-V implementation (Figure 2.4). The generator is assumed to have a constant voltage, V_g, equal to 1 p.u. The equivalent reactance for the transformer, X_T, is equal to 0.01 p.u, and through bus 2 it is connected to two parallel lines, both with a transmission reactance of 0.1 p.u, and zero line resistance. Through bus 3 the two lines are connected to the load, which is defined by a pure active load, nominal reactive load equal to zero and constant power factor, $cos\phi$, equal to 1.
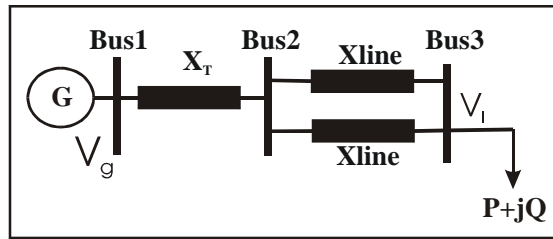
Figure 2.5: Three bus simplified transmission system.

Equations (2.1) and (2.2) define the active and reactive power that can be transmitted to Bus 3:

$$P_l = \frac{V_g \cdot V_l}{Xeq} \cdot \sin\left(\theta_g - \theta_l\right) \qquad (2.1)$$

$$Q_l = \frac{V_g \cdot V_l}{Xeq} \cdot \cos\left(\theta_g - \theta_l\right) - \frac{V_l^2}{Xeq} \qquad (2.2)$$

Where Vg, θ_g, Vl and θ_l are the voltages and angles at the generator and load buses respectively. Xeq is the equivalent reactance of the system.

By combining both equations, equation 2.3 is obtained. Taking into account the relation defined by equation 2.4, the power-voltage function is given by equation 2.5.

$$P_l^2 + \left(Q_l + \frac{V_l^2}{Xeq}\right)^2 = \left(\frac{V_g \cdot V_l}{Xeq}\right)^2 \tag{2.3}$$

$$\tan\theta_l = \frac{Q_l}{P_l} \tag{2.4}$$

Where the subscript l refers to the load

$$P_l = \frac{V_l^2}{Xeq \cdot \left[1 + (\tan\theta_l)^2\right]} \cdot \left[-\tan\theta_l + \sqrt{-1 + \frac{\left[1 + (\tan\theta_l)^2\right] \cdot V_g^2}{V_l^2}}\right] \tag{2.5}$$

The vertex of the parabola, *point of maximum loadability*, is often named point of collapse, but this denomination is no longer true if the load is represented with a characteristic other than constant power. As it will be shown further in this chapter, the voltage dependence characteristic of the load affects voltage stability and therefore the location of the point of collapse. The operating point corresponding to the maximum loadability is calculated by determining the maximum of the function defined in equation 2.5, i.e. the derivative of P_l with respect to V_l equals to zero. This point is thus given by equations 2.6 and 2.7:

$$V_{max} = \frac{V_g}{\cos\theta_l} \cdot \sqrt{\frac{1 - \sin\theta_l}{2}} \tag{2.6}$$

$$P_{max} = \frac{V_g^2}{2 \cdot Xeq \cdot \cos\theta_l} \left(1 - \sin\theta_l\right) \tag{2.7}$$

When the point of collapse is reached, the system becomes unstable, and the voltage starts decreasing quickly since the reactive support of the system under these heavy loaded conditions is not enough. Figure 2.6 shows the P-V representation for different values of *tan ϕ*.
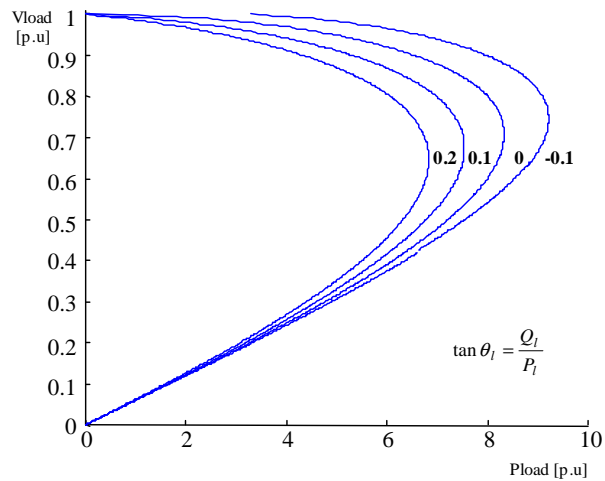
Figure 2.6: P-V curves for different load compensation cases. tanϕ equal to 0.2, 0.1, 0 and –0.1.

By local reactive compensation it is possible to increase the transfer capacity of the system, but at the same time the system operates closer to the security margins, since the point of collapse is placed closer to acceptable voltages.

2.3.3 Influence of the load characteristic on voltage stability

The effect of the load representation on voltage stability, [Johansson and Sjögren, 1995], is studied in this section. The main objective is to prove that under the same conditions in the system, the load representation will affect the location of the operating point in the P-V curves, leading the system closer to or further away from the collapse point. A very optimistic design may lead the system to voltage collapse under severe conditions, while a conservative design will ensure the delivery of energy due to larger security margins.

The importance of using dynamic load models instead of static ones in voltage stability studies is also discussed throughout the section. The use of

dynamic models will provide a more accurate description of the load behavior, making it possible to reduce security margins, and still maintaining high reliability in the system operation.

Static and dynamic characteristic of the load

In order to analyze the effect of power loads on voltage stability, it is necessary to study both the static and the dynamic characteristic of the load. Equation 2.8 describes the voltage sensitivity, given by the parameter α, for general static models in exponential form:

$$Ps = P_o \left(\frac{V}{V_o} \right)^{\alpha} \qquad (2.8)$$

Constant impedance, constant current and constant power characteristics are obtained by using the typical values of α 2, 1 and 0.

To describe the dynamic characteristic of the load, a non-linear dynamic load model with exponential recovery has been chosen [Karlsson and Hill, 1994]. The model, equations 2.9 and 2.10, is characterized by three parameters; α_s is the steady state active load-voltage dependence, α_t is the transient active load-voltage dependence and T_p is the active load recovery time. This model is further studied in Chapter 3.

$$T_p \frac{dP_r}{dt} + P_r = P_o \left(\frac{U}{U_o} \right)^{\alpha_s} - P_o \left(\frac{U}{U_o} \right)^{\alpha_t} \qquad (2.9)$$

$$Pl = P_r + P_o \left(\frac{U}{U_o} \right)^{\alpha_t} \qquad (2.10)$$

Figure 2.7 shows the response of the load when a disturbance is affecting the system. In this case an ideal voltage step has been applied. The response of the load can be divided into a transient characteristic, $P_t(V)$, right after the disturbance, and a steady-state characteristic, $P_s(V)$, after the recovery, [Hill, 1993] and [Karlsson, 1992].
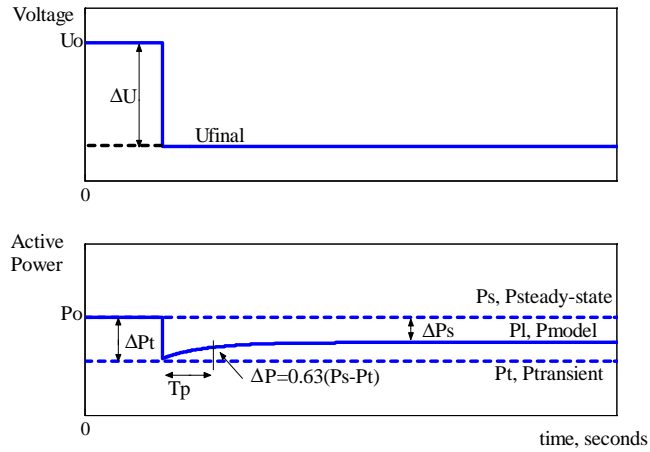
Figure 2.7: Load response under ΔU step, from the Uo-level**.**

Expressions for both characteristics, steady state and transient, are given by equations 2.11 and 2.12 respectively:

$$P_s(V) = P_o \left(\frac{V}{V_o} \right)^{\alpha_s} \tag{2.11}$$

$$P_t(V) = P_o \left(\frac{V}{V_o} \right)^{\alpha_t} \tag{2.12}$$

Dynamic aspects of voltage stability

The stability of the system described in figure 2.5 is studied now, when one disturbance is affecting the system. A disconnection of one of the parallel lines has occurred.

Figure 2.7 shows a simplified scheme of the transmission system under these new conditions.
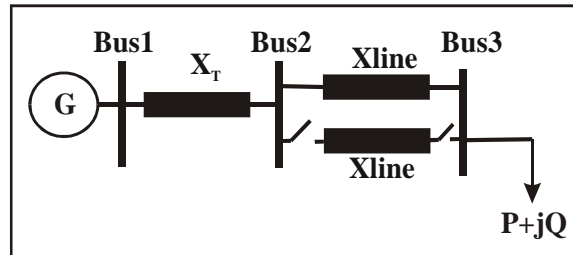
Figure 2.7: Line disconnection on a simplified three-bus transmission system.

Figure 2.8 shows a P-V representation of the pre-disturbance, curve (1), and post-disturbance situation, curve (2). The disconnection of one of the lines reduces the maximum amount of power that can be transmitted by the system. The total reactive consumption in the transmission system is higher and the voltage in the load bus has decreased. The static load characteristic for different values of α, voltage sensitivity, is also shown. Since equations 2.11 and 2.8 have the same form, we will refer the exponent that describes the power-voltage dependency as the parameter α. The negative values of the parameter are associated to a combination of a dynamic restoration of the load and the discrete action of tap changers.

For a typical case where the load power is not affected by the voltage, constant power, the parameter is equal to 0. Those values, which are higher than 0, express load voltage dependency. As exemplified in the figure, the larger this parameter is, the further the new operating point is from the P-V nose. For a static representation, this parameter expresses the load-voltage dependency. For a dynamic representation, the exponent is associated with the long-term characteristic of the load. Those values larger than zero correspond to partial restoration of the load to its pre-disturbance value.

The negative values of the parameter are associated with the long-term dynamic restoration of the load, and the effect of discrete tap changers, i.e. by action of tap changers the voltage in one of the sides of the controlled transformer is regulated to an acceptable value. Since the load representation is voltage sensitive, the load is increasing at the same time as the voltage. If the regulation of the voltage is discrete, there is possibility of overshooting in the voltage and therefore in the load, which means that the steady-state value for the load will be higher than the pre-disturbance one.

The larger the negative value is, the larger is the overshoot in power, indicating that the system is closer to the voltage stability limits. Figure 2.8 shows an unstable situation when α_s is equal to –0.5.
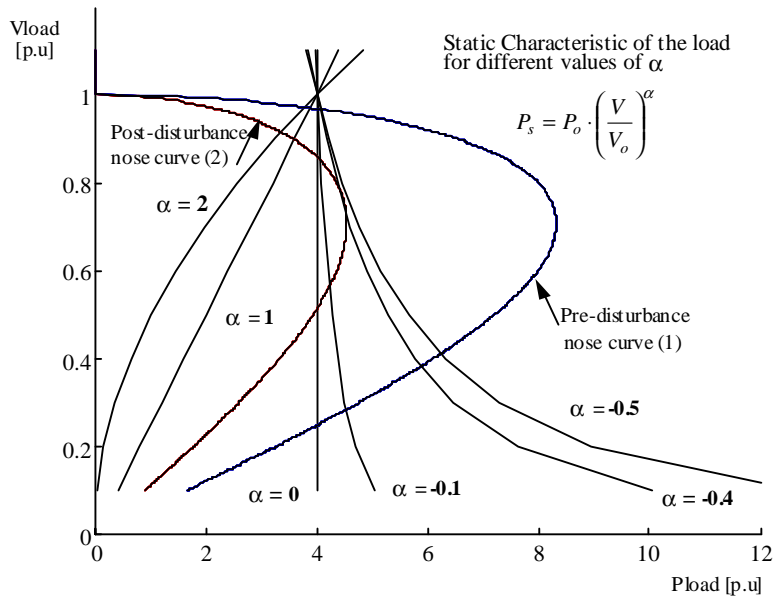
Figure 2.8: Influence of the static load characteristic on PV curves when the disconnection of a parallel line has occurred. The load characteristic is shown for α equal to 2, 1, 0, -0.1, -0.4 and -0.5.

Figure 2.8 has shown how the load representation affects voltage stability and the location of the new operating points, further or not to the collapse point, after a disturbance. From a planning and operating point of view the difference between these new operating points is important.

The traditional way of representing power loads in voltage stability studies is by using static models, and in many cases, assuming a constant power characteristic because of the use of tap changers for voltage regulation, [IEEEStability, 2002]. The fact that loads are generally voltage dependent is a critical aspect of voltage stability studies. Figure 2.9 shows a case where the voltage sensitivity of the load helps the stability of the system, by

providing some system relief. Figure 2.9 corresponds to the case described in Figure 2.7, when one parallel line is disconnected.
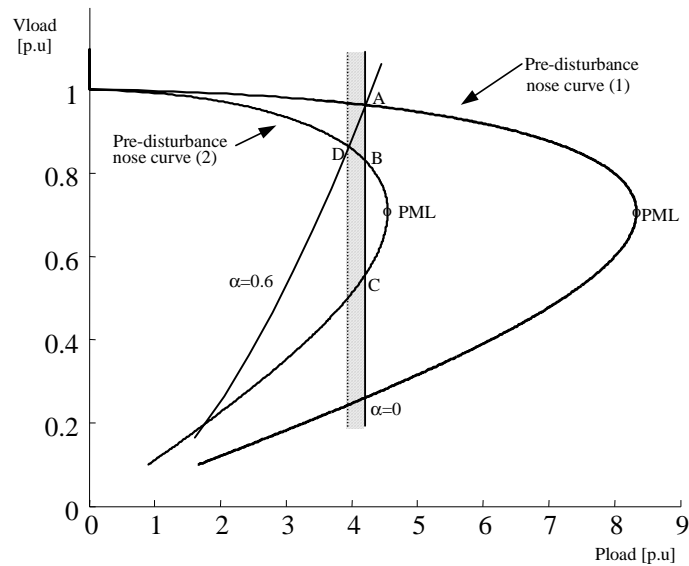
Figure 2.9: Influence of the static load characteristic on PV curves, voltage dependent, $\alpha=0.6$, and voltage independent, $\alpha=0$, when the disconnection of a parallel line has occurred. The exceeded security margins are marked by a shaded area.

By using a constant power representation in power flow calculations, the voltage solution will correspond to the point A and B, before and after the disturbance. However, since most power loads are voltage dependent the load voltage sensitivity, for example for a value of α equal to 0.6, is also shown. The solution is now point D. The difference between these two points D and B is important. The actual situation at D corresponds to less heavy loaded conditions and higher voltage than was predicted by the power flow. In this case, by assuming a constant power characteristic, the impact of the load in the system is over-emphasized and the theoretical transfer capacity is reduced despite increasing security margins, which at the end leads to a poor utilization of the system.

Electric heating, which shows a thermostatic effect, is a special load to take into account. When a disturbance is affecting the system and the voltage is reduced, the drop in power consumption of the individual loads activates the thermostats in order to keep the loads connected longer, i.e. on an aggregated base this means that more electric heating are connected at the same time yielding a higher load. The global effect in load is to increase the nominal load to a level close or equal to the pre-disturbance one, at the post-disturbance voltage. In the case of electric heating loads, this situation is more critical during the winter than the summer, especially in cold countries. The behavior of these loads is well described by equations 2.9 and 2.10. The effect of the thermostat characteristic is important to be considered in long-term simulations, and in those areas where most of the load is of this type and a significant number of on-load tap changers. If the tap changers reach regulation limits after a disturbance, the effect of the dynamic recovery of the loads is critical for voltage stability.

The dynamic representation of this type of load is characterized then, by a transient part, and a long-term part. The change in the characteristic, and the recovery time from the transient state to the steady-state one is critical in voltage stability [IEEEStability, 2002]. By increasing the understanding of this phenomenon, it is possible to take corrective actions quickly enough, such as load shedding, switching capacitors, starting auxiliary gas turbines, and lead the system to stable conditions. Figure 2.10 shows an ideal voltage step in an area where most of the load is electric heating, and both load responses, A) a dynamic model with partial recovery to constant current, and B) a static model with a constant current characteristic. A constant current characteristic is a typical representation for the load in wintertime.

By using a static model it has been assumed that the load behaves as a constant current. In reality, the drop in voltage will reduce the power load. The reduction will activate the thermostats for longer time and this will result in the increase of the aggregated load consumption to a value close or equal to the pre-disturbance conditions. The resulting operating point is more critical than at predicted by the static model, since the load demand is higher, and this may lead the system to a severe situation. However, during the recovery time Tp, there is a relief in load, and by taking an effective and quick action the stability of the system may be maintained.
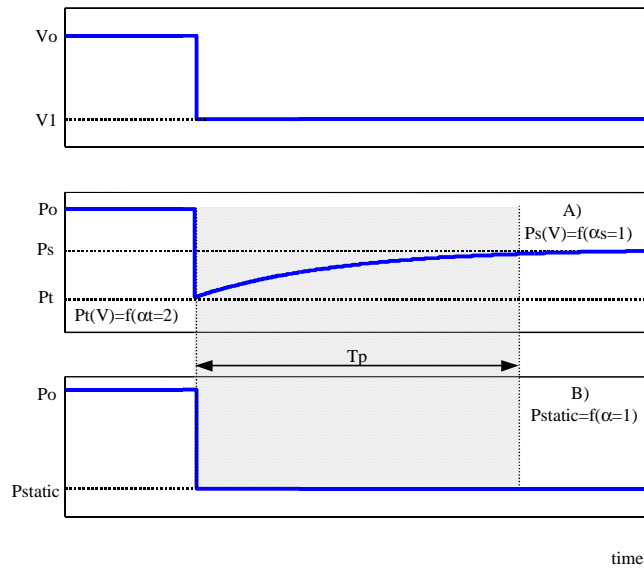
Figure 2.10: Load response under a voltage drop corresponding in an area where most of the load corresponds to electric heating. A) Dynamic representation of the load, B) Constant current representation.

Figure 2.11 shows again the situation described in Figure 2.7. The load is mainly electric heating. The pre-contingency system was operating at the intersection of the load characteristic curve and the pre-disturbance PV-curve, point A, with a voltage of 0.92 p.u and a power transfer of 5.3 p.u. After the disturbance, the system has moved to the point B, with voltage equal to 0.85 and power transfer equal to 4.2 p.u. At this point the voltage has dropped. Also the load demand has decreased, since the load-voltage sensitivity has resulted in a relief in load. However, the thermostatic characteristic of the electric heating will tend to increase the actual load to the pre-disturbance nominal value. The load characteristic will start changing towards a constant power characteristic, (α moving towards zero). The intersection of the new curves with the post-disturbance PV-curve will lead the system to very low voltage operating points and eventually to a voltage collapse, point C.

During the transition it is possible to take some corrective actions in order
to move the operating point to a stable situation in the upper part of the new
curve, point D. Some of these actions are local reactive compensation of the
load, (Figure 2.11), load shedding, starting small-scale gas turbines.
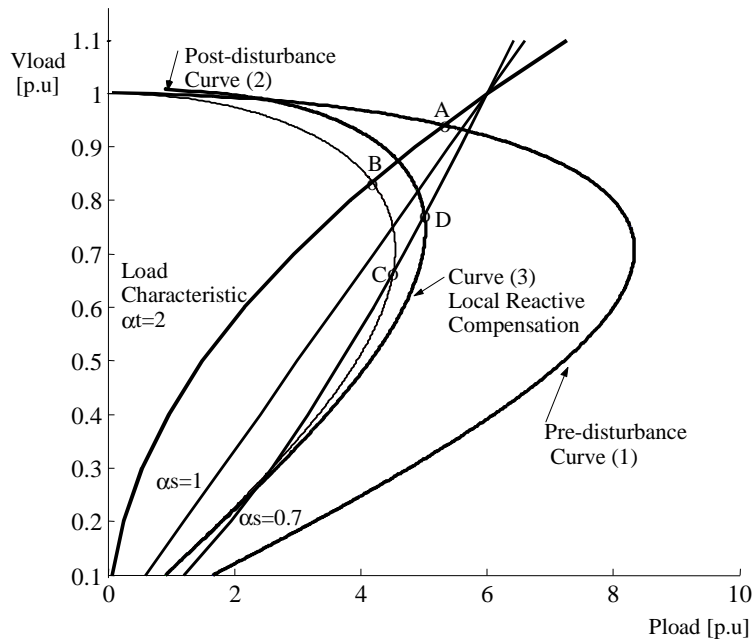
Figure 2.11: Influence of the thermostatic characteristic of electric heating loads in
voltage stability. Curve (1), (2) are the pre- and post-disturbance curves
respectively, and curve (3) corresponds to the system transfer capacity when local
reactive support is used.

2.4   Conclusions

The effect of the load representation on voltage stability has been studied.
Under the same conditions in the system, the load representation affects the
location of the operating point in the P-V curves, leading the system closer

to or further away from the collapse point. Since the load behavior is critical for the stability of the system, more accurate models are necessary. The traditional static models are not enough to represent the load dynamics and therefore dynamic load models have been introduced.

Moreover, some types of load such as electric heating are especially critical for stability because of their thermostatic characteristic. After a disturbance in the system, (voltage and power drop), and due to the effect of the thermostats, the aggregated load tends to increase the load to a level close or equal to the pre-disturbance one, at the low voltage. This situation may result in severe conditions for the system operation. However, during the recovery time it may be possible to take some corrective actions such as local reactive compensation, load shedding, starting small-scale gas turbines, which may lead the system to stable operating points instead.

Chapter 3

Load Modeling

In recent years, the interest in load modeling has been continuously increasing, and power system load has become a new area for researching into power systems stability. Several studies, [IEEEStability 1990], [Taylor 1994], have shown the critical effect of load representation in voltage stability studies, and therefore the need of finding more accurate load models than the traditionally used ones.

Voltage collapse is a phenomenon that in most cases takes several minutes; most of the load modeling work done in the past has been focused on induction machines, critical in the range of some seconds after a disturbance. Other static nonlinear models have been used for analyzing the long-term power system behavior; the load response is then described as a function of voltage [Karlsson and Hill, 1994]. The idea of a dynamic model that is able to cover the short and the long-term has been a goal in the last years. Now it is not only important to study the effect of induction motors, but also how tap-changers, spontaneous load variations as well as other components are affecting the stability of the power system [Johansson and Sjögren, 1995]. The idea of using static load models in stability analysis is changing in favor of dynamic load models.

Even though power system load has gained more attention in the last years, it is still considered as one of the most uncertain and difficult components to model due to the large number of diverse load components, to its high distribution, variable composition with time of day and week, weather and through time, and also because of lack of precise information on the composition of the load. Different utilities are available for load forecasting

31

purposes [Willis, et al., 1995], but also new techniques for the determination of the load characteristics from measured composition data have been developed [Dovan, et al., 1987]. The result of these new techniques will lead to a better understanding of the load dynamics and therefore to an improved load representation, making it possible to decrease uncertainty margins, resulting in a positive impact on both economy and reliability of the system operation. Moreover the combination of an accurate load model and a real-time monitoring application will bring up new competitive possibilities for the electricity industry.

3.1   Introduction

In this section we discuss different modeling approaches and the use of data acquisition that is required to achieve them.

3.1.1 Physical vs. black box models

A model based on fundamental engineering knowledge about the physical phenomena that affect the system is called *physical model*. A basic model based on elementary laws will provide accurate results when simulating, but in case of a high complexity system, the high difficulty in obtaining all the physical laws affecting the system and the specific parameters will make it necessary to develop the model based on empirical laws. When a model is based on the empirical relations between input and output signals, it is called a *black box or empirical model*. Black-box models are thus applied when there is not enough knowledge to create a physical model, or the functioning of the system is very complex, but there is available data to establish a mathematical relation between the input and output measurements of the system.

A physical model, which will be described further in the thesis, has been chosen for the realization of this work. The model complexity is able to describe the load dynamics of interest.

3.1.2 Data for Load Modeling

Two basic approaches are used to obtain data on composite load characteristics; the measurement-based approach, and the component-based approach.

The measurement-based approach involves direct measurements at representative substations and feeders to determine the voltage and frequency sensitivity of the active P and reactive Q load. The data is obtained either from measurements in-situ, and includes voltage and frequency variations, and the corresponding variations in active and reactive load, either to intentional disturbances, test measurements, or to natural events, normal operation data. By fitting the measured data to an assumed model, the parameters of that load model are identified. Such an approach is sometimes called gray-box modeling, since a structure of the model is assumed. The techniques used for the determination are related to the complexity of the assumed model and the characteristics of the field measurements. The identification of the parameters in static load model submitted to voltage steps is straightforward, compared to identifying parameters in dynamic load models using normal operation data.

The main advantage of using a measurement-based approach is the availability of actual data from the system under study, and the possibility to track seasonal variations but also deviations from normal operation. On the other hand, this approach implies economical investment in appropriate equipment for carrying out the measurements and monitoring the most important loads in the system.

The component-based approach involves developing a composite load model [Taylor, 1994] from information on its constituent parts, i.e., mix of classes at the substation, composition of each of those classes, and main characteristics of each single load component. The *load class mix data* describes which is the percentage of each of several load classes such as industrial, residential, commercial, to the load consumption at a specific bus of the system. The *load composition data* describes the percentage of each load component, such as electric heating, air conditioner, induction motors to the active consumption of a particular load class, and the *load characteristic data* is related to the physical characteristics of each one of those load components.

The main advantage of this method is that it does not require field measurements, it is easier to adapt to different systems and conditions, and it is much easier to put into use. On the other hand, since the load class mix data varies from bus to bus and is dependent on weather and time, it is necessary to often determine and update the load class mix data for each bus of the system.

In order to get a better description of the load characteristics, it would be optimal to combine both methods. In this thesis the measurement-based approach has been used.

3.1.3 Type of Measurements

The use of *continuous field measurements* provides real-time information of the status of the system. The collection of data involves a continuous monitoring process to store and to present the information in suitable form, and a data post-processing. When the process is limited to data collection and monitoring, the operators must take the control decisions related to irregularities in the system. Other more advanced solutions integrate the on-line information from the acquisition with an automatic control system, and the observations made by the operators. A disadvantage of carrying out these measurements is the implementation and maintenance cost of the equipment. *Off-line data processing* provides information from the system corresponding to a period of time previous to the data analysis and processing. They make it possible to analyze different characteristics of the system, at different places and times, and basically they constitute rich databases for research purposes. The main disadvantage of these measurements is that the analysis, detection of irregularities in the system and control actions, do not take place in the system, and therefore it is not possible to observe how the system would react to them. Moreover since power system load models show variations in model structure and model parameters due to different system and environment conditions, the quantity of data that needs to be collected off-line is large.

Both measurement techniques can be the result of either *field test measurements* of measurements from *normal operation*. The use of normal operating data is advantageous from the technical and economical point of view. The alternative of running a test involves alterations in the normal operation in the system and inconvenience for the customers. The need for

manpower further results in very expensive tests. From the technical point of view, normal operation data will not only describe a specific phenomenon, but also the effect of all the dynamics that are acting on the system.

Off-line processing of data both from field test and normal operation data have been used in obtaining the results of this thesis.

3.2   Load Characterization

Here we will discuss the different load types that are present in an aggregated load. Typical types of loads are described and various compositions are mentioned.

3.2.1 Load Types

According to the description presented in the previous section, the load composition of a particular area is characterized by the load class data, the composition of each one of the classes, and the characteristics of each single load component. The load class data is often grouped in industrial, residential, commercial and agricultural load data. The *industrial load* is mainly related to industrial processes, and most of the load corresponds to industrial motors, up to 95%. Heavy industries may include electric heating processes such as soldering. The *residential load* includes most of the devices related to housing habits, but also a big percent of electric heating and air conditioner units during winter and summer respectively. The *commercial load* corresponds to air conditioner units and a large percent of discharge lighting, and *agricultural load* to induction motors for driving pumps.

In general the different load components that constitute the different load classes can be included in one of the next four groups;

- Loads with 'fast dynamic' electrical and mechanical characteristics such as induction motors,

- Loads that under voltage excursions present significant discontinuities such as discharge lighting and motor protections,

- Loads whose response to voltage faults does not present significant discontinuities or delays such as incandescent lighting, and

- Loads with 'slow' characteristics such as electric heating.

A brief description of some important load components [Taylor, 1994], [Agneholm, 1999], [Kundur, 1994], [IEEELoad, 1993], induction motors, street lighting, electric heating and LTCs, on load tap changers, follows in this section.

Induction Motors

A large amount of power consumption goes to induction motors at residential, commercial and industrial areas. A common use of motors at residential and commercial areas is for the compressor loads of air conditioning and refrigeration. These loads require nearly constant torque at all speeds, and are the most demanding from a stability viewpoint. On the other hand, pumps, fans and compressors account for more than half of the industrial motor use.

Typically motors consume 60 to 70 % of the total power system energy and their dynamics are important for voltage stability and long-term stability studies.

Lighting

Mercury vapor, sodium vapor and fluorescent loads constitute the main kind of lighting used in industry and street lighting, and correspond to a large percent of the load composition in commercial areas. They are very sensitive to voltage variations, since they extinguish at about 80% voltage. *Mercury devices* are based on the operation of an electric discharge, i.e. when a mercury lamp is switched on it is characterized by a weak blue illumination, that will change into lighter white as long as the pressure and temperature increase. This process takes between 2 and 5 minutes to stabilize, and during that time the consumption corresponds to 40 to 50 % of the stationary value. After a lamp has been switched off, it needs some time,

glowing time, to cool down before the discharge can be re-ignited and then restarted. *Sodium lamps* work in the same way as mercury lamps. Since they work at higher pressure and temperature, the quality of the illumination is better, and the glowing time to be restarted is shorter. *Fluorescent lamps* are the most common type of light used in offices, supermarkets, and in general in commercial areas because their low production cost, and high efficiency to produce light. Just some seconds after the lamp is on, the power consumption reaches more than 90 % of its steady state value.

Thermal Loads

A large percent of loads in residential areas, water heaters, ovens, electric heating, and in industrial areas, soldering and molding machines, boilers, behave similar to a constant resistance in the short-term. Right after a voltage drop the possible variations from power in the input of the device hardly affect the temperature and therefore the resistance characteristic. After some seconds, and since the heat production has decreased, the 'on cycle' of the thermostats in thermal loads will prolong in order to recover the temperature. Under low voltage conditions the temperature will then increase slower than in normal conditions during the 'on cycle' of the thermostat. On the other hand, those thermostats that are in the 'off cycle' will not respond to the voltage drop until they enter in the 'on' period, and therefore the temperature will drop to the same rate during the 'off cycle'.

When the voltage is low the thermostats are mainly working on the 'on cycle' all the time, and therefore the load consumption is similar to the one under normal conditions. This type of load behaves as a constant power load in the long-term. In case of very extreme weather conditions, as in a cold winter day, the full restoration of the load may be impossible since the thermostats are already working 100 % in the 'on cycle'.

Load Tap Changers

Load tap changer transformers do not correspond to a load component, but seen from the transmission system they may be considered as part of the load. After a disturbance, they restore the sub-transmission and distribution voltages to their pre-disturbance values, but they also affect the status of the voltage sensitive loads. The restoration of the voltage, and consequently the

increase of these loads may lead the system to voltage instability and collapse. The restoration process takes several minutes.

3.2.2 Load Composition

The composition of the load is strongly dependent on the time of day, month and season, but also on weather. In most cold countries the winters are characterized by high load consumption mainly related to electric heating, while during the summer the consumption is low and hardly affected by the small percent of air conditioner units. In warmer countries the situation is the opposite, and it is during the summer when the load consumption reaches the highest values due to connection of air conditioning loads. Both air conditioning and electric heating loads vary seasonally, but they are also strongly dependent on the weather conditions. If there is cold and windy weather the electric heating demand will increase, while if there is humid weather the use of air conditioner units will increase.

Weekdays are mainly dominated by industrial and commercial loads. The industrial processes may also correspond to evening hours and weekend days. The commercial load consumption varies mainly when comparing weekdays and weekend, and the larger demand corresponds to the working hours.

3.3   Standard Load Models

As mentioned earlier in this chapter a model is a set of equations to describe the relationship between the input and output of a system. In the case of load modeling this mathematical representation is related to the measured voltage and/or frequency at a bus, and the power consumed by the load, active and reactive. Due to the high diversity and distribution of power system loads it has been difficult to model it, and several alternatives have been proposed troughout the time for its representation, depending on its main purpose.

The main classification is in static and dynamic models. A *static load model* is not dependent on time, and therefore it describes the relation of the active

and reactive power at any time with the voltage and/or frequency at the same instant of time. On the hand, a *dynamic load model* expresses this relation at any instant of time, as a function of the voltage and/or frequency at past instant of time, including normally the present moment. The static load models have been used for a long time for both purposes, to represent static load components, such as resistive and lighting loads, but also to approximate dynamic components. This approximation may be sufficient in some of the cases, but the fact that the load representation has critical effects in voltage stability studies is more and more replacing the traditional static load models with dynamic ones.

3.3.1 Static Load Models

Common static load models for active and reactive power are expressed in a polynomial or an exponential form, and can include, if it is necessary, a frequency dependence term, [IEEELoad, 1993], [IEEELoad, 1995]. A brief description of some of these models follows:

ZIP model or polynomial model

The static characteristics of the load can be classified into constant power, constant current and constant impedance load, depending on the power relation to the voltage. For a constant impedance load, the power dependence on voltage is quadratic, for a constant current it is linear, and for a constant power the power it is independent of changes in voltage. The *ZIP model*, equations (3.1) and (3.2), is a *polynomial model* that represents the sum of these three categories:

$$P = P_o \left[a_1 \left(\frac{V}{V_o} \right)^2 + a_2 \left(\frac{V}{V_o} \right) + a_3 \right] \tag{3.1}$$

$$Q = Q_o \left[a_4 \left(\frac{V}{V_o} \right)^2 + a_5 \left(\frac{V}{V_o} \right) + a_6 \right] \tag{3.2}$$

V_o, P_o and Q_o are the values at the initial conditions of the system for the study, and the coefficients a_1 to a_6 are the parameters of the model.

Exponential Load Model

Equations (3.3) and (3.4) express the power dependence with the voltage, as an exponential function.

$$P = P_o \left(\frac{V}{V_o} \right)^{np} \tag{3.3}$$

$$Q = Q_o \left(\frac{V}{V_o} \right)^{nq} \tag{3.4}$$

The parameters of this model are np, nq, and the values of the active and reactive power, P_o and Q_o, at the initial conditions. Common values for the exponents of the model [Taylor, 1994], [Le Dous, 1999], for different load components are included in Table 3.1.

Load Component	np	nq
Air Conditioner	0.50	2.50
Resistance Space Heater	2.00	0.00
Fluorescent Lighting	1.00	3.00
Pumps, fans other motors	0.08	1.60
Large industrial motors	0.05	0.50
Small industrial motors	0.10	0.60

Table 3.1: Common values for the exponents np and nq, for different load components.

For the special case, where np or nq are equal to 0, 1 and 2, the load model will represent a constant power, constant current or constant impedance model respectively.

Frequency Load Model

The models presented above can also include frequency dependency, by multiplying the equations by the factor of the form (3.5):

$$[1 + A(f - f_o)] \tag{3.5}$$

f_o and f are the rated frequency and the frequency of the bus voltage, and the parameter A represents the frequency sensitivity of the model.

Induction Load Model

A simplified induction motor model can be obtained from the scheme in Figure 3.1.
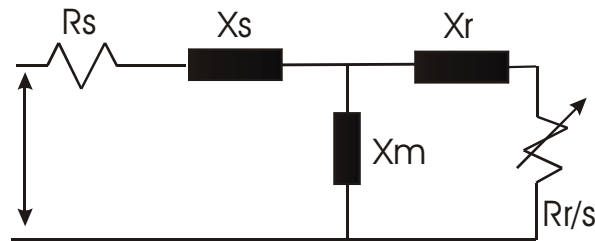
Figure 3.1: Equivalent scheme of a steady-state induction motor.

Rs, Rr, Xs and Xr are the stator and rotor resistances and reactances respectively. Xm is the magnetizing reactance, and s is the motor slip. The stator flux dynamics are normally neglected in stability analysis, and the rotor flux in long-term analysis. Figure 3.2 shows the transient state equivalent circuit, where the induction motor is modeled by a transient emf E' behind a transient impedance X' [Taylor, 1994].
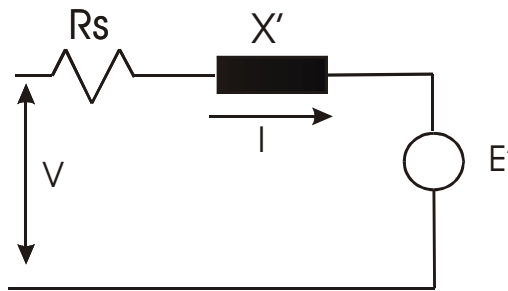
Figure 3.2: Equivalent scheme of a transient-state induction motor.

3.3.2 Dynamic Load Models

When the traditional static load models are not sufficient to represent the behavior of the load, the alternative dynamic load models are necessary. The parameters of these load models can be determined either by using a measurement-based approach, by carrying field measurements and observing the load response as a result of alterations in the system, or by using a component-based approach; first by identifying individual load characteristics and then by aggregating them in one single load.

The literature for dynamic load models is quite large depending on the results from different field measurements and their purposes [Lin, et al., 1993], [Ju et al., 1996], [Lian et al., 1998], [Karlsson, 1985]. The main interest of this thesis is related to exponential dynamic load models, and more specifically to [Karlsson and Hill, 1994].

3.4   Exponential Dynamic Load Model

Due to the large amount of electrical heating loads in Sweden and its critical effect on voltage stability [Karlsson and Hill, 1994] have proposed a load model with exponential recovery. The model is presented below, as a set of non-linear equations, where real (active) and reactive power have a non-linear dependency on voltage.

$$T_p \frac{dP_r}{dt} + P_r = P_o \left(\frac{U}{U_o} \right)^{\alpha_s} - P_o \left(\frac{U}{U_o} \right)^{\alpha_t} \tag{3.6}$$

$$Pl = P_r + P_o \left(\frac{U}{U_o} \right)^{\alpha_t} \tag{3.7}$$

The U_o and P_o are the voltage and power consumption before a voltage change. P_r is the active power recovery, P_l is the total active power response, T_p is the active load recovery time constant, α_t is the transient active load-voltage dependence, and α_s is the steady state active load-voltage dependence. Similar equations are also valid for reactive power.

Figure 6.3 shows the meaning of equation (3.6) and (3.7), when an ideal voltage step is applied.
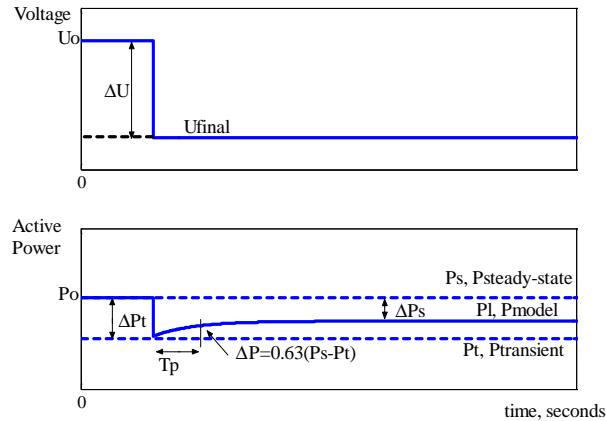
Figure 3.6: Load response under ΔU step, from the Uo-level.

The load behavior is thus characterized by a time constant, and transient and steady state load-voltage dependence parameters. *Tp* represents the time that the power recovery needs to reach 63% of its final value, α_s or the steady state load-voltage dependence quantifies how much load has been restored after the recovery; a value equal to 0 means a fully restored load, while a different value indicates partly restored load. Furthermore, the parameter α_s, steady state voltage dependency, may present negative values. The stationary level reached by the load after the recovery is then higher than the expected one, resulting in an overshooting in the load. α_t or the transient load-voltage dependence, describes how the load behaves at the disturbance moment. If α_t is equal to 0, the load behaves as a constant power, if it is equal to 1 the load behaves as a constant current, and if it is equal to 2 as constant impedance.

Chapter 4

Field Measurements

The main contribution of this chapter is a continuous recording of field measurements from normal operation. The use of normal operating data is advantageous from a technical and economical point of view. The alternative of running a test involves alterations in the normal operation at the substation and inconveniences for the customers due to repeated switching of capacitors. The need for manpower further results in very expensive tests. From a technical point of view, normal operation data will not only describe a phenomenon like load-voltage characteristics, but also the effect of all the dynamics that are acting on the system. In that way, by analyzing the load-voltage characteristics we will observe that the load response is caused by the effect of voltage variations, but also by load variations from the consumer side, i.e. spontaneous load variations. Voltage step variations are of special interest due to its relation with daily normal operation at a substation, i.e. connection and disconnection of capacitors and tap changer operations. In conclusion, the extra information obtained from normal operation helps to understand the nature of the load dynamics, and therefore to decrease uncertainty margins.

4.1   Field Measurements

Field measurements from two different experiments are presented in this chapter, called test No.1 and test No.2. The recordings included in test No.1 are part of the results obtained from a previous field test [Le Dous, 1999],

carried out during 1996 in the South East of Sweden, Blekinge. Test No.2 describes the mentioned continuous acquisition field measurement process from normal operation, including a description of the data acquisition process and the measuring equipment. The test was carried out during the period July 2001-June 2002, in the South of Sweden, in a branch of the distribution system at Tomelilla. The fact that both tests, No.1 and No.2 have been run under different periods of time and in different load areas, i.e. load composition is not the same, will make it possible to study the effect of different conditions in the results presented further in this thesis.

The provided information from the continuous recording process is large and of great interest due to its relation to normal operation. A post-processing of the data from test No.2 is presented in this chapter. It includes treatment of signals such as filtering, determination of daily, weekly, monthly and seasonal consumption load average profiles, description of daily normal operations at the substation, as well as possible deviations from normal operation.

4.2   Test No.1

Test No.1 is a part of the recorded data during a field test in the South East of Sweden [Le Dous, 1999], Blekinge, in the distribution area of Sydkraft during June 1996.

4.2.1. Load area description

The total load of the measurements area was around 115 MW, which consisted mainly of countryside and private homes and farms of different sizes. Two larger industries were fed with approximately 20 MW. Part of the test grid is a village with a load of about 30 MW. The industrial load consisted mainly of induction motors, around 13% of the average total load. Figure 4.1 shows the composition of the load in the area of measurements. The test was carried out during June 1996, a Saturday night and Sunday morning; hence a large part of the load consisted of street lighting. The outdoor temperature was about 10°-11°C and approximately 20% of the load in the area consisted of electrical heating.
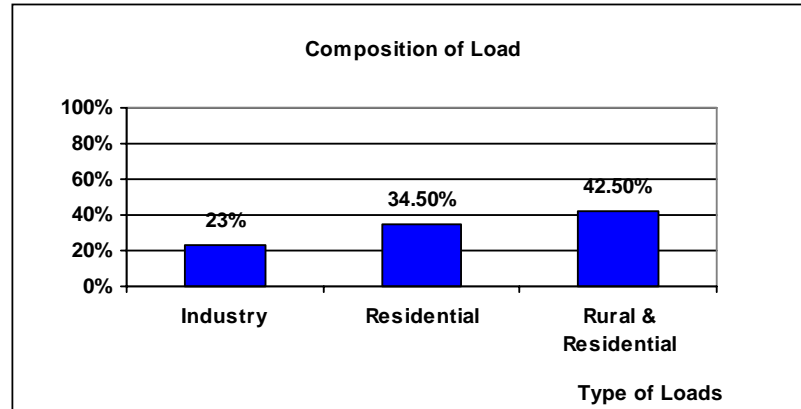
Figure 4.1: Composition of load in %, in the measurement area from test No.1.

4.2.2. Measurement description

The data originate from six different experiments in the 400-130 kV-transmission system. The voltage changes were made by simultaneous manual operation of the tap changers on the 400/130 kV transformers. By acting 1, 2 and 3 steps in both directions, the voltage changes are up to ±5%. An outline of the test system is presented in Figure 4.2. Measurements of voltage, active and reactive load on the 130 kV-side were selected for the analysis of the dynamic relation between voltage and load. The model aggregates all the loads up to the 130 kV-level.

In the original experiment, an extra test consisting of switching off a 90 MVar shunt capacitor bank connected to the 130 kV-bus was realized. This operation resulted in an instantaneous voltage step. The data resulting from this last test has not been used in this thesis.
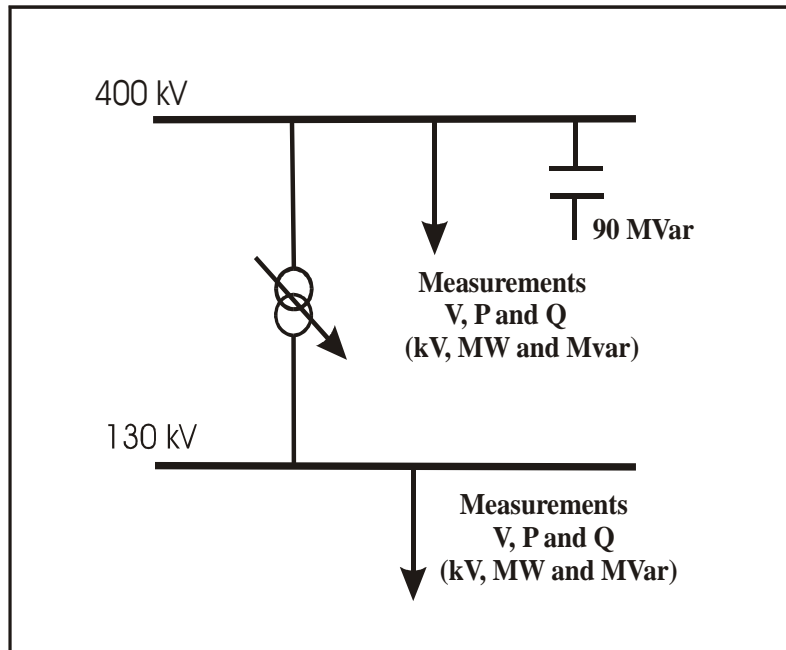
Figure 4.2: Simplified outline of the test system No.1.

4.2.3. Voltage signals

During test No.1 voltage variations because of ideal voltage steps have been recorded. The test has been performed as shown in Figure 4.3. By the action of 1, 2 and 3 taps in both directions and taking into account that the tap size is equal to 1.67%, the resulting variations are in the orders of ± 1.7%, ± 3.4% and ± 5.0%. Notice that the steps that require the action of more than 1 tap in the same direction are not completely ideal, since there is a short time-delay between each tap changer action. Figure 4.4 shows the mentioned voltage variations, where a), b), c), d), e) and f) correspond to – 1.7%, +1.7%, -3.4%, +3.4%, -5% and +5% respectively.
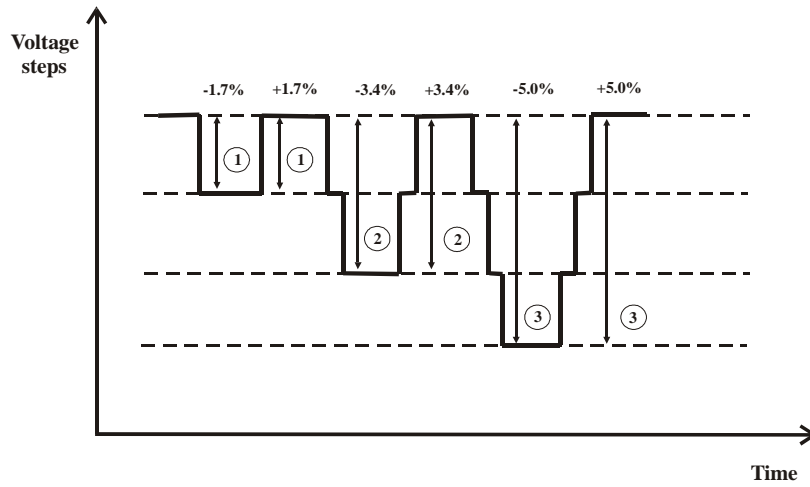
Figure 4.3: Implemented voltage steps.
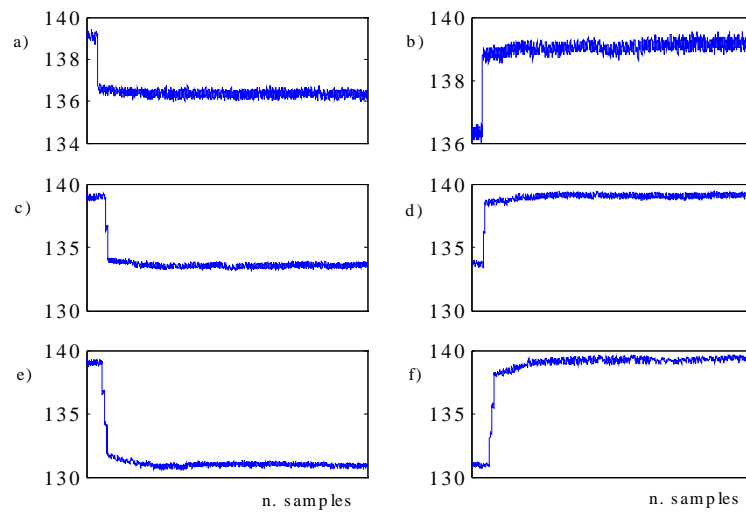
Figure 4.4: Measured voltage variations corresponding to a) –1.7%, b) +1.7%, c) -3.4%, d) +3.4%, e) -5% and f) +5%.

4.3   Test No.2

Test No.2 deals with field measurements resulting from a continuous acquisition of data from normal operation.

The concept of running new measurements arises in view of the fact that a continuous acquisition of data from normal operation, will not only track daily, weekly and seasonal variations in load, but also will catch large deviations from normal operating ranges. The continuous recording process brings up large amounts of information related to both, the daily operation, but also to the nature of the load dynamics affecting the system at every instant. The analysis of this data then will make it possible to study daily normal operation activities, but it will also contribute to a better understanding of the load behavior, which is necessary for obtaining a more accurate load representation.

4.3.1. Load area description

The measurements have been carried out in a branch of the distribution system in the South of Sweden, at Tomelilla, during the time July 2001-June 2002. Since the weather conditions differ during the measurements, the outdoor temperature is varying and therefore updated information has been necessary. Based on data from the Danish Meteorological Institute [Meteorol., 2002] two places have been selected for reading weekly and monthly temperatures, Københavns Lufthavn, Copenhagen Airport, and Dueodde, which is situated on Bornholm, the Danish island southeast of Ystad.

Figure 4.5 shows a map of the South of Sweden. Malmö is located on the West part as a reference, and Tomelilla is placed in the Southeast part of the country. In Appendix I the recorded temperatures during the test are documented.

Figure 4.5: Map of the county Skåne (Scania) in the south part of Sweden.

A simplified scheme of the test area is shown in Figure 4.6. It includes the distribution system from the 130 kV-level and downward. At the 130 kV bus, two three windings 100/100/40MVA, 130/50/20 kV tap changing transformers are connected in parallel. They are both operating during winter due to the increase in power demand, while on summer only one of them is active. On the 130 kV bus bar, two manually controlled capacitor banks of 20 and 40 MVar respectively are connected. They make reactive compensation from 20 to 60 MVar possible. The connection and disconnection of the capacitor is controlled from the operation center in Malmö twice a day, morning and evening. However, and based on the recorded data, it will be shown further in this thesis that this switching

operation is quite irregular in typical daily operations. The tap changers, which are controlling the voltage at the 20 kV-level, are placed on the 130 kV windings. The minimum tap size of the tap changers at Tomelilla is equal to 1.67 % of the voltage level.
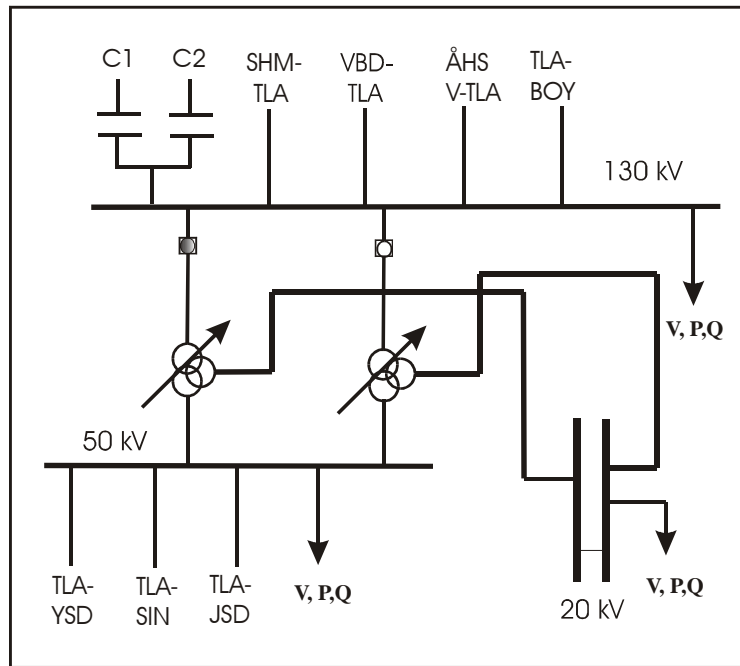
Figure 4.6: Simplified test system at Tomelilla. Measurements of voltage, active and reactive power, are expressed in kV, MW and MVar respectively.

A load of about 62 MW is connected to the 20 kV side of the transformers. A large percent of the load corresponds to residential and rural type, around 53%. This residential load includes mainly private houses, block of flats and public service buildings. On the other hand, the rural type aggregates the demand of the countryside, i.e. farms of different sizes with own production, such as corn, milk and meat production. The residential and rural load mainly corresponds to electric heating, radiators and boilers, as well as some heat pumps and electric/oil combined heating. A large industrial customer, around 15 MW, and other minor industries are directly

fed from the 20 kV level; their load is primarily constituted of induction motors and electric heating.

It has to be taken into account that the load composition will depend not only on the type -- residential, rural, commercial and industrial -- but also on weather conditions and variations in load demand during the measurements. As an example, the effect of electric heating will be larger during cold periods and therefore in wintertime. During the summer time, the heating demand will increase and consequently the electric heating effect in the load, but, and due to air conditioner actions, the percent of induction motors in the total load may increase. Figure 4.7 shows the composition of the load at the 20 kV-level. It is classified in residential, rural, industrial and commercial types. More details about the composition of the load are shown in Appendix I.
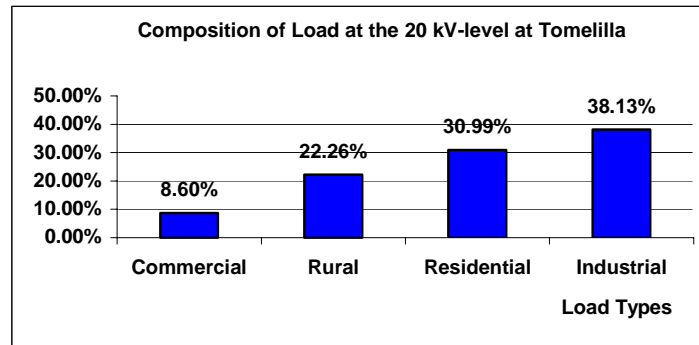
Figure 4.7: Composition of load at the 20 kV-level at Tomelilla.

The 50 kV side of the transformers is connected to a 50/20 kV substation at Järrestad. Besides, the 50 kV bus feeds mainly secondary distributors, i.e. companies supplying power to the cities Ystad and Simrishamn. Part of the load on the 50 kV bus emanates from a converter station for the railway. Further analysis at this level is not included in this study.

4.3.2. Measurement description

The measurement equipment is a Macintosh computer with 4 GBytes hard disk capacity, which allocates an analog input card, National Instruments

MIO16, and software for the configuration and activation of the functions of the card (LABVIEW). Thirteen different channels have been used during the acquisition, see Table 4.1.

TOMELILLA MEASUREMENTS						
CH	OBJECT	SIGNAL	MEASURE VALUE	OUT [V]	VOLTAGE RATIO	CONVERSION FACTORS
0	T1/T2 20 kV	U	0-22 V	0-5	22/0.11	0.012695 kV/bit
1	T1/T2 50 kV	U	0-55 V	0-5	55/0.11	0.03222 kV/bit
2	TLA-BOY	U	0-137.5 V	0-5	132/0.11	0.080566 kV/bit
3	ÅHS V-TLA	U	0-137.5 V	0-5	132/0.11	0.080566 kV/bit
4	VBD-TLA	U	0-137.5 V	0-5	132/0.11	0.080566 kV/bit
5	T1 20 kV	P	0-60 MW	0-5	22/0.11	0.0292 MW/bit
6	T1 20 kV	Q	-30-0-30 MVar	0-5	22/0.11	0.0292MVar/bit-30 MVar
7	T2 20 kV	P	0-60 MW	0-5	22/0.11	0.0292 MW/bit
8	T2 20 kV	Q	-30-0-30 MVar	0-5	22/0.11	0.0292MVar/bit-30 MVar
9	T1 50 kV	P	0-130 MW	0-5	55/0.11	0.063476 MW/bit
10	T1 50 kV	Q	-70-0-70 MVar	0-5	55/0.11	0.068359MVar/bit-70 MVar
11	T2 50 kV	P	0-130 MW	0-5	55/0.11	0.063476 MW/bit
12	T2 50 kV	Q	-70-0-70 MVar	0-5	55/0.11	0.068359MVar/bit-70 MVar

Table 4.1: Characteristics of the signals chosen for the acquisition, and conversion factors between the substation and the analog input card.

Note that four different signals are necessary for measuring active and reactive load on the 50 kV and 20 kV sides of the three winding transformers. During winter both transformers will be connected, and the active and reactive load consumption will be the sum of the recordings at T1 and T2. During the summer one of the transformers will be disconnected, so two of the signals will be zero. The data is sampled with a frequency of 3 Hz, and it is stored continuously in files of 12 hours duration, labelled with date and time. The program includes a real time monitoring of the size of the files and the recorded values in the substation expressed in binary code. Different transformation factors are necessary to convert directly, on real time, from binary code to real numbers (see Table 4.1). Since the aim is to analyze the load-voltage characteristic in a time frame of about 10 seconds to 10 minutes, the choice of the proper sampling frequency is crucial for the acquisition of significant information during the test. The chosen frequency of 3 Hz is sufficiently fast to capture the transient dynamics of the load. Spontaneous variations due to load switching operations from the customer side are also captured.

4.3.3 Measurement results

The measurements presented in the thesis correspond to recorded voltage, active and reactive load at 130 kV, 20 kV and 50 kV under the period July 2001 to June 2002. Due to the length of the test and to technical problems in the hardware, some periods of time are missing, however the acquired data fulfils the requirements of this project. The available data from the recording process is presented in Figure 4.8.

Figure 4.8: The available data from the recording process.

4.4   Analysis of Normal Operation Data

The measurements resulting from test No.2 provide a large amount of information, which is especially advantageous since it originates from continuous recording from normal operation. An off-line processing of the data will make the most of this information, and will evidence the importance of running these measurements instead of running shorter tests, which involve alterations in the normal operation at the substation. The data is relevant from the technical point of view, its analysis will make it possible to describe typical operations at the substation such as, switching of capacitors related to reactive compensation actions, voltage regulation due to tap changer operations, high and low voltage warning situations, but also to study the load-temperature characteristic, and to obtain monthly, weekly and daily load consumption profiles. Moreover, the data contains repeated voltage step variations, which, as mentioned earlier in this thesis result in an exponential recovery of the load, and consequently they are of great interest for analyzing the load-voltage characteristic in a time frame of

10 seconds to 10 minutes. At last, a proper filtering of the data will eliminate possible effects of high frequency noise during the acquisition.

Due to the large amount of information and results, only a reduced part is presented in this chapter. Further information can be found in [Romero1, 2001], [Romero2, 2001]. Different aspects are presented in the following pages:

- Voltage, active and reactive load at 20 and 50 kV;

- Load consumption profiles;

- Typical daily operations;

- Analysis of the load-temperature characteristic;

- Voltage step variations.

4.4.1 Measured voltage and power

Figures 4.9 and 4.10 show the recorded voltage, active and reactive load response at the 20 and 50 kV-level during the Thursday 23 August 2001. In Figure 4.9, it is observed that during the first hours in the morning until around 6:00 a.m, the active load demand remains constant and at a low level. During the night there is hardly consumption at residential areas, only a small percent corresponds to electric heating in winter, and to air conditioner in summer. A larger percent of the consumption during these hours corresponds to street lighting and to some industrial processes, which are active during the night.

Between 6:00 and 8:00 a.m, the daily activities in residential areas start. Notice that the data corresponds to a weekday, and therefore, it is expected not only an increase because of pure domestic use but also, because of offices and business activities, and at industrial areas, because of connection of some industrial processes. The load consumption increases around a 50 % between those hours and it reaches its peak consumption at around 12:00 p.m. The load consumption during the time frame between 8:00 a.m and 4:00 to 5:00 p.m is mainly related to commercial and industrial activities,

and the load during those hours remains at a high level. From around 5:00 p.m to 10:00 p.m most of the consumption is due to pure domestic use and industrial processes, since the commercial schedule is finished. After 10:00 p.m, the demand newly varies, to a low value due to disconnection of industrial processes and the decrease of activities at residential area.
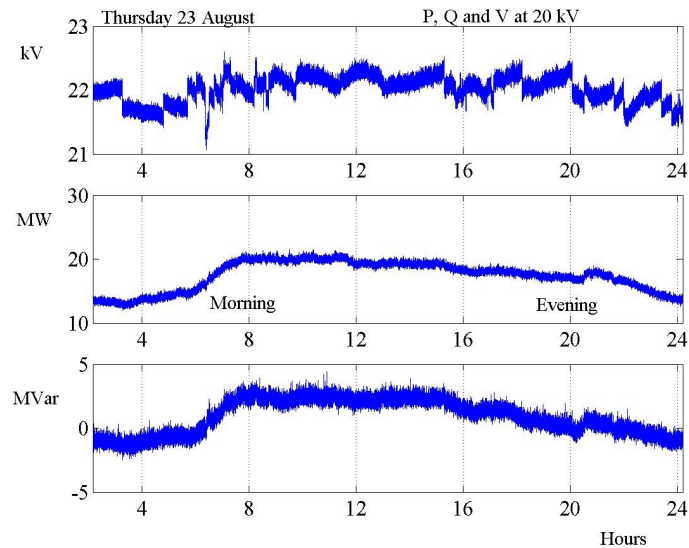
Figure 4.9: Voltage, active and reactive load at 20 kV at Tomelilla, on Thursday 23/08/01.

In relation to the reactive load consumption, when the network is heavily loaded during the morning or during peak loads, the reactive consumption of the lines increases proportional with the square of the current, and therefore reactive compensation is necessary to improve the power transfer capability and the voltage stability. Operations of switching capacitors are scheduled to be done manually, twice a day, morning and evening, at the operation center at Malmö. However, the scheduled time for the operations is altered very often during the daily operations.

By checking the reactive load profile in Figure 4.9, at around 6:00 a.m, when the active load demand starts to increase a capacitor connection is done in order to compensate the reactive consumption of the lines and

transformers. In the evening, at around 6:00 p.m to 7:00 p.m, the capacitors are disconnected.

Notice that in figure 4.9, at 20 kV, at around 8:00 p.m there is an increase in the active demand, probably due to the connection of an industrial load. At the same time, and at non-scheduled time, a new capacitor connection is realized due to the requirements at the substation.

The description above for the measured voltage and power in the 20 kV-level can be also applied to the 50 kV-level. Figure 4.10 shows the recorded voltage, active and reactive load response at 50 kV-level.
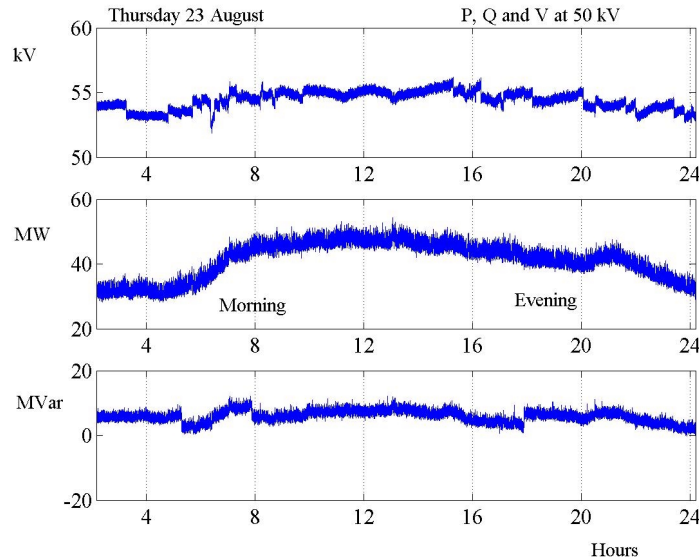
Figure 4.10: Voltage, active and reactive load at 50 at Tomelilla, on Thursday August 23, 2001.

After a general description of the active and reactive load behavior during 24 hours, it is interesting to compare if there is any difference, and in that case, which are the differences in load profile during a weekday and a weekend-day, and which are the peak hours in load demand for both cases. Figure 4.11 shows the voltage, active and reactive load at 20 kV during the weekend 13-14-15 July, (starting on Friday 13 in the evening).
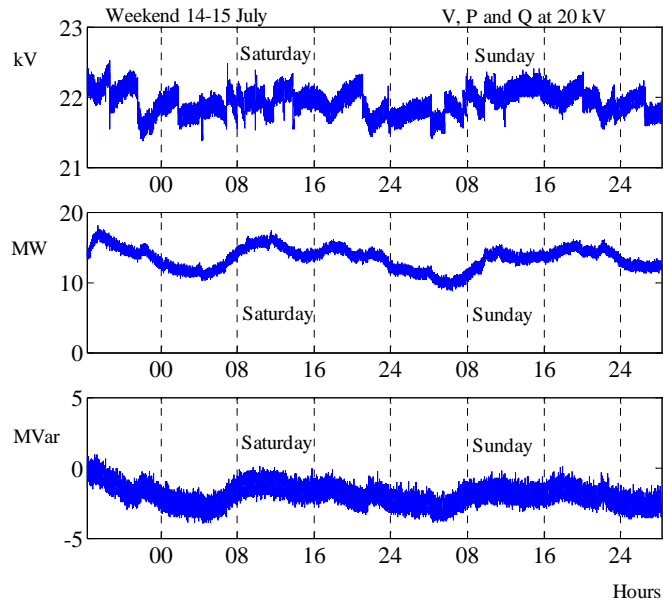
Figure 4.11: Voltage, active and reactive load at 20 kV during the weekend 14-15 July.

The main difference between a week-day and a weekend day load consumption is that the first one presents a load profile more homogeneous since a big percent of the consumption corresponds to industrial and commercial operations, i.e. the load demand increases when the working time starts, it reaches a maximum at around 12:00 p.m, and it starts to decrease when the working hours are over. On the other hand, the load profile during Saturdays and Sundays is more irregular, and the load consumption is mainly due to domestic use, and some commercial operations during the Saturday morning. The load profile follows domestic habits and the increasing slope during the morning, at around 8:00 a.m is softer than during a weekday. The load demand during a weekend-day remains on a high level until later hours at night probably due to different activities during holidays. However, and based on the recorded information the average load consumption seems to be higher during a week-day than during a weekend-day, but the peak load values are higher on weekend time rather than during the rest of the week.

The same conclusions can be applied to 50 kV. Figure 4.12 shows the voltage, active power and reactive power responses at 50 kV during the weekend of 14-15 July. The results show that the active load consumption at 50 kV is slightly higher than at 20 kV. The active load profile during a week-day behaves in the same way as explained above for 20 kV, i.e. the load demand starts to increase at around 8:00 a.m, starting time for business and commercial activities, it reaches it maximum, peak load, at around 12:00 p.m, and remains constant until around 8:00 p.m, where it decreases to a low value. The load demand during a weekend-day presents different peak load hours, and its load profile is more irregular, mainly due to its relation to domestic activities. The average load consumption seems to be higher during a weekday than during a weekend-day, but on the other hand, the peak loads are higher on weekend time.
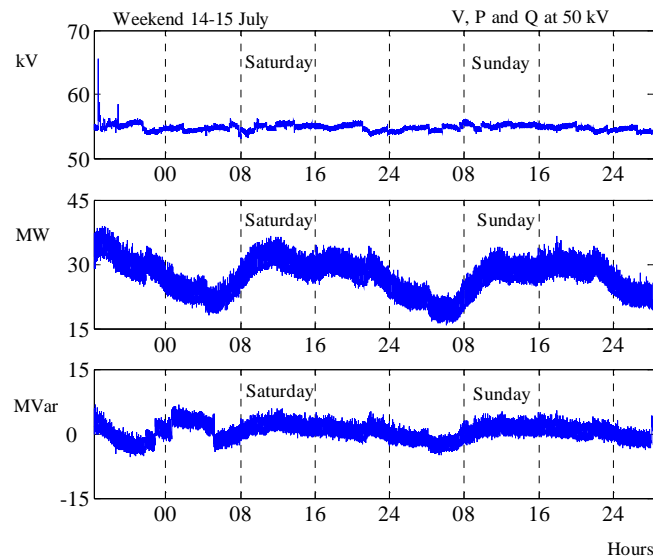
Figure 4.12: Voltage, active and reactive load at 50 kV during the weekend 14-15 July.

It was mentioned in Section 4.3.1 that the composition of the load will not only depend on the load type, -- residential, rural, commercial and industrial, -- but also on the weather conditions. The changes in temperature during a year affect the distribution in the load composition, and the average

load demand. Figure 4.13 shows a comparison between the active and reactive load consumption at 20 kV during a summer and a winter day, Monday 13 August 2001 and Monday 18 February 2002. The outdoor temperature was about 9.5 to 27.5°C, and -5.7 to 3.8°C respectively.
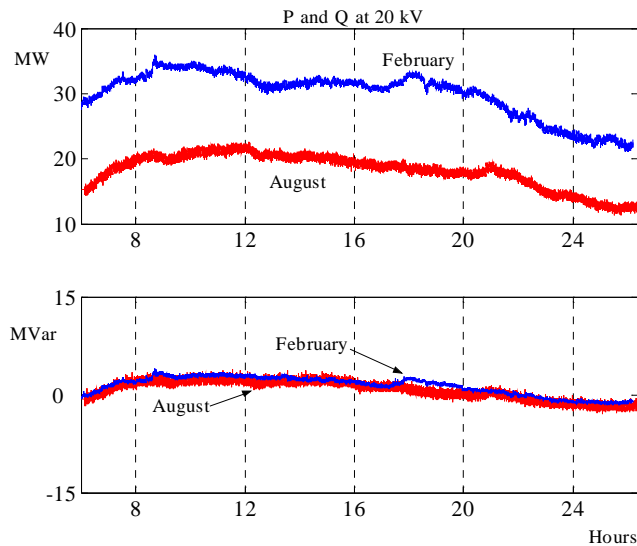
Figure 4.13: Active and reactive load consumption at 20 kV, during Monday 13.

In Sweden, in general, the average load demand is higher during wintertime. Checking Figure 4.13, the average load at 20 kV during Monday 18 February is approximately 70 % higher than during Monday 13 August. In the area of the measurements, South of Sweden, and during the winter the temperatures have moved in the range of -12.3 to 11.3°C. Due to those temperatures, electric heating in the houses is necessary. A large percent of the load during this period of time consists of electric heating, either radiators or boilers, and heat pumps. During the summer the temperatures have varied in the range from 5.1 to 27.5°C, and owing to the mild conditions heating is not necessary, and air conditioners are hardly used. Moreover, the consumption can be considerably lower during July and August since they are holiday months and some commercial and industrial activities are stopped until late August. At Tomelilla, the described two three windings 130/50/20 kV tap changer transformers connected in parallel

(see Figure 4.7), will be both operating during winter and high power demand situations, while during the summer only one of them, T1, will be in service. Figure 4.14 shows a comparison between the active and reactive load consumption at 50 kV during a summer and a winter day, Monday 13 August 2001 and Monday 18 February 2002
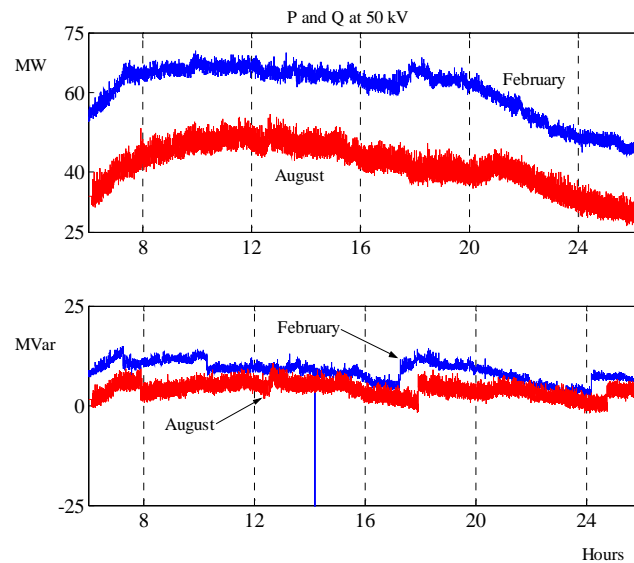
Figure 4.14: Active and reactive load consumption at 50 kV, during Monday 13 and February 18 February 2002.

4.4.2. Daily operations

Normal operating data are of great value for understanding typical daily operations at a substation, but also to detect unusual situations that deviate from normal operation and may drive the system to severe conditions. At the operation centers the information from normal operation is continuously updated. This information is normally stored in large databases. With help of the reported log-files at the Malmö operation center and by checking the recorded data it is possible to determine if there is any pattern in the

schedule of the realization of the operations at Tomelilla, and to obtain detailed information of how the operations are performed.

Figure 4.15 shows the measured voltage at 20 kV during Monday 13 August. As an example two voltage regulation operations are pointed at the figure. The regulation is performed by the action of tap changers and, in this case, it has taken around one minute to perform it.
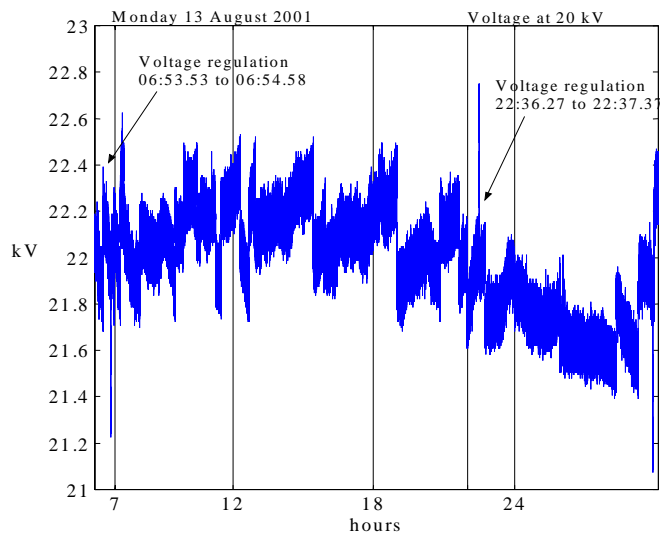
Figure 4.15: Voltage regulation due to action of tap changers during Monday 13 August.

In Figure 4.16 one of these operations is described. At 22.36.27, the tap changers start regulating the voltage to a higher value, since the active load demand is decreasing. The action is done by two upward tap operations. Since the tap changers are working on a discrete-tap mode, each tap operation corresponds to a step variation in the order of 1.67%. After the second tap connection, the newly reached voltage is too high and therefore it needs to be regulated. A warning signal is detected at the operation center in Malmö, and a manual disconnection of capacitors is performed to finally stabilize the voltage.
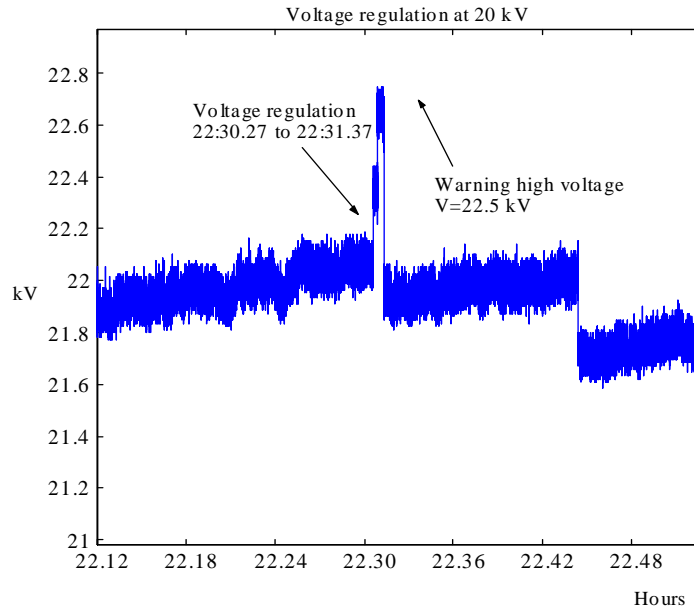
Figure 4.16: Voltage regulation and disconnection of capacitors due to high voltage conditions.

Figure 4.17 shows the measured voltage at two different places at 130 kV during Friday 17 August. At 07.09.26 hours a capacitor connection is realized to compensate the increasing load demand in the first hours of the day (check figure). In the evening the opposite operation is performed. The voltage variation due to switching capacitors is in the order of ±3 %.

During the day different critical situations are detected at the operation center. The figure shows how at 10:00 a.m the voltage has reached a very high value, a warning signal is received at the operation center, and voltage regulation by the action of tap changers is started until an acceptable value is reached again.
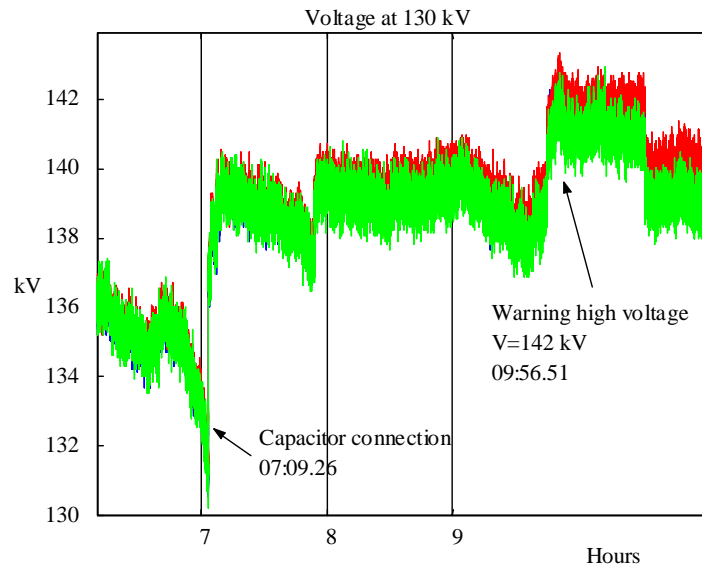
Figure 4.17: Capacitor connection and voltage regulation due to high voltage conditions at 130 kV.

In spite of the fact that the switching capacitor operation is usually ordered twice a day, morning and evening, and since it is an operation that requires manpower, there are often many irregularities in the scheduled hours for its realization. As an example Figure 4.18 shows voltage, active and reactive load at 20 kV, during the first weekend of February, 2 and 3 of February. During these two days it is possible to check the differences in time for connecting and disconnecting capacitors. C1 and C2 correspond to two different connections in the morning, while D1 and D2 corresponds to disconnections in the evening.

Weekend1 2/02/02 to 3/020/02

- C1 Connection of capacitor at 130 kV. Saturday 02/02/02, time 09.50.00

- D1 Disconnection of capacitor at 130 kV. Sunday 03/02/02, time 03.11.48

- C2 Connection of capacitor at 130 kV. Sunday 03/02/02, time 09.11.47

- D2 Disconnection of capacitor at 130 kV. Sunday 03/02/02, time 23.11.47
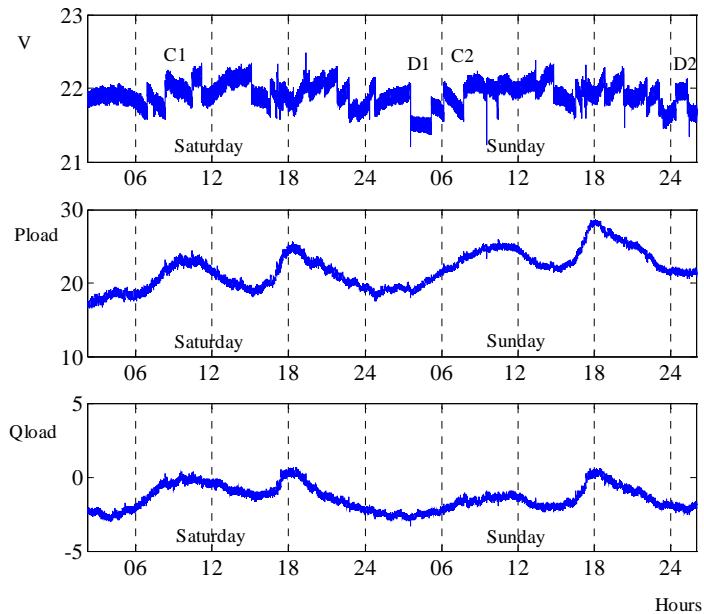
Figure 4.18: Voltage, active and reactive load at 20 kV during Saturday 2 and Sunday 3 of February. Typical daily operations at 20 kV.

4.4.3. Voltage step variations

The data described throughout this Section 4.4 represent valuable information for studying the load-voltage characteristic in a time frame of about 10 seconds to 10 minutes.

During the recording time repeated voltage step variations due to switching capacitor and tap changers operations have occurred. The minimum voltage variation at Tomelilla because of those operations corresponds to the tap

size in the tap changers and is equal to 1.67 %, while the variations due to switching capacitors are in the order of ±3% or larger. The effect of a voltage step variation will result, as mentioned in earlier chapters, in a pure exponential recovery of the load.

More aspects related to voltage variations and their detection, will be discussed further in Chapter 6.

Chapter 5

Determination of Parameters in Dynamic Load Models

5.1   Introduction

Chapter 5 presents an improved method for the estimation of parameters in dynamic load models. Instead of curve fitting and manual inspection technique a more accurate procedure has been used. The method avoids possible errors by manual inspection, gives an accurate solution and reduces the time for the parameter determination.

The method will make it possible the study of the time-varying active and reactive load parameters. The variation in time constants and transient, as well as steady state voltage dependency, give an idea of how fast the recovery of load is after a change in voltage, the composition of the load, and how well the load fits in the proposed model.

5.2   Linearisation

The described dynamic load model introduced in Chapter 3, is presented as a set of non-linear equations, equations (5.1) and (5.2), where real (active) and reactive power have a non-linear dependency on voltage. The nonlinearities are necessary to reproduce variations in power for large

changes in voltage, even though the changes are very rare. Furthermore, the non-linear representation complicates the identification procedure since it is not possible to apply the general identification methods because they are only valid for linear systems. Linearising the system, makes the model valid only for small variations, but simplifies parameter identification drastically.

$$T_p \frac{dP_r}{dt} + P_r = Po\left(\frac{U}{Uo}\right)^{\alpha_s} - Po\left(\frac{U}{Uo}\right)^{\alpha_t} \tag{5.1}$$

$$Pl = P_r + Po\left(\frac{U}{Uo}\right)^{\alpha_t} \tag{5.2}$$

Considering the model described in (5.1) and (5.2), the first step is to linearise around an operating point (U^*). Small deviations around the nominal point are denoted by Δ, and by using Taylor series expansion and removing all the constant terms, the model is given by:

$$\Delta P_l = \Delta P_r + \alpha_t \cdot P_0 \cdot \left(\frac{U^*}{U_0}\right)^{\alpha_t - 1} \cdot \frac{\Delta U}{U_0}$$

$$T_p \frac{\Delta P_r}{dt} = \alpha_s \cdot P_0 \cdot \left(\frac{U^*}{U_0}\right)^{\alpha_s - 1} \cdot \frac{\Delta U}{U_0} - \alpha_t \cdot P_0 \cdot \left(\frac{U^*}{U_0}\right)^{\alpha_t - 1} \cdot \frac{\Delta U}{U_0} - \Delta P_r \tag{5.3}$$

By introducing new quantities, A, B and u, the identification process is simplified. The state space representation of the model is given by (5.4) and (5.5):

$$A = \alpha_t \cdot \left(\frac{U^*}{U_0}\right)^{\alpha_t - 1} \qquad B = \alpha_s \cdot \left(\frac{U^*}{U_0}\right)^{\alpha_s - 1} \qquad u = \frac{\Delta U}{U_0}$$

$$\Delta P_l = \Delta P_r + A \cdot P_0 \cdot u \tag{5.4}$$

$$T_p \cdot \frac{\Delta P_r}{dt} = B \cdot P_0 \cdot u - A \cdot P_0 \cdot u - \Delta P_r \tag{5.5}$$

By applying Laplace- transformation and introducing $T_1 = T_p \cdot A$, the load variation ΔP_l is given by (5.7):

$$\Delta P_l = \frac{B - A}{1 + s \cdot T_p} \cdot P_0 \cdot u + A \cdot P_0 \cdot u$$

$$\frac{\Delta P_l}{P_0} = \frac{B + s \cdot A \cdot T_p}{1 + s \cdot T_p} \cdot \frac{\Delta U}{U_0}$$

(5.6)

$$\boxed{\frac{\Delta P_l}{P_0} = \frac{B + s \cdot T_1}{1 + s \cdot T_p} \cdot \frac{\Delta U}{U_0}}$$

(5.7)

Equation (5.7) represents the load response when a voltage change is occurring in the system. It is characterized by three parameters, steady state voltage dependency B, transient voltage dependency A, and time constant T_p. ΔP_l and ΔU represent deviations from the steady state values Po and Vo. ΔP_l represents the difference between the initial value Po, and the last value P after a voltage variation. ΔU is the difference between the initial Uo and the voltage U after a variation. By checking equation (5.7), when s goes to zero the value for the steady state parameter B is obtained. While when s goes to ∞ we will obtained ($T1/Tp$), i.e. the transient parameter A.

Figure 5.1 shows a comparison between the non-linear and linear model, when a voltage step of -1.8% from the nominal point (130 kV) has been applied. Both models capture the dynamic response, and agree well with each other. The difference between the measured and simulated data corresponds to spontaneous load changes. They are thus not related to voltage variations, and to the load exponential response, which is the matter of this study. It can be thus concluded that the linearised model is sufficiently accurate for our identification purposes.
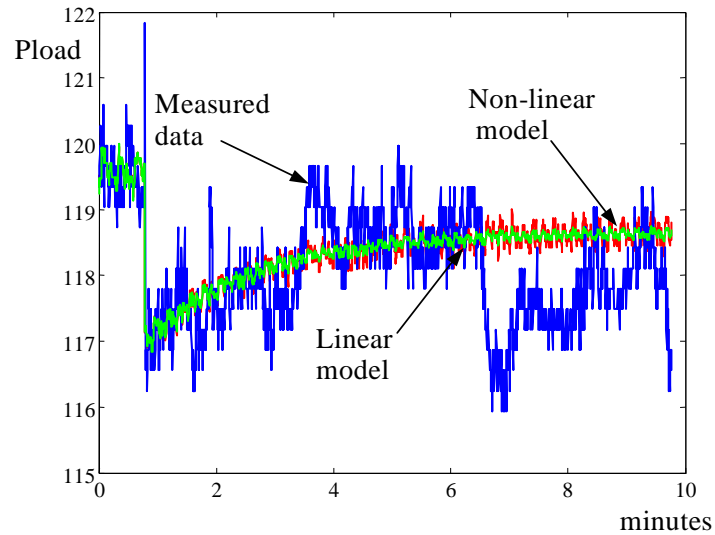
Figure 5.1: Measured and simulated load response (linear and non-linear models), for ΔV of -1.8% at the 130 kV level.

5.3   Optimization

An automatic determination of parameters is meant to be used on continuously recorded data. The result of that determination will give information about the time variations of the parameters. The aim is then to use the described linearised model (5.7) and to identify its parameters with measured data.

The algorithm uses N samples of input signals (*voltage, $V(t_k)$*) and output signals (*power, $P(t_k)$*), $k=1...N$, and the objective is to obtain estimates of the parameter vector $\theta=(T_p, \alpha_s, \alpha_t)$ to minimize the difference between the measured and the simulated data (as a quadratic criterion). The measured data corresponds to the load response when a voltage variation has occurred on the system, while the model described by (5.7) represents the variation of the load from its steady state value *(ΔP)* due to the voltage variation; i.e. the

total simulated load response will be equal to its initial value *Po*, plus that variation *(ΔP)*. The objective function to be minimized using a quadratic least square criterion is:

$$F\ (\boldsymbol{\theta}) = \sum_{k=1}^{N} (Psimulated(t_k,\boldsymbol{\theta}) - Pmeasured(t_k,\boldsymbol{\theta}))^2 \qquad (5.8)$$

$$F_N(\boldsymbol{\theta}) = \sum_{k=1}^{N} ((Po + \Delta Pl) - Pmeasured(t_k,\boldsymbol{\theta}))^2 \qquad (5.9)$$

Where,

$$\Delta Pl = Po \cdot \frac{B + s \cdot T_1}{1 + s \cdot T_p} \cdot \frac{(\Delta U)}{Uo}$$

$$\Delta Pl = (Po - Psimulated\ (t_k,\boldsymbol{\theta}))$$

$$\Delta U = (Uo - U\ (t_k,\boldsymbol{\theta}))$$

The least squares optimization algorithm is used to minimize the function (5.9) and to obtain the initial values of the parameter vector *θ*. By using iteration for the data sequence, the final values for the linear model are calculated, and the corresponding non-linear model parameters are straightforward to determine by using equations (5.10) and (5.11):

$$B = \alpha_s \cdot \left(\frac{U^*}{U_0}\right)^{\alpha_s - 1} \qquad (5.10)$$

$$A = \alpha_t \cdot \left(\frac{U^*}{U_0}\right)^{\alpha_t - 1} \qquad (5.11)$$

By using equation $A = T_1/T_p$, it is possible to obtain the value of the time constant *Tp*. The equations above are solved by iteration. Assuming that $U^* = U_0$, the first estimates are given by:

$$\alpha_{s,0} = B \quad \alpha_{t,0} = A$$

The general expression for the following estimates is given by (5.12):

$$\alpha_{s,k+1} = \frac{B}{\left(\dfrac{U*}{U_0}\right)^{\alpha_{s,k}-1}} \quad \alpha_{t,k+1} = \frac{A}{\left(\dfrac{U*}{U_0}\right)^{\alpha_{t,k}-1}} \tag{5.12}$$

The procedure presented determines the value of the linear model parameters. By assuming that large disturbances are not affecting the system, the non-linear model parameters can be calculated from the linearised model parameters.

5.4   Robustness of the Model Simulations

Based on the field measurements corresponding to Test No.1, which is described in Chapter 4, the introduced method for estimation of parameters in dynamic load models has been tested. The simulations presented in this section represent an extension of previous studies [Le Dous, 1999], [Karlsson, 1992], [Karlsson and Hill, 1994], and they prove the robustness of the method, i.e. possible errors by manual inspection are avoided, and accurate solutions are obtained.

The data originates from six different experiments in the 400-130 kV-transmission system. The voltage changes were made by simultaneous manual operation of tap changers on the 400/130 kV transformer feeding one area with an aggregated load of 150 MW. By acting 1, 2 and 3 steps in both directions, the voltage changes are up to about ±5%. Measurements of voltage, active and reactive load on the 130 kV-side were used for analysis of the dynamic relation between voltage and load. The model aggregates all the loads up to the 130 kV-level. For six different sets of data, the identification process has been applied. Both the non-linear and the linear models have been fitted to the data. Tables 5.1 and 5.2 show the results of the identification for both, the active and reactive response respectively.

No	$\Delta V/V_0$ [%]	T_p [s]	α_t	α_s
1	-1.8	135	1.36	0.25

2	+1.9	40	1.70	-0.10
3	-3.7	61	1.31	-0.16
4	+3.7	74	1.35	-0.54
5	-5.3	70	1.65	-0.32
6	+5.4	78	1.60	-0.08

Table 5.1: Identified parameters for active response under six different voltage steps.

No	$\Delta V/V_0$ [%]	T_q [s]	β_t	β_s	Qo [Mvar]
1	-1.8	89	-181.18	7.90	-0.974
2	+1.9	256	-687.20	975.60	-0.046
3	-3.7	88	87.67	31.86	-2.850
4	+3.7	105	104.50	-148.56	0.867
5	-5.3	78	77.89	19.35	-2.840
6	+5.4	94	94.18	-49.75	1.254

Table 5.2: Identified parameters for reactive response under six different voltage steps. Normalizing factor of the reactive load *Qo*.

From the results presented in the tables, and under voltages steps in the order of ±1.8% to approximately ±5.4% from the nominal value (130 kV level) it can be concluded that:

- The active load (Table 5.1) behaves much like a resistance for fast voltage changes (transient). α_t is in the order of 1.35 to 1.7.

- The exponential recovery of the active load shows time constants of 40 to 135 seconds.

- The steady state voltage dependency parameter α_s, in some of the cases, presents a negative value. The stationary level reached by the load after the recovery is equal to (around 0) or higher than the expected one, probably due to the effect of the on load tap changer action, i.e over and undershooting.

- In general, both the active and reactive load time constants are in the same order, even though the reactive load recovery seems slightly slower. The recovery of the reactive power is mainly produced by the increase of the reactive losses due to the active recovery of the load at low voltage. The main differences in the order of the time constants is probably related to the effect of spontaneous load demand variations, and therefore unrelated to voltage variations.

The obtained values for the reactive transient (β_t) and steady state (β_s) parameters fit the proposed model, however, they deviate from the expected values probably due to the fact that the value Qo used in the normalization in equation (2) may be equal to zero because of the effect of reactive compensation. Table 5.3. shows the results obtained by normalizing the reactive dynamic load in equation (2) with So, sum of the active and reactive load just before the voltage variation, instead of by only using Qo. This problem will be discussed further in Chapter 6.

No	$\Delta V/V_0$ [%]	T_q [s]	β_t	β_s
1	-1.8	88	2.43	0.12
2	+1.9	165	2.02	-0.64
3	-3.7	88	2.08	-0.77
4	+3.7	89	2.42	-0.98
5	-5.3	78	2.22	-0.48

| 6 | +5.4 | 92 | 2.62 | -0.49 |

Table 5.3: Identified parameters for reactive response under six different voltage steps. Normalizing factor of the reactive load *So*.

- The steady state voltage dependency parameter β_s presents negative values in some of the cases probably due to the effect of tap changer actions, in the same way as it has been described above for the active load steady state parameter α_s.

- The transient voltage dependency parameter β_t is mainly related to the load composition and its percent of induction motor loads. Since the field measurements from test No.1 corresponds to approximately the same hours of the day and the same season, the composition of the load is stable, and the parameter β_t hardly varies, moving in the range of 2 to 2.6.

Figure 5.2 and 5.3 show the voltage variation, and both, the active and reactive response for two of the cases presented above.
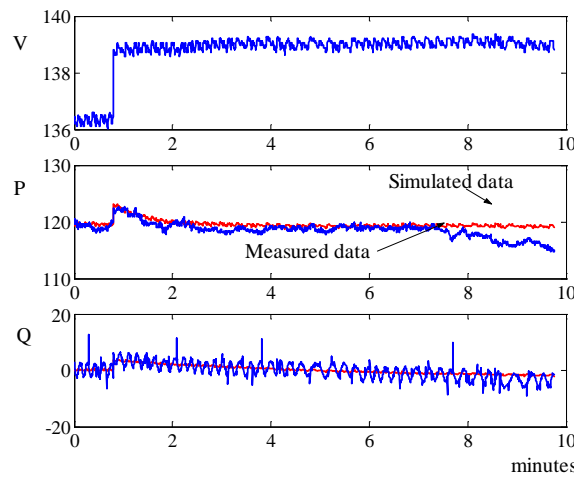
Figure 5.2: Measured and simulated load response (active and reactive), *ΔU* of +1.9% (case No.2) from the 130 kV level, during 10 minutes.
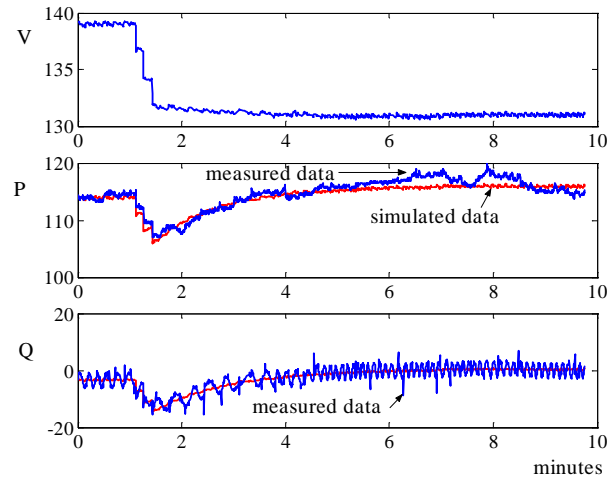
Figure 5.3: Measured and simulated load response (active and reactive), ΔU of – 5.3% (case No.5) from the 130 kV level, during 10 minutes.

5.5   Effect of Spontaneous Load Variations

The load demand is the amount of power needed by the consumers in a specific area, under normal conditions of voltage and frequency. This quantity is predicted based on detailed information from the consumption side, such as characteristics of the single loads, but also histograms, average load profiles of the area, and taking into account the transfer limits of the network. On the other hand, the amount of power measured under particular conditions of voltage and frequency is called load, and this value usually differ from the forecasted demand.

Figure 5.4 shows a simplified scheme of a distribution network. The variations in the active and reactive power load, P and Q, are due to both changes on the generation side and on the consumer side. On the generation side, the action of tap changers and the switching capacitor operations result in voltage variations, voltage steps, and thus in a load variation with exponential recovery. On the consumer side, the spontaneous connection

and disconnection of individual loads will alter the load. Since this phenomenon is unrelated to voltage changes, it will be uncorrelated with the exponential recovery of the load described by equations (5.1) and (5.2).
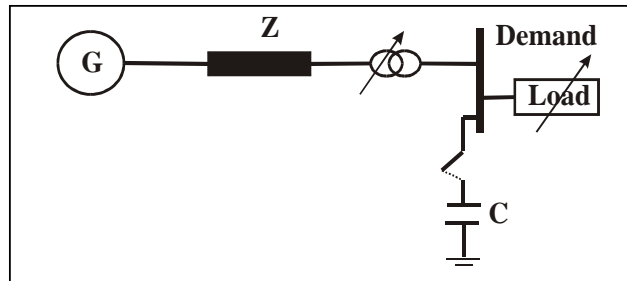
Figure 5.4: Simplified scheme of a distribution network for describing both actions, from generation and consuming side that produce load variations.

As it has been shown throughout the chapter, a voltage step gives enough information to determine the transient behavior α_t with good accuracy. On the other hand the steady state load-voltage dependency, and the time constant estimates are less accurate due to the effect of the spontaneous changes in the active load. The accuracy of those two parameters is depending on the measuring time used for the identification purpose. There is a trade-off between the minimum measuring time for the identification and the influence of spontaneous changes in the load response. If the load is strongly affected by spontaneous changes, the measuring time for capturing the effect of a voltage step should be short (trying to avoid other kind of information), but if this time is very small, there will not be enough information (sample points) for capturing the real dynamics of the system.

The active load recovery leads to a stable value approximately 10 minutes after the step has occurred. At this time the spontaneous changes still do not affect the response much. In case of the reactive power the effect of these variations does not cause any problems. The reactive load response follows the behavior of the voltage, and it is hardly affected by spontaneous changes in the load. Figure 5.5 shows a comparison between the simulated and the measured load response (P and Q), during 20 minutes. After 6.5 minutes the active load response is strongly affected by spontaneous changes. As it is shown in Figure 5.5, during the first 6.5 minutes, there is enough information to describe the transient and exponential behavior of the load.
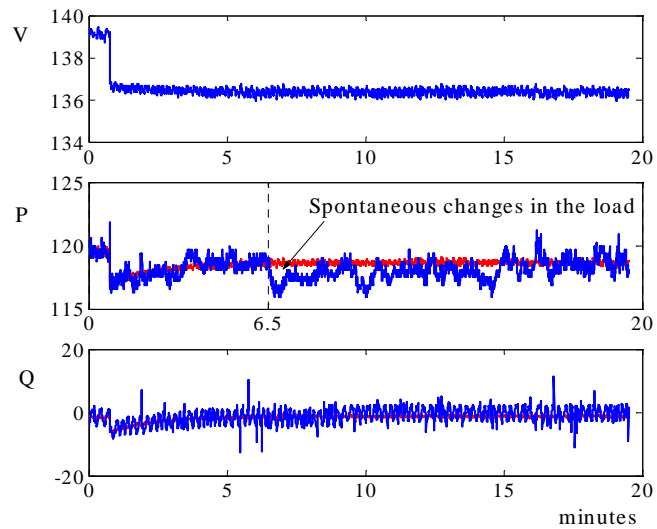
Figure 5.5: Influence of spontaneous changes in the load response. ΔU of -1.8 % (case No.1) from the 130 kV level. Simulation time of 20 minutes.

To conclude, there is a great uncertainty in determining the proper analysis window for every case of data since spontaneous load variations may occur in the system, and therefore the realization of an on-line identification of parameters on dynamic loads is more complicated. This problem will be discussed throughout the next chapter.

Chapter 6

Automatic Determination of Parameters

The desired on-line identification requires an automatic process, i.e. continuous acquisition of data, automatic detection of voltage variations, and identification of parameters. Figure 6.1 shows a simplified scheme of the process.
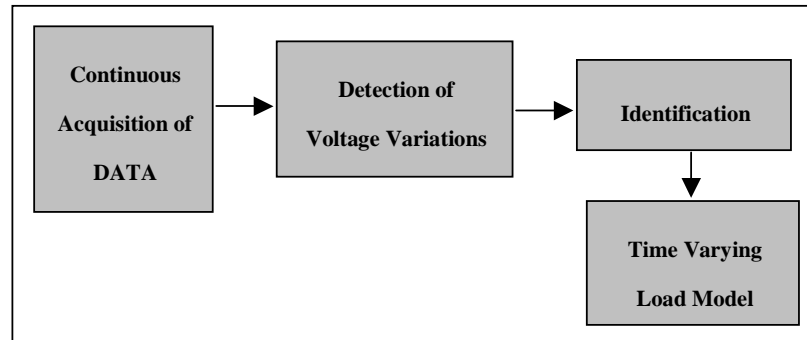
Figure 6.1: Simplified scheme of an automatic process for determination of parameter in dynamic load models.

The continuous acquisition of normal operation data will result in non-stationary load data sequences, i.e. every data case differs from the others, and different considerations will have to be taken into account for analyzing the information.

The Chapter describes the difficulties that may appear and the conditions that must be set up for carrying out the desired parameter estimation, i.e. the detection of significant voltage variations and the determination of the analysis window for every data set. In Section 6.7, the critical effect of the normalization factor in the reactive load representation has been studied, and it has been found that an inappropriate value will affect the variability of the identified reactive load parameters.

6.1   Conditions for Parameter Estimation

In order to get useful results from the identification, it is important to determine which kind of input signal, voltage variation, is of interest, and to ensure that the signal has significant excitation on the physical model under study [Bergh, 1996]. Afterward, and since the recorded data provides long sequences of information, a procedure for detecting the voltage variations must be applied. The first challenge is thus to detect when the excitation starts. At that point, the detection is stopped, and the analysis for studying the physical process and to identify the load parameters is started. Right after this procedure is finished, the detection will continue.

As mentioned in Chapter 5, the determination of the window length for the identification is not an easy task, since the data is strongly affected by the presence of spontaneous load variations. Moreover, the data must be filtered in order to reduce the noise introduced by the measuring devices or originated by the process itself during the acquisition.

6.2   Excitation

The interest of this thesis is focused on studying the load-voltage characteristics on a time scale of about 10 seconds to 10 minutes. Voltage step variations are basically the most important excitation signals in this test, since their effect will result in a pure exponential recovery of the load, as mentioned in Chapter 3. Furthermore, a step includes enough information to identify the transient behavior of the load variation, but also, and after the

step, the voltage remains constant for enough time, to make it possible to describe the recovery of the load.

During normal operation at Tomelilla, step changes in voltage are caused by switching capacitors and by tap changer operations. The minimum voltage step related to these operations corresponds to one tap change, i.e. equal to ± 1.6%, and therefore it will be interesting to study variations in the order of ± 1.6% or larger.

6.3   Detection of Voltage Variations

Since the acquisition process provides long data sets, a procedure for detecting excitation must be applied. As explained above, the detection stops when a voltage variation occurs, and the analysis of data to study the load dynamics is then started.

 The procedure is applied to the 12 hours files acquired at Tomelilla, and it reacts when a significant voltage variation is detected. The variations are detected by comparing the mean value of the last old 20 samples with the mean value of the newest 20 acquired samples. In case there is a significant change, in the order of ± 1.6% or larger, a window of 650 samples is opened. During those 650 samples and by following the same method of comparing the old samples with the newest acquired ones, it is also checked if a new variation is occurring. If this happens a new window of 650 samples is opened at that point. It is checked if the previous window is long enough to study the exponential recovery of the load. Before the detection starts, the data is low-pass filtered and resampled to 1 Hz, eliminating the effects of high frequency noise during the acquisition process. Figure 6.2 shows a flow chart describing the detection procedure.

The detection procedure has been tested with reported information from daily operations at Tomelilla, but also by comparing the results with those coming from other work on detection [Svantesson, 2002]. Figure 6.3 shows the data corresponding to voltage at the 20 kV-level during 2/02/02.
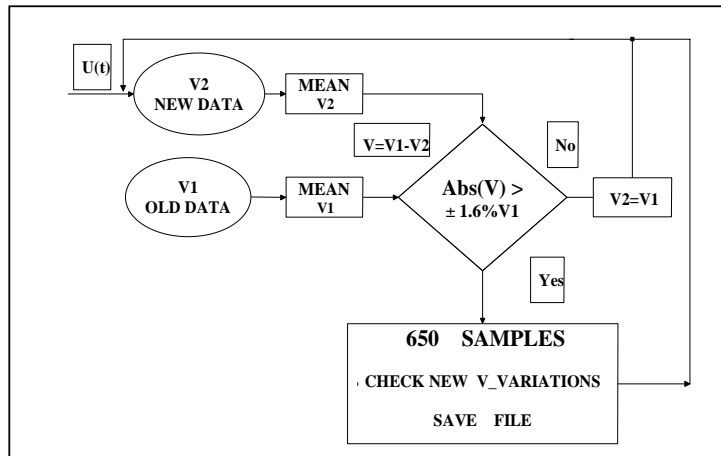
Figure 6.2: Flow chart for detection of voltage variations in the order of ± 1.6% or larger from normal operation.
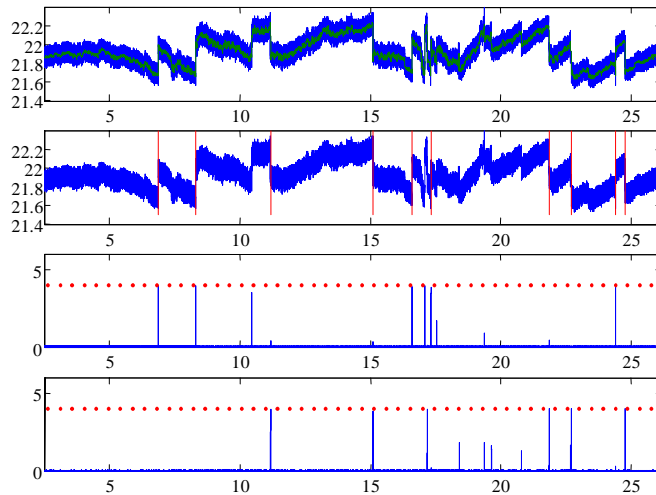
Figure 6.3: Detection of voltage steps at the 20 kV-level during Saturday 2/02/2002. The first part of the plot presents the recorded data, while the second one points at the detected steps. The third and fourth part of the figure shows the positive and negative detected steps.

6.4   Data Sequence Length

The number of samples used for the identification strongly affects the quality of the estimates, and therefore its selection is critical for the accuracy of the results. As described in Chapter 5, a large measuring time could lead to a situation much affected by possible spontaneous load variations, i.e. connection or disconnection of loads, variations due to tap changer operations, and therefore to corrupted information. On the other hand, a very short identification time will result in a sufficiently accurate value for the transient characteristic, but inadequate for calculating time constant and steady state value, because the load response will not yet have reached a stable level. Thus there is a trade-off between the minimum measuring time for the identification and the influence of spontaneous changes in the load response.

6.4.1. Data analysis

Measurements at the 20 kV-level during Saturday 14 July 2001 from test No.2 have been selected for studying the influence of the number of samples during the identification. Table 6.1 shows the results obtained by applying the voltage detection process described in section 6.2 and the identification procedure for 150, 200, 300 and 400 samples respectively.

The quality and robustness of the results for the different data sequence lengths have been checked by using curve fitting, and by calculating the residuals of the model [Ljung, 1995]. The values in bold represent the best estimates for every voltage variation, based on the mentioned tests.

No.	L	PLOAD			QLOAD		
		Saturday 14 July 2001 at Tomelilla 20 kV level
		T_p	α_t	α_s	T_q	β_t	β_s
1	150	245	2.40	-0.30	34	-7.00	-9.00
	200	**110**	**2.30**	**1.30**	312	-8.60	-5.30

	300	110	2.30	0.50	**244**	**-8.0**	**-6.00**
	400	235	2.20	0.70	422	-9.30	-0.90
2	150	9	1.00	1.20	18	-7.60	-5.90
	200	**153**	**1.30**	**0.80**	**219**	**-7.00**	**-2.50**
	300	187	1.30	0.60	520	-7.00	2.90
	400	197	1.20	0.70	604	-7.20	5.40
3	150	**87**	**1.60**	**-0.80**	**181**	**-3.50**	**-4.50**
	200	19	1.80	0.60	270	-3.30	-6.00
	300	606	0.70	1.20	599	-2.40	-14.80
4	150	40	1.30	2.20	446	-5.70	-8.00
	200	**179**	**1.40**	**2.40**	**238**	**-5.70**	**-3.20**
	300	240	1.50	2.60	148	-6.60	-3.50
	400	811	1.40	6.41	172	-6.50	-3.50

Table 6.1: Results from the identification by using 150, 200 and 300 samples respectively.

Figure 6.4 shows the detected voltage variation and its corresponding dynamic active and reactive response for case No.2.

Residuals and curve fitting tests have been applied, and the results are included in Table 6.2. Ok or Not Ok define if the result of a test is accepted and if the quality of the estimates is good enough.
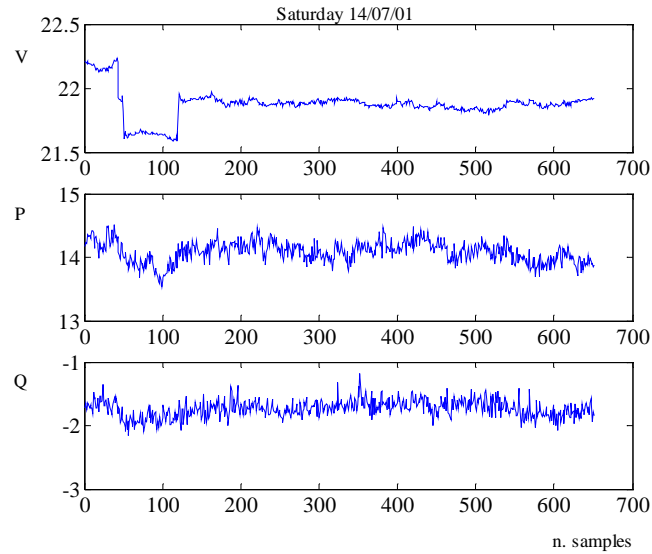
Figure 6.4: Detected voltage variation and its corresponding dynamic active and reactive response, for case No.2.

Saturday 14 July 2001 at Tomelilla				
L	**RESIDUALS**		**FITTING**	
	P	**Q**	**P**	**Q**
150	Ok	Ok	Not Ok	Not Ok
200	Ok	Ok	Ok	Ok
300	Not Ok	Ok	Ok	Ok
400	Not Ok	Ok	Not Ok	Ok

Table 6.2: Curve fitting and residuals.

Figure 6.5 shows a comparison between the simulated and the measured load during 10 minutes. The load response is strongly affected by

spontaneous variations during the first samples, i.e. disconnection of a load. At around sample no 250 the load response reaches a stable value. After 300 samples some oscillations, overshooting and undershooting due to tap changer operations may affect the accuracy of the identification. The second plot in Figure 6.5 describes the difference between the measured and simulated data. This difference corresponds to all the variations mentioned above, that are not included in the physical model describing the exponential recovery of the load.
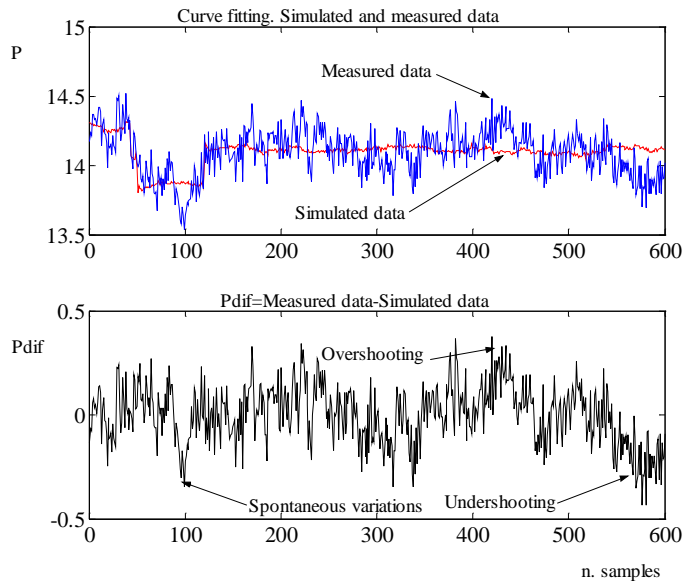
Figure 6.5: Influence of spontaneous variations in the load.

Figure 6.6 shows the correlation of the residuals of the system when 200 samples have been used for the identification. The result deviates from the expected white noise profile, which can be justified by those variations not included in the identification model.

The lower part of Figure 6.6 displays the autocorrelation function of e, residuals or prediction error, and the cross correlation between e and the inputs. A 99% confidence interval for those variables is also displayed, assuming that e is white noise and independent from the input u. If the

correlation function goes significantly outside of that interval the model cannot be accepted because there is linear dependency in the residuals and consequently the model is not properly fitting the data. Correlation between e and u for negative lags means output feedback, and it is not a reason to reject the model. Only correlation on positive lags is of interest for validation, i.e. only when the data is shifted to later dates.
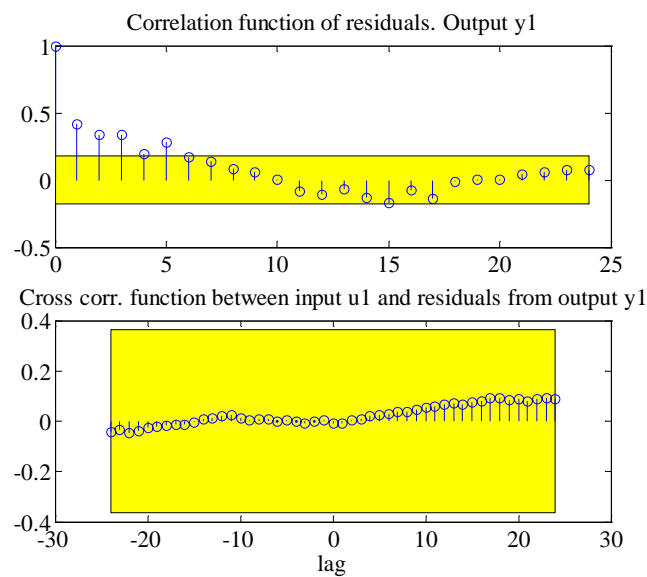
Figure 6.6: Calculated residuals for 400 samples.

The reactive response is hardly affected by spontaneous load variations. Figure 6.7 verifies that this influence is small. In Figure 6.8 the residuals of the system when 200 samples have been used for the identification are presented.
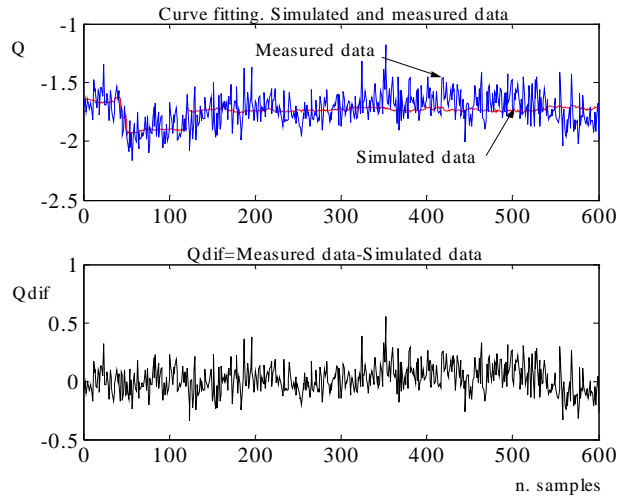
Figure 6.7: Influence of spontaneous variations in the load.
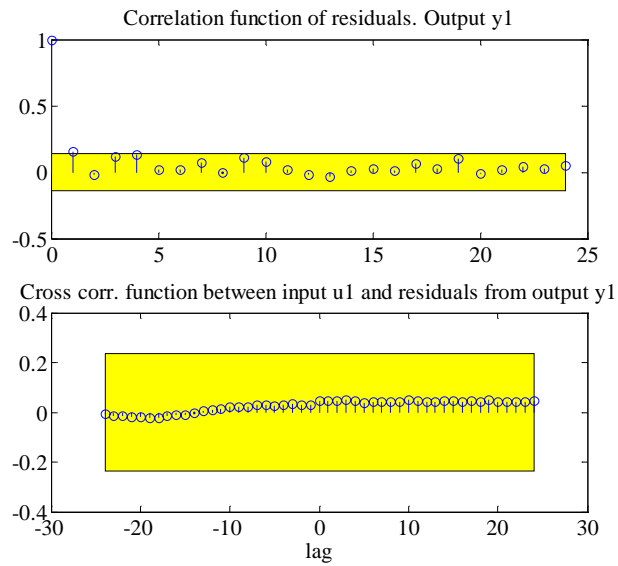
Figure 6.8: Calculated residuals for 200 samples.

If we increase the number of samples used for the identification, the quality of the estimates will be compromised and the residual plot will result in a less accurate profile. Figure 6.9 shows the result of the residuals when 400 samples have been used in the identification.
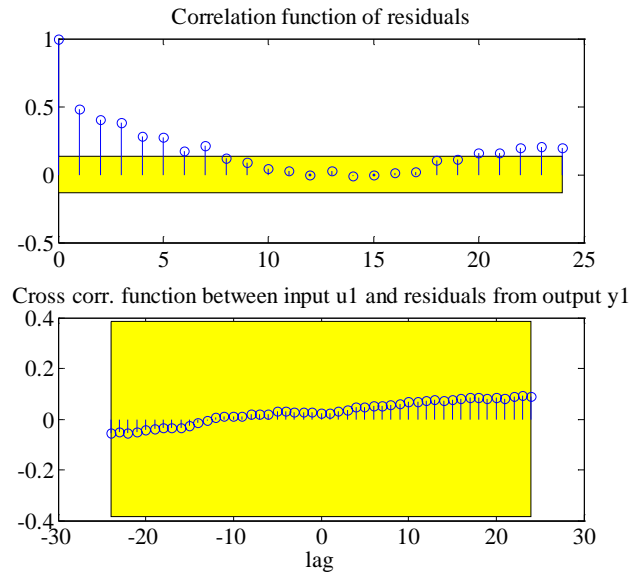
Figure 6.9: Calculated residuals for 400 samples.

In general, we can conclude that a good estimation is obtained by choosing the measuring time to about 2.5-3 times the value of the load time constant, after the voltage variation has happened.

6.4.2. Resistive characteristic of the load

Whereas this window length achieves accurate estimates for the three parameters, the measuring time can be considerably reduced to a value close to the disturbance time if the identification purpose is limited to determining the transient behavior of the load.

In the transient frame the active power demand of most loads, including heating and motors, behave like constant impedance. This is equivalent to

an algebraic quadratic voltage dependence, which corresponds to the value 2 of the exponent α_t. Figure 6.10 shows the voltage in File No.1, a step change.
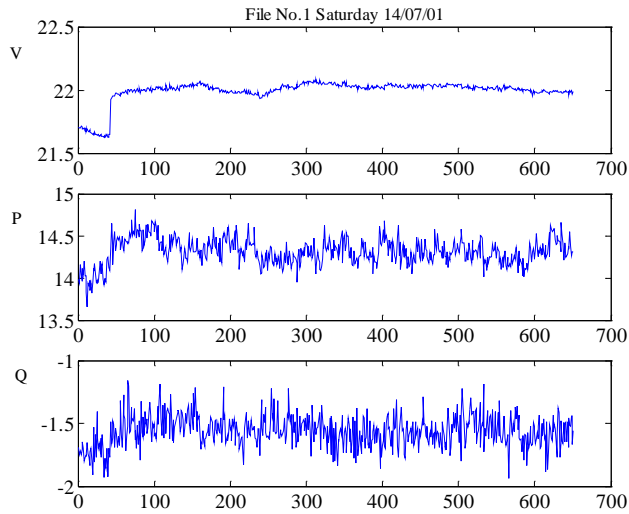
Figure 6.10: Voltage variation, active and reactive power.

Tables 6.3 and 6.4 show the values for the transient estimates for active and reactive load, α_t and β_t respectively, using different number of samples just after the step has occurred (t=43 seconds). Assuming that α_t should be in the neighborhood of 2, we can evaluate the values in table 6.3.

Active Transient Characteristic of the load		
Percent of Tp	**Window Length**	α_t
5%	49	1.69
10%	54	1.99
15%	60	2.32

20%	65	2.06
25%	71	1.99
30%	75	1.80

Table 6.3: Identification of the transient behavior for active load under a step change at t=43 seconds. Tp=110 seconds.

Reactive Transient Characteristic of the load		
Percent of Tq	**Window Length**	β_t
5%	55	-11.30
10%	67	-4.30
15%	80	-6.30
20%	92	-7.87
25%	104	-7.97
30%	116	-7.47

Table 6.4: Identification of the transient behavior for reactive load under a step change at t=43 seconds. Tq=244 seconds.

According to these results, and depending on the identification purpose, it is possible to study the dynamic load response in a shorter or longer term. Figure 6.11 shows the principal behavior of the exponential recovery of the load after a voltage step.

A window length of approximately 15% of the value of the load time constant is enough for identifying accurately the short-term characteristic of the load. During (15-30)% of the value of the load time constant, the load has a resistive characteristic. By increasing the window length to 2.5-3

times the load time constant, we will also obtain an accurate value for the steady state behavior and for the time constant.
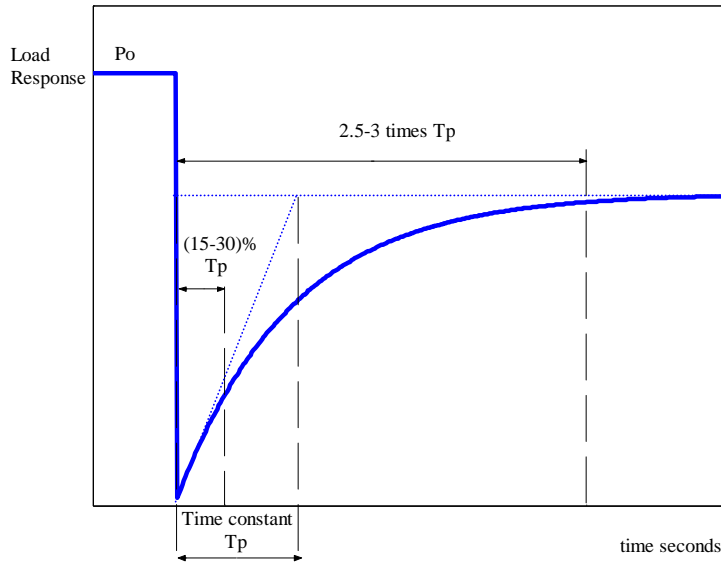
Figure 6.11: Exponential recovery of the load.

6.5   Normalization of Dynamic Reactive Load Models

The critical effect of the normalization factor in the variability of the reactive load parameters has been mentioned in Chapter 5, where the identified reactive steady-state and transient parameters deviated to very large values, when the value Qo used in the normalization in Equations (6.1) and (6.2), was close to zero.

In this section, and by using measured data from normal operation it is shown that the reactive power level, which has previously been used as normalization factor is inappropriate. If instead apparent power level is used for normalization, the variability in the parameters that describe the reactive load response is drastically reduced.

The common value *Qo* used in the normalization of the reactive load models may be close to zero due to the effect of reactive compensation, and therefore the reactive load parameters that describe the load response will deviate to very large values. The measured data is collected with different amounts of reactive compensation. This makes it possible to describe how the reactive load parameters change with the value of *Qo*.

6.5.1 Determination of parameters in reactive load models

Based on the described nonlinear model in Chapter 5, equations (5.1) and (5.2), the corresponding reactive load representation is given by (6.1), (6.2), and characterized by three parameters, reactive steady state load-voltage dependence, reactive transient load-voltage dependence and a load-recovery time constant.

$$T_q \frac{dQ_r}{dt} + Q_r = Qo\left(\frac{U}{Uo}\right)^{\beta_s} - Qo\left(\frac{U}{Uo}\right)^{\beta_t} \tag{6.1}$$

$$Q_l = Q_r + Qo\left(\frac{U}{Uo}\right)^{\beta_t} \tag{6.2}$$

Uo and *Qo* are the voltage and power consumption before a voltage step change. *Qr* is the reactive power recovery, Q_l is the total reactive power response, T_q is the reactive load recovery time constant, β_t is the transient reactive load-voltage dependence, and β_s is the steady state reactive load-voltage dependence. In analogy with Chapter 5 the non-linear model is simplified to a linear identification problem by linearizing around an operating point (U*). New quantities have been introduced, and the state space representation is given by (6.3) and (6.4):

$$Aq = \beta_t \cdot \left(\frac{U*}{U_0}\right)^{\beta_t - 1} \qquad Bq = \beta_s \cdot \left(\frac{U*}{U_0}\right)^{\beta_s - 1} \qquad u = \frac{\Delta U}{U_0}$$

$$\Delta Q_l = \Delta Q_r + Aq \cdot Q_0 \cdot u \tag{6.3}$$

$$T_q \cdot \frac{\Delta Q_r}{dt} = Bq \cdot Q_0 \cdot u - Aq \cdot Q_0 \cdot u - \Delta Q_r \tag{6.4}$$

By introducing $Tq_1 = T_q \cdot Aq$, the reactive load variation ΔQ_l is given by (6.5). A similar equation can be derived for the active load variation.

$$\frac{\Delta Q_l}{Q_0} = \frac{Bq + s \cdot Tq_1}{1 + s \cdot Tq} \cdot \frac{\Delta U}{U_0} \qquad (6.5)$$

The transfer function (6.5) represents the load response when a voltage change is occurring in the system. It is characterized by three parameters, reactive steady state voltage dependency Bq, reactive transient voltage dependency Aq, and reactive time constant T_q. ΔQ_l and ΔU represent deviations from the steady state values Qo and Uo. The reactive load equation has been normalized by using Qo. The aim is then, to use the described linearised model (6.5) and to identify its parameters with measured data. The least squares optimization algorithm is used in the identification.

6.5.2 Normalization in dynamic load models

The identification process proposed above has been applied to different sets of data, as exemplified by test No.6.1 and 6.2.

<u>Test No.6.1</u>

The test, check Section 4.2, is based on previous measurements in the power system in the South of Sweden, and they represent an extension of previous studies [Le Dous, 1999], [Karlsson, 1992]. The data originates from six different experiments in the 400-130 kV-transmission system during June 1996. The voltage changes were made by simultaneous manual operation of tap changers on the 400/130 kV transformer. Six different sets of data have been used in the simulation.

No	$\Delta V/V_0$ [%]	T_p [s]	α_t	α_s
1	-1.8	135	1.36	0.25

2	+1.9	40	1.70	-0.10
3	-3.7	61	1.31	-0.16
4	+3.7	74	1.35	-0.54
5	-5.3	70	1.65	-0.32
6	+5.4	78	1.60	-0.08

Table 6.5: Identified parameters for active load response under six different voltage steps.

No	$\Delta V/V_0$ [%]	T_q [s]	β_t	β_s	Qo [Mvar]
1	-1.8	89	-181.80	7.90	-0.974
2	+1.9	256	-687.20	975.60	-0.046
3	-3.7	88	87.67	31.86	-2.850
4	+3.7	105	104.50	-148.56	0.867
5	-5.3	78	77.89	19.35	-2.840
6	+5.4	94	94.18	-49.75	1.254

Table 6.6: Identified parameters for reactive load response under six different voltage steps. Normalizing factor of the reactive load Qo.

The identified parameters for the active load, Table 6.5, exhibit low variability and correspond to acceptable values. The reactive parameters, however, are less reliable. Even though the reactive transient (β_t) and steady state (β_s) parameters fit the proposed model in each case, they deviate from the expected values. An important factor contributing to this may be that the value *Qo* used in the normalization in equations (6.2) may be close to zero because of the effect of reactive compensation. By checking the factor *Qo*

in Table 6.6 it is observed that for those values closer to zero, the deviation in the identified parameters is larger. Figure 6.12 shows a simple representation of the total load as the sum of the effect of the active and reactive power.
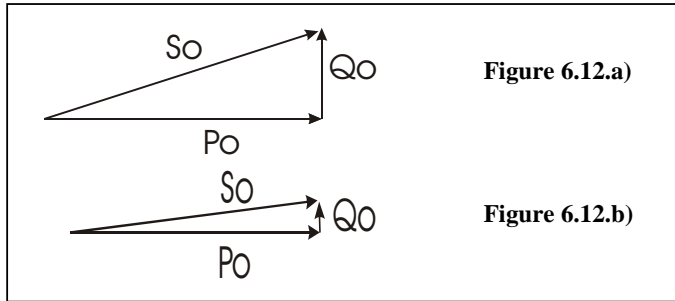
Figure 6.12: Total load *So*, as the sum of the active and reactive effect, *Po* and *Qo*, when reactive compensation is and is not needed, figure b) and a) respectively.

The load response in figure 6.12.a is not affected by reactive compensation while it is in figure 6.12.b. The value *Qo* is reduced to a value closer to zero due to the effect of capacitors, but *Po* remains constant. Since theoretically, when *Qo* tends to zero, the model parameters will go to infinity, it is necessary to normalize the reactive load model by some other factor that is not affected by this phenomenon.

Suggested candidates are *Po* or *So*. By normalizing by *So* the reactive load representation is then given by equations (6.6) and (6.7):

$$T_q \frac{dQ_r}{dt} + Q_r = So\left(\frac{U}{Uo}\right)^{\chi_s} - So\left(\frac{U}{Uo}\right)^{\chi_t} \tag{6.6}$$

$$Q_l = Q_r + So\left(\frac{U}{Uo}\right)^{\chi_t} \tag{6.7}$$

Uo and *So* are the voltage and apparent power levels before a voltage step change. *Qr* is the reactive power recovery, *Ql* is the total reactive power response, T_q is the reactive load recovery time constant, χ_t is the transient reactive load-voltage dependence, and χ_s is the steady state reactive load-

voltage dependence. Table 6.7 shows the results obtained by normalizing the reactive dynamic load in equation (6.2) by *So*. The quality of the reactive power parameter estimates is now similar to those for the active power.

No	$\Delta V/V_0$ [%]	T_q [s]	χ_t	χ_s
1	-1.8	88	2.43	0.12
2	+1.9	165	2.02	-0.64
3	-3.7	88	2.08	-0.77
4	+3.7	89	2.42	-0.98
5	-5.3	78	2.22	-0.48
6	+5.4	92	2.62	-0.49

Table 6.7: Identified parameters for reactive load response under six different voltage steps. Normalizing factor of the reactive load *So.*

Test No.6.2

The data originates from a continuous acquisition from normal operation data in the 130-50-20 kV distribution system in the South of Sweden, see Section 4.3. Due to the fact that the continuous acquisition of data provides large amount of information that corresponds to non-stationary load data sequences, i.e. every data case differs from the others, it has been possible to study the impact of reactive compensation during daily operations on the representation of the reactive load.

Measurements at the 20 kV-level during February 2002 have been selected for the analysis. The identification procedure described in this thesis has been applied to the mentioned data.
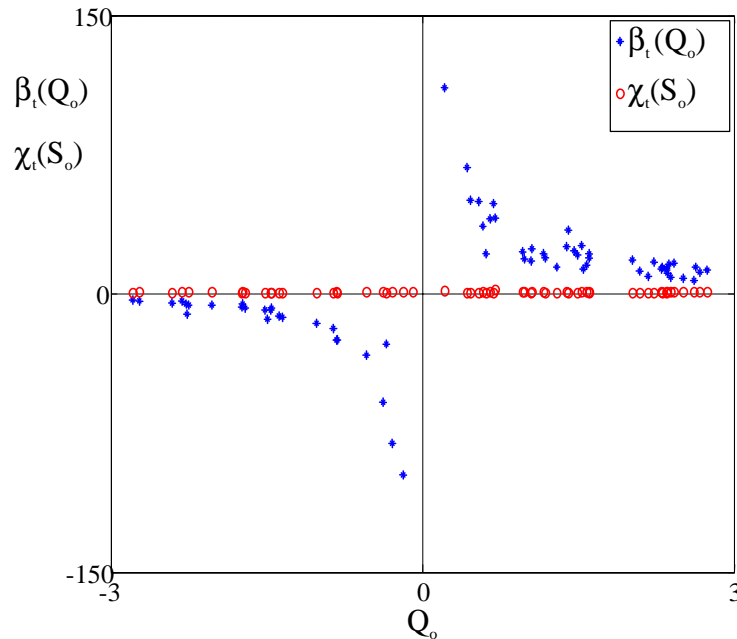
Figure 6.13: Effect of the reactive compensation in the identification of the parameter χ_t, using the normalization factor Qo and So respectively.

Figure 6.13 shows the result of the identification for the reactive transient part of the load, plotted against the power level *Qo*, when the reactive load equation has been normalized by *Qo,* asterisk '*', and by *So*, circle 'o', respectively. By normalizing with *Qo*, when the value *Qo* goes to zero, the transient parameters, β_t, tend to plus or minus infinity, and they apparently deviate significantly from their normal values. On the other hand, by normalizing with *So*, the transient parameter χ_t, exhibits small variability. When the value *Qo* is in the neighborhood of 0, the parameters do not deviate from the physically expected values , since *So* is hardly affected by the effect of reactive compensation.

Figure 6.14 presents the result of the identified parameter χ_t, when the normalization factor is *So*. The identified parameters remain in a limited interval.
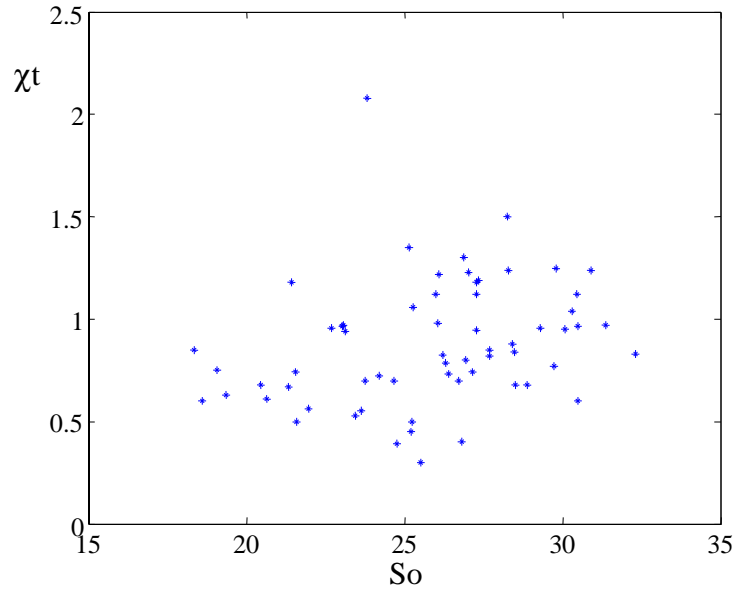
Figure 6.14: Effect of the reactive compensation in the identification of the parameter χ_t using the normalization factor *So*.

6.5.3 Conclusions

The effect of normalization on dynamic load models has been studied. The factor *Qo* previously used to normalize the reactive load model is inappropriate since it may be equal to zero due to the effect of switching capacitor operations. The identification of parameters for the reactive load model when normalizing by *Qo* shows that these parameters tend to infinity when *Qo* goes to zero. On the other hand, an accurate representation of the reactive load is achieved by normalizing with the factor *So*, since this factor is hardly affected by reactive compensation.

Chapter 7

Analysis of Experimental Results

Daily, weekly and seasonal variations of the load model parameters will be studied throughout this chapter. This has not been studied before, but is made possible by the collected data. The process for determining parameters of dynamic load models described in Chapters 5 and 6 has been applied to data from normal operation during the periods indicated in Figure 7.1. The identified parameters and associated time of day are addressed in several tables in Appendix I.

Figure 7.1: Periods of normal operation during July 2001-June 2002, when data has been acquired.

7.1   Analysis of Variability of the Parameters

The large amount of information presented in Appendix I makes the study of the variability of the parameters difficult, because it corresponds to different seasons and times of the year, but also because it includes large variety of load processes. Sections 7.1.1 and 7.1.2 present the annual and daily variability of the parameters respectively.

Due to the fact that the amount of available data for some periods of time is shorter than others due to initial problems during the acquisition of data, some deviations in the expected parameters have been obtained.

7.1.1 Annual variability

The monthly mean value and standard deviation for each of the identified parameters have been calculated, and they are presented in Table 7.1.

DATE	PLOAD			QLOAD		
	T_p	α_t	α_s	T_q	β_t	β_s
July 01	145 (112)	1.58 (0.33)	1.20 (1.43)	196 (60)	0.87 (0.21)	0.61 (0.67)
Aug. 01	140 (79)	1.43 (0.37)	0.81 (1.21)	180 (76)	1.20 (0.35)	0.39 (0.94)
Sept. 01	168 (156)	1.52 (0.27)	0.65 (0.69)	155 (96)	1.31 (0.30)	0.51 (0.38)
Jan. 02	127 (52)	1.84 (0.50)	0.63 (1.00)	126 (48)	0.79 (0.22)	0.48 (0.59)
Feb. 02	161 (104)	2.08 (0.62)	0.60 (0.90)	151 (78)	0.87 (0.30)	0.30 (0.48)
Apr. 02	134 (55)	1.75 (0.51)	0.57 (1.23)	132 (55)	0.77 (0.22)	0.58 (0.66)
May 02	123 (51)	1.65 (0.63)	0.44 (1.24)	132 (52)	0.95 (0.32)	0.58 (0.78)
June 02	123 (56)	1.38 (0.67)	0.34 (1.16)	126 (51)	1.11 (0.37)	0.75 (0.79)

Table 7.1: Monthly mean values for the identified parameters in the proposed dynamic load model. Standard deviations are shown within parentheses.

Figure 7.2 shows the variability of each one of the above mentioned parameters, active power time constant Tp, active power transient voltage dependency α_t, active power steady state voltage dependency α_s, reactive power time constant Tq, reactive power transient dependency β_t, and reactive power steady-state dependency β_s, during the period of time July 2001 to June 2002.
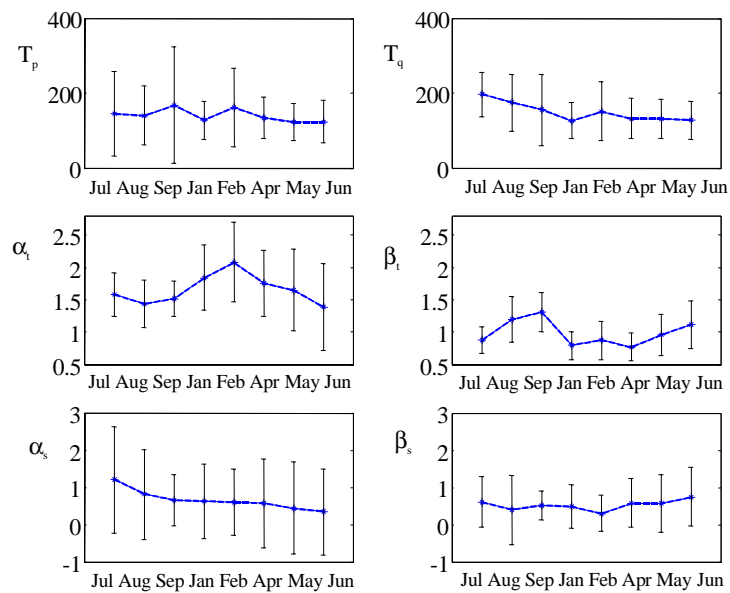
Figure 7.2: Annual variability of active and reactive power parameters in dynamic load models based on monthly averages.

Based on both Table 7.1 and Figure 7.2 it has been observed:

Time constants, *Tp* and *Tq*

- In general the active recovery of the load seems slightly faster in summer than in winter. The monthly active time constant for September (Figure 7.2) shows a different pattern. This value is not trustable since it has been calculated using very few data points.

- The value of both the active and reactive time constants move in the same order in a range of about 80 to 200 seconds. Figure 7.3 shows the correlation between these two parameters for all the available data from July 2001 to June 2002. A correlation factor equal to 0.41 has been found. The figure shows a high concentration around the mentioned range, while the disparity in the results increases for values larger than 200 or smaller than 80 seconds.
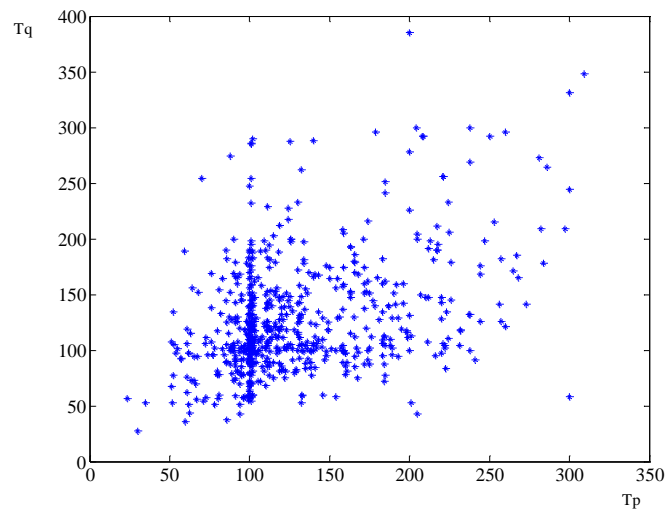
Figure 7.3: Correlation between active and reactive load time constants.

- The differences in the order of the time constants, the reactive load recovery seems slightly slower, is probably related to the effect of spontaneous load demand variations, but the main recovery of the reactive load is produced by the increase of the reactive losses due to the active recovery of the load at low voltages. This conclusion is justified further in this chapter.

- Figure 7.3 shows, especially between 80 to 200 seconds, how the variability of the correlation between both parameters is not constant. For example for a 100 seconds active time constant, different values for the reactive time constant have been

obtained and therefore different correlation between both parameters. The real and reactive powers are coupled and both real and reactive power load models should be simultaneously identified, with coupling effects. The correlation is not constant all the time, since it is depending on how much other external stochastic disturbances affect the system, i.e. spontaneous load variations or other unmodeled dynamics. A more accurate dynamic model will be desired in order to decrease uncertainty in the determination of these two parameters. A good suggestion for future work is the implementation of a dynamic model as a combination of the studied physical model and a stochastic extension.

- Figure 7.4 shows the correlation between the active and reactive load time constants, when instead of using all the available data like in Figure 7.3, the monthly average active and reactive time constants are used. A correlation factor of 0.50 has been obtained.
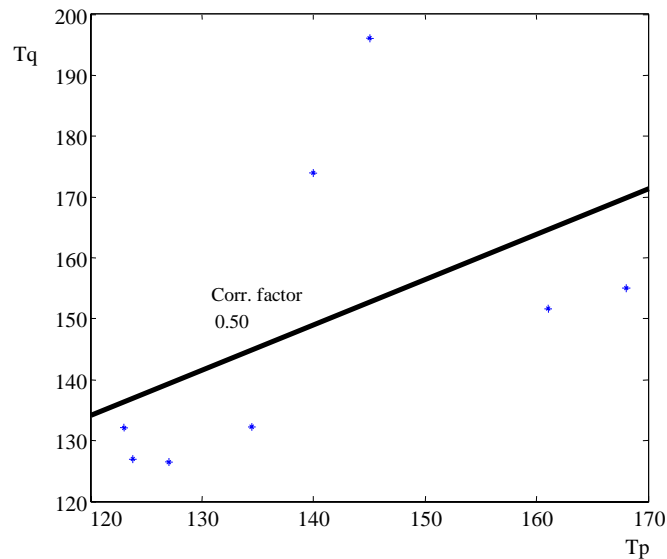
Figure 7.4: Correlation between the monthly average active and reactive load time constants during July 2001-June 2002.

- • There is one outlier in the data corresponding to July. July has few data points, and the weekend is a significant part of the data. This factor may have affected the value of the identified time constants. During the weekends most of the load type is residential. However industrial processes, which are characterized by larger time constants, may be started during Saturday and Sunday nights.

The standard deviation for the identified values of the active and reactive time constants shows a large variability of the parameters. The reason is related to the daily diversity of load processes. The measured load aggregates different load classes, industrial, residential and commercial, but also different load compositions, induction motors, electric heating, street lighting, which are described by different load characteristics. Table 7.2 shows the time constant values of some of the most common loads.

Type of Load	Load Recovery Time Constant
Induction Motors	Few seconds
Tap Changers & Voltage Regulators	10 seconds-several minutes
Constant energy resistive loads	Several minutes
Fluorescent Lamps	1-2 minutes

Table 7.2: Approximate time constant values for some of the most common loads.

Active transient load voltage dependence α_t

- • During the winter and due to the low temperatures, the heating demand increases, and therefore the use of heating with thermostat control. This kind of device presents a resistive characteristic. Table 7.1 shows α_t moving on a range of 1.30 to 2.10. The value 2.10 has been obtained for the coldest month, and it is associated to a pure resistive behavior of the load. The active transient part of the load is strongly correlated to the temperature, i.e. the colder it is the larger parameter α_t is

obtained. Figure 7.5 shows this correlation. Correlation factor of –0.82.
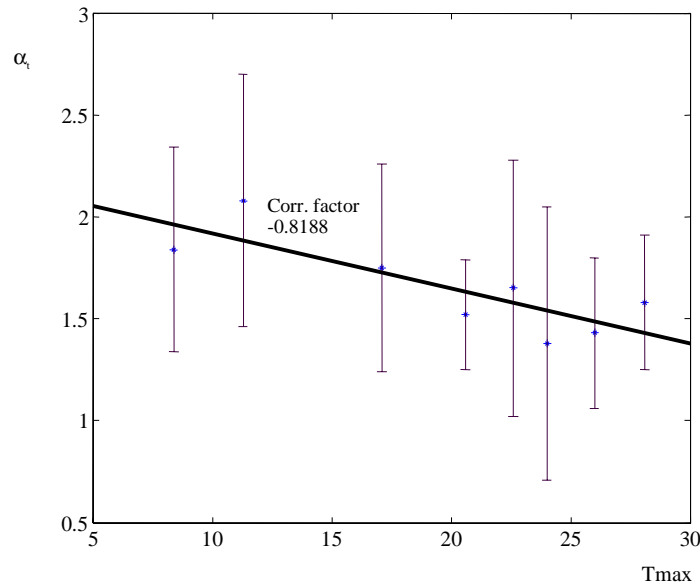
Figure 7.5: Correlation between the monthly average values for the active transient load voltage dependence α_t and the corresponding maximum average temperature for every month.

Reactive transient load voltage dependence β_t

- The obtained values of β_t are in the range of 0.70 to 1.30. The parameter β_t is depending on the temperature, (see Figure 7.2). The parameter is higher during warm months and lower during winter. Since the measurements have been carried out in the same area, and the load composition hardly has changed, the variability of the parameter is probably due to dis/connection of air conditioners and heat pumps, and other similar loads during winter/summer. Figure 7.6 shows the estimated correlation between this parameter and the temperature.
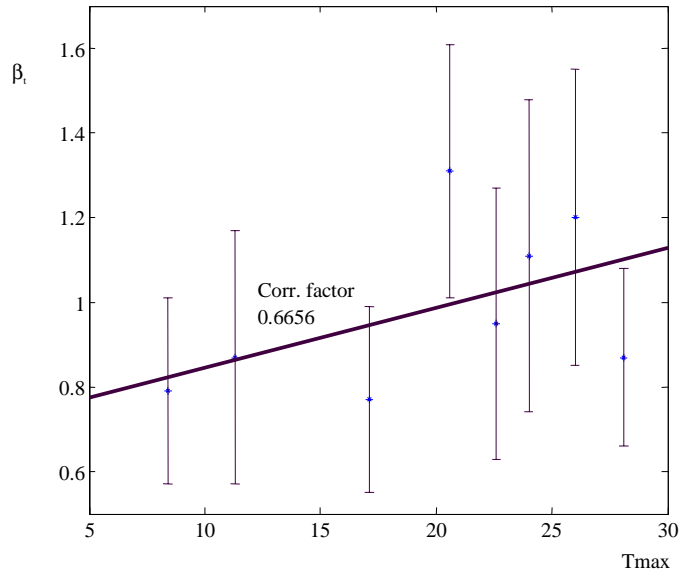
Figure 7.6: Correlation between the monthly values for the reactive transient load voltage dependence β_t and the corresponding maximum average temperature for every month.

Active and reactive steady state load voltage dependence α_s, β_s

- Table 7.1 shows that the parameters α_s and β_s move in a range of about 0.30 to 1.20 and 0.30 to 0.75 respectively. Furthermore, the identified parameters present a large variability that can be associated to the large diversity of load processes mentioned before.

- In some cases the parameters present negative values. The stationary level reached by the load after the recovery is equal to or higher than the expected one, probably due to the effect of the tap changers, resulting in an over or undershooting of the load. An important contribution to voltage instability may be done by unexpected values of these parameters, such as active or reactive load overshooting resulting from negative values of α_s or β_s.

7.1.2 Daily variability of the parameters

Since the variability of the values of the time constants and steady state characteristics is still very large, a new distribution of the results has been done. The 24 hours of a day has been divided into three periods of time, as follows:

- Period I: Day, for the interval of hours from 6:30 to 17:30. This period of time includes the commercial and working hours.

- Period II: Evening, for the interval of hours from 17:30 to 22:00. The time corresponds mainly to residential activity and some street lighting.

- Period III: Night, for the interval of hours from 22:00 to 6:30. This period of time correspond to some industrial activity during the night, but mainly to street lighting.

For each one of the identified parameters presented in Appendix I it has been calculated monthly mean value and standard deviation for day, evening and night hours. The results are presented in the next three tables, Table 7.3 for monthly variability during the day, Table 7.4 for monthly variability during the evening, and Table 7.5 for the variability during the night.

DAY	PLOAD			QLOAD		
	T_p	α_t	α_s	T_q	β_t	β_s
July	195 (98)	1.60 (0.46)	1.07 (1.53)	216 (51)	0.91 (0.20)	0.33 (0.56)
Aug	133 (92)	1.52 (0.19)	0.60 (1.70)	176 (80)	1.34 (0.36)	0.49 (0.26)
Sept	168 (156)	1.52 (0.27)	0.65 (0.69)	155 (96)	1.31 (0.30)	0.51 (0.38)
Jan	122 (45)	1.89 (0.43)	0.39 (1.00)	129 (53)	0.87 (0.21)	0.66 (0.63)
Feb	125 (68)	2.03 (0.55)	0.40 (0.85)	142 (71)	0.88 (0.32)	0.52 (0.63)
Apr	136 (61)	1.70 (0.56)	0.46 (0.41)	138 (58)	0.81 (0.23)	0.56 (0.64)

May	122 (49)	1.53 (0.56)	0.48 (1.21)	136 (54)	1.04 (0.32)	0.64 (0.74)
June	125 (53)	1.50 (0.80)	0.68 (1.17)	128 (44)	1.17 (0.37)	0.82 (1.03)

Table 7.3: Variability of load model parameters during day hours.

EVEN.	PLOAD			QLOAD		
	T_p	α_t	α_s	T_q	β_t	β_s
July	99 (11.30)	1.45 (0.07)	0.90 (0.80)	163 (109.00)	0.72 (0.14)	1.65 (0.26)
Aug	122 (64.27)	1.26 (0.74)	0.93 (0.97)	214 (73.00)	1.33 (0.15)	0.66 (0.59)
Sept	168 (156.00)	1.52 (0.27)	0.65 (0.69)	155 (96.00)	1.31 (0.30)	0.51 (0.38)
Jan	124 (51.00)	1.76 (0.55)	0.73 (0.88)	122 (45.00)	0.76 (0.17)	0.36 (0.55)
Feb	119 (53.00)	1.85 (0.47)	0.59 (0.72)	127 (65.00)	0.80 (0.25)	0.36 (0.52)
Apr	147 (55.00)	1.67 (0.43)	0.31 (0.85)	137 (54.50)	0.79 (0.16)	0.67 (0.60)
May	126 (55.26)	1.78 (0.59)	0.42 (1.28)	122 (44.49)	0.89 (0.27)	0.56 (0.70)
June	107 (38.39)	1.40 (0.73)	0.63 (1.12)	118 (35.16)	0.96 (0.23)	0.83 (0.96)

Table 7.4: Variability of load model parameters during evening hours.

NIGHT	PLOAD			QLOAD		
	T_p	α_t	α_s	T_q	β_t	β_s
July	133 (64.00)	1.61 (0.27)	0.86 (0.76)	205 (29.69)	0.90 (0.37)	0.41 (0.09)
Aug	141 (111.00)	1.45 (0.28)	0.60 (0.17)	189 (79.00)	1.00 (0.31)	0.05 (1.10)
Sept	168 (156.00)	1.52 (0.27)	0.65 (0.69)	155 (96.00)	1.31 (0.30)	0.51 (0.38)
Jan	134 (58.00)	1.82 (0.51)	0.68 (0.90)	126 (42.00)	0.73 (0.23)	0.39 (0.55)

Feb	126 (65.00)	2.23 (0.53)	0.43 (0.25)	140 (61.00)	0.67 (0.21)	0.33 (0.59)
Apr	134 (49.00)	1.71 (0.46)	0.45 (0.60)	116 (45.00)	0.72 (0.24)	0.51 (0.61)
May	119 (46.52)	1.65 (0.50)	0.60 (0.99)	138 (59.03)	0.75 (0.28)	0.40 (0.86)
June	118 (55.47)	1.37 (0.58)	0.58 (1.14)	133 (62.80)	0.96 (0.27)	0.55 (1.28)

Table 7.5: Variability of load model parameters during night hours.

In general, the standard deviation of the identified time constants has decreased probably because of the fact that the results have been grouped into three different classes with different load characteristics, and therefore the diversity of load processes in each of these groups has decreased. On the other hand, even though the standard deviation has decreased considerably in some of the cases, there is still large variability. To achieve more accurate results it would be necessary to apply more advanced data analysis techniques. By sorting the data differently the results may be improved further. A new classification could be by grouping the data in a weekend and week type, especially in July 2001 when the weekend is a significant part of the available data. Other suggestion is to group in relation to the type of process, -- industrial residential, commercial, rural --, or even considering different patterns for a weekday (day, evening and night), a Saturday, and a Sunday.

Based on the information in Tables 7.3, 7.4 and 7.5, a comparison of the variability during the day, evening and night hours for each one of the parameters has been done. The information from September is not included, since the few acquired samples during this period make the data unreliable. It has been observed:

Active and reactive time constants

- Figure 7.7 shows the variability of the active time constant. The variability of this parameter seems very uncertain and difficult to track. On one hand it seems that the recovery of the load is slightly faster during the summer than the winter, check Figure 7.7 during June, July and August. This may be due to the fact that during summertime the demand of electric heating is

considerably reduced, the effect of thermostats is reduced, most of the load is street and commercial lighting, and therefore the recovery of the load is lower i.e. shorter time to reach the steady-state. The lowest values of the time constants are obtained during the evening hours, and during summer time. The load processes are related to residential activity. On the other hand unexpected fast recoveries during February, and slightly differences with summertime values during January have been obtained.

- The only conclusion the author could draw with certainty is that the variability of the time constants may be dependent on temperature but mainly on the composition of the load. The fact that aggregated load has been used for this work make it difficult to study how the different load processes affect the value of the variability of the parameter.
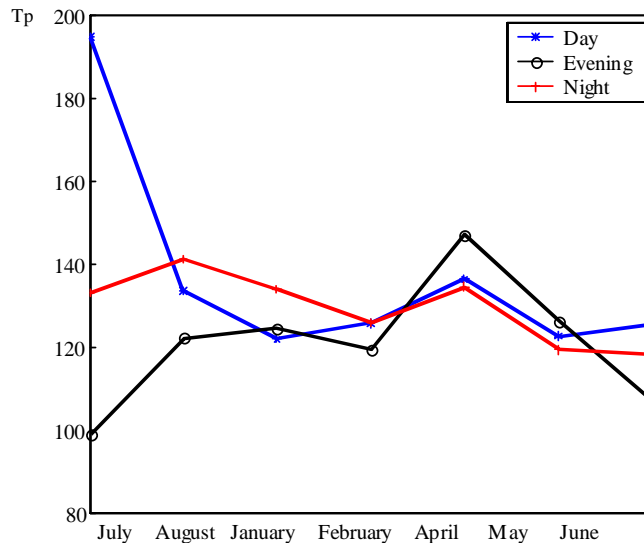
Figure 7.7: Annual variability of the active time constant for day, evening and night hours.

- Both active and reactive time constant values move approximately in the same order.

<u>Active transient load voltage dependence α_t</u>

- Figure 7.8 shows the dependency of this parameter on the temperature for the three times of the day. The larger values have been obtained for the colder months and the lower to the warmer ones because of the variation in heating demand.

- During the summer the parameter exhibits the lowest values; values during evening and night hours are 1.4 and 1.3 respectively. Higher values correspond to day hours. The reason is probably due to the mild weather and the increase of light hours, which will change the residential habits, and therefore decrease the heating demand.
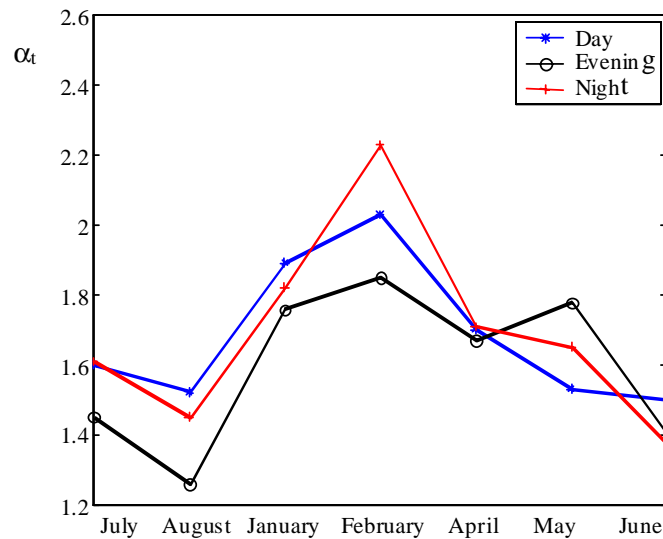
Figure 7.8: Annual variability of the active transient load voltage dependence α_t for day, evening and night hours.

- During the winter, the higher values are associated to the night hours, which is justified by the large percent of electric heating connected due to the extreme cold temperatures.

Reactive transient load voltage dependence β_t

- The Figure 7.9 shows the dependency of this parameter on temperature; the values are larger during the summer and lower during the winter. Since the summers in the South of Sweden are characterized by mild temperatures the connection of air conditioner units is hardly necessary, and – if it occurs - only during the day hours. The lowest parameter values have been obtained during night hours, while the highest ones during day hours.

- During the winter the parameters exhibit low values for the three times of the day. The highest values correspond to day hours, mainly associated to industrial processes.
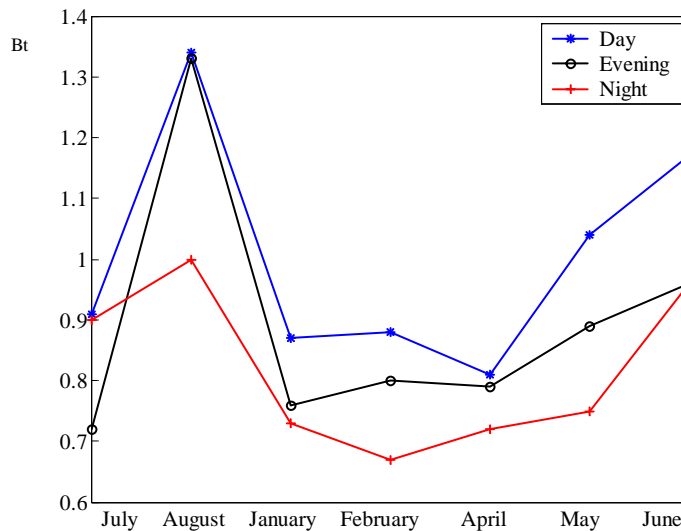
Figure 7.9: Annual variability of the reactive transient load voltage dependence β_t, during day, evening and night hours.

Active and reactive steady state load voltage dependence α_s β_s

- Figure 7.10 shows the variability of the active steady state load voltage dependence of the load. The values of this parameter are associated to the values obtained for the respective active time constant.

- For wintertime the values of α_s are closer to 0 and therefore to a full restoration of the load. During wintertime most of the load is electric heating and the energy demand is high. The thermostats in the heating are active almost all the time, and the load fully recovers, α_s is zero, or even reaches values larger than in the pre-disturbance situation, values smaller than zero. Larger values of the parameter have been found for summer time when electric heating is not a big percent of the load.
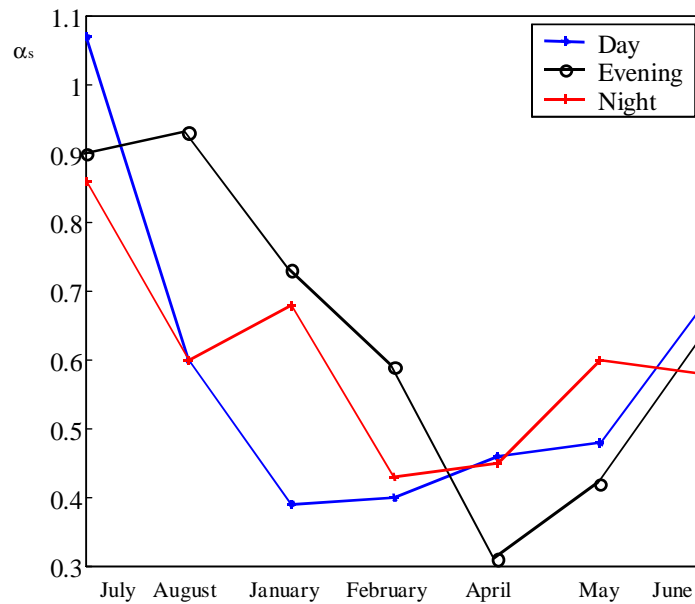
Figure 7.10: Annual variability of the active steady state load voltage dependence α_s for day, evening and night hours.

- Figure 7.11 shows that there is correlation between the parameter α_s and the load recovery time constant. The correlation function corresponds to day hours, with a correlation coefficient of 0.88. Smaller correlation coefficients have been found for evening and night hours, -0.70 and 0.30 respectively.
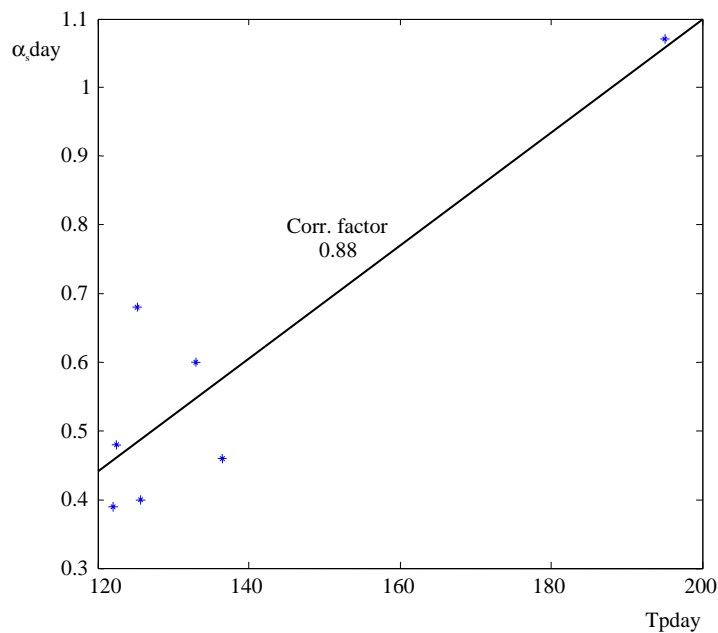
Figure 7.11: Correlation between the monthly values for the active steady state load voltage dependence α_s for day hours, and the corresponding monthly values for the active time constant.

- The value corresponding to July strongly affects the correlation sign between both parameters. A comparison with the other obtained values shows a difference in the range of Tp and α_s, but still correlation between both parameters. This may be related, as mentioned before in this chapter, to the reduced number of data points available during that month, and the significant percent of weekend days in the data.

The conclusions described above for the active steady state parameter, and its relation with the active recovery time of the load can be applied in the same way for the reactive steady state parameter and the reactive recovery time constant. The correlation coefficients obtained for day, evening and night hours are then, -0.86, 0.31 and –0.56 respectively.

7.2   Active and Reactive Load Correlation

Regarding the time constant values presented in the previous section in Table 7.1 it has been shown that both the active and reactive time constants move in the same range of about 80 to 200 seconds, and are correlated to each other with a correlation factor equal to 0.50. See Figure 7.4. The reason of this correlation is studied throughout this section.

The small differences in the order of both active and reactive time constants are probably related to spontaneous load variations, and therefore unrelated to voltage variations, but the main recovery of the reactive load is produced by the increase of the reactive losses due to the active recovery of the load at low voltage.

In order to check whether the reactive recovery really originates from the mentioned increased reactive losses, the simplified distribution system model shown in Figure 7.12 has been used to estimate those losses. The complete distribution system under the recording point at the 130 kV level has been modeled with a series reactance equal to the sum of both reactances at 130 and 20 kV according to Appendix II. The measured values at the 20 kV-level have been used to determine the value of the losses (*Qlosses*).
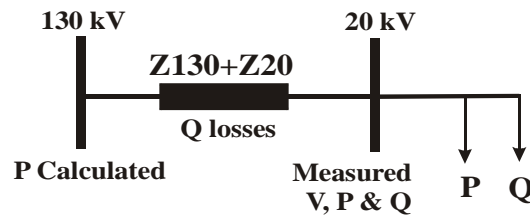
Figure 7.12: Simplified distribution system from the 130 kV- level to the 20 kV-level for determining the reactive load losses.

Figure 7.13 shows the calculated *Qlosses* curve together with the curves for the active and reactive consumption at the 20 kV. All the quantities are presented in per unit. The value before the voltage change for each one of the quantities has been chosen as the base value.
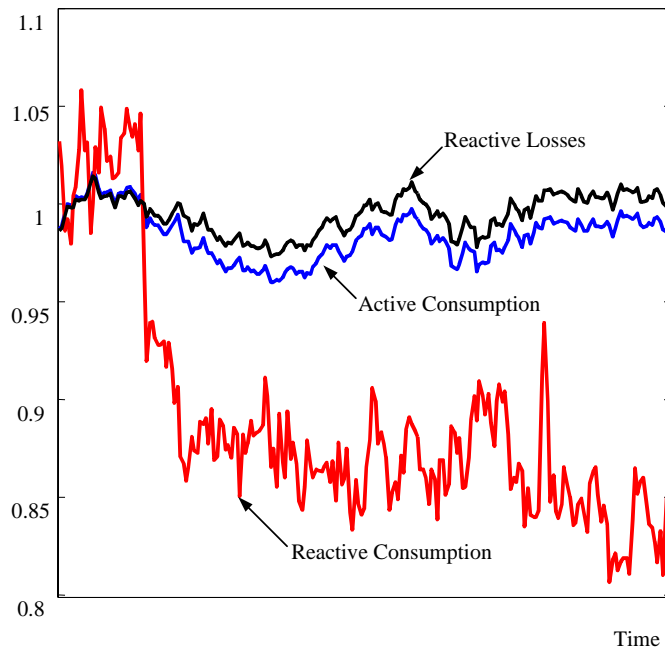
Figure 7.13: Comparison of the reactive losses and the active consumption curves.

7.3   Conclusions

An identification process for determining the active and reactive parameters in dynamic load models from normal operation data has been applied. The monthly and daily standard deviations of the resulting identified parameters show a large variability in the distribution of the results, probably due to the

high diversity of load processes, even during the day. The values of both time constants move in the same order and they are correlated to each other. The difference in the order of the time constants is probably related to the effect of spontaneous load demand variations. The active and reactive transient load voltage dependence α_t and β_t exhibit a strong dependency with the outdoor temperature, and therefore with the season and time of the day. The active and reactive steady state load voltage dependence α_s and β_s, are correlated to their respective active and reactive time recovery. It has been found that during wintertime the parameter α_s is closer to 0 and therefore to a full restoration of the load.

The distribution of the identified time-varying active and reactive load parameters, the calculated correlation factors, and in general the material presented throughout this chapter offers unique and pioneer information for the study of the load time-varying characteristic and the analysis of the load dynamics. Other previous studies in dynamic load models do not include the mentioned results.

Chapter 8

Conclusions

As an extension of previous studies on modeling and identification of non-linear dynamic load models, and motivated by finding more accurate ones for better description of the dynamic load characteristic and its relation to voltage stability, the work presented here has focused on the mentioned load characteristic, by identifying the active and reactive parameters in non-linear dynamic load models [Karlsson and Hill, 1994].

An automatic method for the determination of the load parameters from normal operation data is proposed. The non-linear model is reduced to a linear identification problem by linearisation, and the identification of the load parameters is achieved straightforward by using the Least Squares criterion. The method is robust with respect to the data, provided that data has been properly screened.

The availability of continuous normal operation data has provided large amount of information that has been critical for the accomplishment of this work. The realization of expensive tests has been avoided, and information of high value related to the load dynamics has been provided. This information has helped to track seasonal variations in load and to analyze typical daily operations at a substation.

8.1   Summary of the Results

The main conclusions of the thesis are summarized below, and are the result of applying the proposed automatic method to the field measurements described in Chapter 4.

Influence of the load characteristic in voltage stability

The effect of the load characteristic in voltage stability studies has been investigated. The use of the traditional static load models is changing more and more in favor of the dynamic ones in order to get a better representation of the load, and therefore to optimize the system operation.

The fact that loads are generally voltage dependent is a critical aspect for the design of security margins. A very pessimistic design may over-weight this security and this may result in a poor utilization of the system. On the other hand, a very optimistic design may lead the system to voltage collapse. It has been also studied that the voltage sensitivity of the load may help the stability of the system by providing some system load relief.

Moreover, some types of load such as electric heating are especially critical for stability because of their thermostatic characteristic. After a disturbance in the system, (voltage and power drop), and due to the effect of the thermostats, the aggregated load tends to increase the nominal load to a level close or equal to the pre-disturbance one, at the low voltage. This situation may result in severe conditions for the system operation. However, during the recovery time it may be possible to take some corrective actions such as local reactive compensation, load shedding, starting small-scale gas turbines, which may lead the system to stable operating points instead.

Window length

The influence of the data sequence length has been studied. A good estimation is achieved by choosing a window length of 2.5-3 times the load time constant, after a voltage change. If the identification is limited to determining the transient characteristic of the load, the measuring time can be considerably reduced to an approximate value of 15% of the time constant. Moreover, the measurements have verified that during the first 15-

30% of the recovery the load behaves as a resistance, i.e. transient characteristic in the neighborhood of 2.

Normalization on reactive dynamic load models

The influence of the normalization in dynamic reactive load models has been studied throughout Section 6.4. By using measured data from normal operation it is illustrated that the reactive power level Qo traditionally used to normalize reactive load models is inappropriate, since it may be equal to zero due to the effect of reactive compensation. The identification of parameters for the reactive load model when normalizing by Qo provides values that tend to infinity when Qo goes to zero.

If instead active power level Po, or apparent power level So is used as a base, the variability in the parameters that describe the reactive load response is drastically reduced.

Dynamic load parameters

According to the identified results from the determination of the active and reactive load parameters in Chapter 7 the following has been achieved:

Active and reactive time constants

In general, the values of both time constants move in the same order in a range of about 80 to 200 seconds, and they are correlated to each other with a correlation factor of 0.50. The difference in the order of the time constants is probably related to the effect of spontaneous load demand variations, but the main recovery of the reactive load is produced by the increase of the reactive losses due to the active recovery of the load at low voltage.

The average seasonal and daily time constant values indicate, faster recovery of the load during warmer months. The lowest values correspond to evening hours during summertime when the load demand reaches its minimum due to holidays season and to low consumption of electric heating. However, the monthly and daily standard deviation of the parameters, show a large variability in the distribution of the results due to the high diversity of load processes, even during the day. In order to group

the results more accurately, it would be useful to apply alternative analysis techniques as well as other ways of grouping the data.

Active transient load voltage dependence α_t

The obtained correlation factor (-0.82) between this parameter α_t, and the outdoor temperature during the measurements shows the strong dependency of the active transient characteristic of the load with the season, time of the day and weather conditions. The larger values of this parameter, close to 2, correspond to the colder months of the year, especially during the night, and they show a pure resistive characteristic of the load, which is related to the increase in using electric heating load. On the other hand, the lower values of the parameter correspond to summertime where the heating load consumption is very low.

Reactive transient load voltage dependence β_t

The parameter β_t is associated to the load composition and the presence of induction motors in it, but also to the effect of distribution transformers operating in saturation.

A high dependency of this parameter on the temperature has been found, where the higher values correspond to summertime and day hours, and the lower to wintertime and night hours. Since the measurements correspond to the same area, the main varying condition is the temperature, and the low variability in the parameter is probably related to connection/disconnection of air conditioners, heat pumps, and other similar loads during winter and summer.

Active and reactive steady state load voltage dependence α_s β_s

The active and reactive steady-state characteristics of the load, α_s and β_s, describe the respective active and reactive time recovery. It has been found that during wintertime the values of α_s are closer to 0, and therefore to a full restoration of the load, while larger values are obtained during summertime.

Moreover, some of the results exhibit negative values, corresponding to overshooting in the recovery of the load because of the action of discrete tap changers under low voltage conditions, that may contribute critically to the voltage stability of the system.

8.2   Future Research

The time-varying parameters for the active and reactive dynamic representation of the load have been identified and studied by using normal operation data at the 20 kV-level during July 2001-June 2002. The first objective in the continuing work is the identification and analysis of those parameters at the 50 kV-level in order to increase the understanding of the load dynamics and their representation, but also to quantify the similarities and differences with the results presented in this thesis for the 20 kV-level.

A second objective is to study the applicability of the results for optimizing the determination of the transfer limits and the maximum transfer capacity of the power system. The recording of the load behavior directly provides information about operating conditions, and this information might be used in the calculation of security limits. The main challenge is how to manage an on-line utility able to identify the time-varying parameters of the load, as described throughout the thesis, and how to deal with this information to make it useful in an on-line security assessment analysis.

The on-line security assessment on a power system determines its security level on a real-time basis. According to the obtained level of security after a disturbance, if the power system is found to be insecure, it will be necessary to take preventive actions in order to make the system secure again. An on-line security assessment consists mainly of a *preprocessing* of information, which mainly includes static state estimation and event screening and ranking, a *security assessment* to determine the level of security in the system, a *post-processing* to estimate the dynamic status of the system (stable or unstable), the determination of stability margins and the sensitivity of the transfer limits to those margins, and finally a *control process* to implement the appropriate actions to ensure security in the system again. On-line security assessment packages are commercially available today [IEEEStability, 2002]. Its accuracy is still limited by load model uncertainty.

Furthermore, the exponential dynamic model used during the work has been chosen because its adequacy to represent the load response in a load area mostly composed by electric heating and tap changers (area of study). However, and based on the results obtained in Chapter 7, this model representation can be improved. The normalization factor used in the

reactive load representation *Qo* is not appropriate and *So* is used instead. Besides, correlation between the active and reactive time constants has been found. The real and reactive powers are coupled and both real and reactive power load models should be simultaneously identified, with coupling effects. The correlation is not constant for all situations since it is depending on how much other external stochastic disturbances affect the system. A more accurate dynamic model is then desired.

A good suggestion for future work is the implementation of a dynamic model as a combination of the studied physical model and a stochastic extension. The basic deterministic and physically based model of the load will be described by the proposed set of non-linear differential equations, [Karlsson and Hill, 1994], and the stochastic part will include the noise term, but also the representation of disturbances to the system which are not measured or known, or unmodeled dynamics of the system.

The large amount of data from field measurements described throughout the thesis will hopefully be a valuable source for the continuation of this work and for reducing uncertainty in the load representation.

References

[Agneholm, 1999] E. Agneholm, 'Cold load pick-up'. Technical Report No.354. Department of Electric Power Engineering. Chalmers University of Technology. Göteborg, Sweden 1999.

[Arnborg, 1997] S. Arnborg, 'Emergency Control of Power Systems in Voltage Unstable Conditions'. Technical Report TRITA-EES-9701 ISSN 1100-1607. Department of Electrical Power Engineering. Royal Institute of Technology. Stockholm. Sweden 1997.

[Arnborg, et al., 1998] S. Arnborg, G. Andersson, D.J. Hill and Ian A. Hiskens, 'On influence of load modeling for undervoltage load shedding studies'. IEEE Transactions on Power Systems, Vol.13, No.2, pag. 395-400, May 1998.

[Åström and Wittenmark, 1984] K.J. Åström, B. Wittenmark, 'Computer Controlled Systems. Theory and Design'. Prentice-Hall, Inc., Englewood Cliffs, N.J. 07632. USA 1984.

[Bearden, 2000] T.E.Bearden, 'The Unnecessary Energy Crisis: How to Solve It Quickly'. Association of Distinguished American Scientists (ADAS). Final Draft. June 24, 2000.

[Bergh, 1996] S.G. Bergh, 'Diagnosis problems in wastewater settling'. Technical Report No. 91-88934-01-2. Department of Industrial Electrical Engineering and Automation. Lund Institute of Technology. Sweden 1996.

[CIGRE, 1993] CIGRE TF 38-02-10, 'Modeling of Voltage Collapse Including Dynamic Phenomena', 1993.

[Lin, et al., 1993] C. Lin, Y. Chen, C. Chiou, C. Huang, H. Chiang, J. Wang, L. Fekih-Ahmed, 'Dynamic Load Models in Power Systems Using the Measurement Approach'. IEEE Transactions on Power Systems, Vol. 8, No. 1, pp 309-315, February 1993

[Dovan, et al., 1987] T. Dovan, T.S. Dillon, C.S. Berger, K.E. Forward, 'A Microcomputer Based On-line Identification Approach to Power System Dynamic Load Modeling' IEEE Transactions on Power System, Vol. PWRS-2, No. 3, August 1987, pp 539-533.

[Hill, 1993] D.J. Hill, 'Nonlinear dynamic load models with recovery for voltage stability studies'. IEEE Transactions on Power Systems, Vol.8, No.1, pp. 166-176, February 1993.

[Hill and Hiskens, 1994] D.J. Hill and Ian A. Hiskens, 'Modeling, stability and control of voltage behavior in power supply systems'. IV Symposium of Specialists in Electrical Operational and Expansion Planning, Foz do Iguacu, Brazil, May 1994.

[IEEE, 1990] IEEE Committee Report, 'Voltage Stability of Power Systems: Cocepts, Analytical Tools, and Industry Experience', IEEE/PES 90[TH]0358-2-PWR, 1990.

[IEEELoad, 1993] IEEE Task Force on Load Representation for Dynamic Performance, 'Load representation for dynamic performance analysis'. IEEE Transactions on Power Systems, Vol.8, No.2, pp. 472-482, May 1993.

[IEEELoad, 1995] IEEE Task Force on Load Representation for Dynamic Performance, 'Standard load models for power flow and dynamic performance simulation'. IEEE Transactions on Power Systems, Vol.10, No.3, pp. 1302-1313, August 1995.

[IEEEStability, 1990] IEEE Stability Special: 'Voltage Stability of Power Systems: Concepts, Analytical Tools and Industry Experience' IEEE Special Publication, 90[TH]0358-2-PWR, 1990.

[IEEEStability, 2002] IEEE Stability 'Voltage Stability Assessment: Concepts, Practices and Tools'. IEEE/PES Special Publication. Power System Stability Subcommittee. August 2002.

[Johansson, 1993] R. Johansson, 'System Modeling and Identification'. Prentice-Hall, Englewood Cliffs, NJ 1993.

[Johansson and Sjögren, 1995] S. Johansson, F. Sjögren, 'Voltage Collapse in Power Systems. 'The influence of generator current limiters, on-load tap changers and load dynamics'. Technical Report No. 192L. Department of Electrical Power Engineering. Chalmers University of Technology. Göteborg, Sweden 1995.

[Ju, et al., 1996] P. Ju, E. Handschin and D. Karlsson, 'Nonlinear dynamic load modeling: model and parameter estimation'. IEEE Transactions on Power Systems, Vol.11, No.4, pp. 1689-1697, November 1996.

[Karlsson and Pehrsson, 1985] D. Karlsson and T. Pehrsson, 'A dynamic power system load model and methods for load model parameter estimation'. Technical Report 22L. Department of Electrical Power Systems. Chalmers University of Technology, Sweden. 1985.

[Karlsson, 1992] D. Karlsson, 'Voltage stability simulations using detailed models based on field measurement'. Technical Report No. 230. Department of Electrical Power Systems. School of Electrical and Computer Engineering. Chalmers University of Technology, Göteborg. Sweden 1992.

[Karlsson and Hill, 1994] D. Karlsson and D.J. Hill, 'Modeling and identification of nonlinear dynamic loads in power systems'. IEEE Transactions on Power Systems, Vol.9, No.1, pp. 157-166, February 1994.

[Kundur, 1994] P. Kundur, 'Power System Stability and Control'. Pp 17-40, 271-312, 959-1000. Electric Power Research Institute, McGraw-Hill, USA, 1994.

[Larsson, 2000] M. Larsson, 'Coordinated voltage control in electrical power systems'. Technical Report No. ISBN 91-88934-17-9. Department of Industrial Electrical Engineering and Automation. Lund University 2000. Sweden.

[Le Dous, 1999] G. Le Dous, 'Voltage stability in power systems. Load modeling based on 130 kV field measurements'. Technical Report No. 324L. Department of Electrical Power Engineering. Chalmers University of Technology. Göteborg, Sweden 1999.

[Liang et al., 1998] Y. Liang, R. Fischl, A. DeVito and S.C. Readinger, 'Dynamic reactive load model'. IEEE Transactions on Power Systems, Vol.13, No.4, pp. 1365-1372, November 1998.

[Ljung, 1995] L. Ljung, 'System Identification TOOLBOX', User's Guide. The Math Works Inc. August 1995.

[Machowski, et al., 1997] J. Machowski, J.W. Bialek, J.R. Bumby, 'Power System Dynamics and Stability'. Pp. 74-83, 235-253, Jonh Wiley & Sons. England 1997.

[Meteorol, 2002] Danish Meteorological Institute. Average monthly and weekly temperatures during July 2001-June 2002. www.dmi.dk/vejr/index.html

[Nordel, 1999] Nordel Annual Report. http://www.nordel.org/

[Olsson and Piani, 1992] G. Olsson and G. Piani, 'Computer systems for automation and control'. Technical Report No. ISBN 0-13-457581-4. Prentice Hall International (UK) Ltd., 1992.

[Padiyar, 1996] K.R. Padiyar, 'Power System Dynamics. Stability and Control'. Pp 3-9, 567-570. Indian Institute of Science, Bangalore. John Wiley & Sons (Asia) Pte Ltd and Interline Publishing Pvt. Ltd (India) 1996.

[Price, et al., 1993] William W. Price, Kim A. Wirgau, A. Murdoch, James V. Mitsche, E. Vaahedi and Moe A. El-Kady, 'Load modelling for power flow and transient stability computer studies'. IEEE Transactions on Power Systems, Vol.3, No.1, pp. 180-187, February 1988.

[Repo, 2001] S. Repo, 'On-line voltage stability assessment of power system-An approach of black-box modeling'. Publications 344. Tampere University of Technology. Tampere 2001. Finland.

[Romero1, 2001] I. Romero Navarro, (2001). 'Recording of Voltage, Active and Reactive Power at Tomelilla. TOMELILLA I'. Technical Report, CODEN: LUTEDX/(TEIE-7150). 2001 IEA, Lund, Sweden.

[Romero2, 2001] I. Romero Navarro, (2001). 'Recording of Voltage, Active and Reactive Power at Tomelilla. TOMELILLA II'. Technical Report, CODEN: LUTEDX/(TEIE-7151). 2001 IEA, Lund, Sweden.

[Roos, 2002] F. Roos, 'Coordinated Voltage Control'. Technical Report LUTEDX/(TEIE-5158)/1-35/(2002). Department of Industrial Electrical Engineering and Automation. Lund University. Sweden 2002.

[Sekine and Ohtsuki, 1990] Y. Sekine and H. Ohtsuki, 'Cascaded voltage collapse'. IEEE Transactions on Power Systems, Vol.5, No.1, pp. 250-255, February 1990.

[Svantesson, 2002] T. Svantesson, 'Automated Manufacture of Fertilizing Agglomerates from Burnt Wood Ash'. Technical Report No. ISBN 91-88934-24-1. LUTEDX\(TEIE-1032)/1-207/(2002). Department of Industrial Electrical Engineering and Automation. Lund University 2000. Sweden.

[Taylor, 1994] C.W. Taylor, 'Power System Voltage Stability', pp 17-135. Electric Power Research Institute, McGraw-Hill, USA, 1994.

[Willis, et al., 1995] H. Lee Willis, Linda A. Finley, M. Buri, 'Forecasting Electric Demand of Distribution Planning in Rural and Sparsely Populated Regions'. IEEE Transactions on Power Systems, Vol. 10, No.4, pp 2008-2013, November 1995.

[Xu and Mansour, 1994] W. Xu and Y. Mansour, 'Voltage stability analysis using generic dynamic load models'. IEEE Transactions on Power Systems, Vol.9, No.1, pp. 479-486, February 1994.

Appendix I

Results from the Identification

The appendix confines the results from applying the automatic determination process for identifying parameters in dynamic load models described in chapter 6.

July, August and September

TOMELILLA I at 20 kV. Friday 13/07/01 to Tuesday 17/07/01								
DATE	**FILE**	**TIME**	**PLOAD**			**QLOAD**		
			T_p	α_t	α_s	T_q	β_t	β_s
Friday 13/07/01	1	21.04	37	1.40	3.30	86	0.62	1.84
Saturday 14/07/01	2	10.36	245	2.40	-0.33	300	1.03	0.67
	3	16.16	153	1.30	0.78	163	0.82	0.37
	4	6.65	87	1.65	-0.81	160	0.85	0.32
	5	26.12	179	1.42	2.40	226	1.17	0.48
Sunday 15/07/01	6	4.86	80	1.40	1.20	120	0.80	0.40
Monday 16/07/01	7	13.34	750	1.40	3.70	216	0.90	-0.62
	8	26.12	87	1.80	2.33	384	0.64	0.34
Tuesday 17/07/01	9	8.31	43	1.30	0.78	205	0.65	0.42
	10	14.19	385	1.62	0.46	200	1.19	0.82
	11	21.58	91	1.50	1.50	241	0.83	1.47

TOMELILLA I at 20 kV. Sunday 12/08/01 to Saturday 18/08/01

DATE	FILE	TIME	PLOAD			QLOAD		
			T_p	α_t	α_s	T_q	β_t	β_s
Sunday 12/08/01	12	22.13	27	1.75	-0.38	30	0.57	1.20
	13	25.75	95	1.65	0.05	300	0.70	6.00
Monday 13/08/01	14	9.07	36	1.40	1.84	60	1.87	0.88
	15	9.46	17	1.32	-2.88	74	1.16	0.75
	16	24.78	84	1.20	0.62	141	1.16	0.89
	17	32.16	72	1.00	1.70	107	1.01	0.73
Tuesday 14/08/01	18	12.28	82	1.31	-1.20	120	0.69	0.16
	19	24.29	34	1.55	0.67	300	0.65	0.74
Wednesday 15/08/01	20	12.27	415	1.31	2.22	253	1.35	1.64
	21	15.37	113	1.83	1.88	201	1.64	0.74
	22	26.14	370	1.52	0.15	204	1.13	-0.42
Thursday 16/08/01	23	18.13	58	0.22	0.50	300	1.12	1.07
	24	26.11	40	1.42	0.10	178	1.39	-0.14
	26	25.21	126	1.03	0.84	244	1.11	-0.96
Saturday 18/08/01	27	13.33	53	1.85	-0.32	201	1.64	0.74

TOMELILLA I at 20 kV. Tuesday 21/08/01 to Sunday 26/08/01

DATE	FILE	TIME	PLOAD			QLOAD		
			T_p	α_t	α_s	T_q	β_t	β_s
Tuesday 21/08/01	28	25.86	151	1.10	32.70	163	1.40	-1.91
Wednesday 22/08/01	29	8.38	909	1.60	3.10	297	0.72	1.02
	30	18.24	111	1.40	0.97	121	1.45	0.82
Thursday 23/08/01	31	8.65	273	1.60	-1.60	281	1.40	-2.25
	32	18.40	211	1.99	0.00	217	1.45	-0.22
Friday 24/08/01	33	9.07	160	1.54	0.36	183	1.65	0.21
	34	23.88	874	1.85	3.00	88	0.96	1.05
Saturday 25/08/01	35	13.62	150	1.34	0.86	95	1.41	0.86
	36	21.50	106	1.43	2.26	221	1.30	0.96
Sunday 26/08/01	37	12.80	31	1.66	1.17	131	1.27	0.26

TOMELILLA I at 20 kV. Monday 03/09/01

DATE	FILE	TIME	PLOAD			QLOAD		
			T_p	α_t	α_s	T_q	β_t	β_s
Monday 03/09/01	38	15.11	348.0	1.80	0.00	109	1.57	0.89
	39	22.31	331.9	1.71	0.32	300	1.20	-0.01

| 40 | 26.30 | 18.5 | 1.28 | 1.92 | 110 | 1.55 | 0.51 |
| 41 | 32.68 | 89.3 | 1.31 | 0.36 | 102 | 0.93 | 0.66 |

January

TOMELILLA V at 20 kV. Tuesday 08/01/02 to Thursday 31/01/02								
DATE	**FILE**	**TIME**	**PLOAD**			**QLOAD**		
			T_p	α_t	α_s	T_q	β_t	β_s
Tuesday 08/01/02	1	19.80	223	1.50	-0.07	100	0.65	0.66
	2	21.60	142	1.58	0.11	102	0.77	0.30
Wednesday 09/01/02	3	4.82	106	1.73	0.78	142	1.25	0.25
	4	8.15	56	1.88	1.28	67	0.91	0.56
	5	9.35	124	1.91	0.01	138	0.89	0.40
	6	12.05	44	1.71	0.77	177	0.79	0.51
	7	17.65	124	1.54	1.10	130	0.66	0.78
	8	18.56	198	2.00	1.43	247	0.91	-0.43
	9	20.25	126	1.80	-0.24	131	0.73	-0.20
Thursday 10/01/02	10	4.8	300	1.87	2.40	238	0.61	1.20
	11	5.65	107	1.97	-0.73	111	0.64	-0.65
	12	5.80	138	1.75	1.49	76	0.78	0.45
	13	6.85	87	1.56	1.73	172	0.79	1.44
	14	17.25	168	2.41	0.80	168	1.56	1.26
	15	20.6	54	1.40	0.8	71	0.93	0.53
	16	21.9	110	1.43	-0.10	103	0.78	0.91
	17	22	62	2.12	0.5	61	0.98	0.56
Friday 11/01/02	18	5.01	115	1.80	0.43	87	0.47	0.67
	19	5.95	126	1.20	-0.35	111	0.60	0.59
	20	7.45	150	1.40	0.48	116	0.94	0.43
	21	7.78	75	1.71	1.27	122	1.10	1.03
	22	9.90	198	1.51	0.66	109	0.69	0.72
	23	12.10	76	1.87	0.67	61	1.00	0.43
	24	13.9	162	2.00	-0.94	185	0.76	-0.01
	25	19.80	200	2.11	1.03	171	0.72	0.37
	26	21.60	182	1.72	0.14	101	0.94	-0.15
	27	22.95	107	1.93	1.36	76	0.78	0.24
Saturday 12/01/02	28	1.75	103	1.85	1.97	110	0.60	0.32
	39	4.00	90	2.00	1.01	86	0.72	0.11
	30	9.80	182	1.80	1.01	183	0.62	0.88
	31	16.35	95	2.28	1.02	108	0.88	0.85
	32	17.30	85	2.44	-0.90	166	0.68	0.19
	33	18.80	112	2.02	0.83	176	0.64	0.25
	34	20.50	96	1.92	0.88	100	0.82	-0.23
	35	21.65	51	2.07	0.90	178	0.61	0.01
Sunday 13/01/02	36	5.60	80	2.16	-0.13	94	0.65	-0.43
	37	7.10	102	1.70	1.41	78	0.63	0.59
	38	10.30	113	2.32	-0.59	184	0.68	0.22
	39	12.10	107	1.99	0.65	111	0.51	0.50

	40	19.80	55	1.40	1.60	99	1.20	-0.52
	41	21.10	146	2.02	1.50	102	0.61	1.01
	42	22.45	230	2.39	0.88	79	1.13	0.51
	43	23.05	112	1.35	0.27	184	0.62	0.74
Monday 14/01/02	44	1.30	159	1.55	0.31	101	0.60	0.70
	45	4.70	123	1.70	-1.70	102	0.62	1.31
	46	5.35	125	2.35	1.14	86	0.97	0.62
	47	8.65	135	1.90	-0.89	127	0.78	-0.01
	48	11.85	111	1.46	0.94	102	1.06	0.44
	49	13.50	126	2.12	0.19	257	1.06	1.30
	50	16.20	132	2.78	-0.5	99	1.15	-0.55
	51	18.05	144	1.60	-0.75	124	0.85	0.52
	52	21.50	77	0.84	0.77	139	0.47	0.21
	53	21.75	133	1.52	1.24	82	0.49	0.41
Tuesday 15/01/02	54	4.95	127	1.62	0.60	181	0.37	0.22
	55	5.55	166	1.75	-0.21	101	0.84	0.74
	56	5.75	217	2.12	1.22	124	1.05	0.25
	57	6.00	129	2.03	1.38	104	0.98	1.84
	58	6.60	218	2.04	0.84	119	0.86	1.50
	59	7.95	183	2.16	1.05	102	1.01	1.22
	60	11.85	98	2.35	0.08	94	0.71	0.80
	61	15.90	185	1.87	0.70	267	1.06	1.73
	62	16.20	103	1.60	1.04	145	0.75	1.70
	63	18.95	122	2.09	1.80	102	0.90	0.57
	64	20.55	143	2.52	-0.61	111	0.81	0.76
	65	20.75	128	1.64	1.34	102	0.57	0.72
	66	21.05	85	2.22	-0.04	95	0.92	0.16
	67	22.00	103	1.85	1.02	101	0.60	0.72
Wednesday 16/01/02	68	4.82	81	2.57	0.30	109	0.78	-0.09
	69	8.15	92	1.50	1.77	101	0.81	0.93
	70	9.35	122	2.41	-0.38	111	0.91	0.68
	71	12.05	60	1.70	1.20	146	0.74	0.80
	72	16.20	98	1.50	0.47	213	1.01	-0.21
	73	17.65	60	1.20	0.29	102	0.76	1.68
	74	18.56	97	1.68	0.39	62	0.74	0.31
	75	20.25	117	1.71	0.81	198	0.81	-0.09
	76	21.50	81	2.86	1.56	92	0.88	0.16
Thursday 17/01/02	77	4.21	99	1.49	1.47	212	1.0	-0.2
	78	5.68	60	1.20	2.29	102	0.7	1.68
	79	6.57	97	1.68	0.39	62	0.74	0.31
	80	8.28	116	1.71	0.81	198	0.81	-0.09
	81	9.50	81	2.86	1.57	92	0.88	0.16
	82	13.56	151	1.72	0.73	172	0.79	2.20
	85	21.88	144	2.25	-0.46	101	0.77	0.21
	86	22.86	286	2.27	-0.54	101	0.58	0.54
Friday 18/01/02	87	1.77	102	1.36	0.70	142	0.91	0.64
	88	4.50	71	1.89	0.98	100	1.12	-0.18
	90	9.47	104	1.50	1.65	101	0.83	0.48
	91	14.93	117	1.80	-1.27	80	0.79	0.11
	92	17.93	121	2.05	1.68	116	0.95	0.81

	93	18.40	118	1.67	0.87	199	0.84	1.55
	94	19.26	145	2.27	-0.44	95	0.66	-0.01
	95	23.50	106	1.65	1.75	183	0.55	0.96
	96	24.70	81	1.91	0.29	220	0.64	0.33

Saturday 19/01/02	97	2.20	101	2.42	0.60	83	1.00	0.37
	98	9.82	104	1.70	-0.88	231	0.73	0.16
	99	15.80	93	2.29	1.77	212	0.48	1.61
	100	17.73	288	1.81	0.58	140	0.60	0.17
	101	18.84	285	1.52	-1.78	101	0.48	0.52
	102	23.89	228	3.01	1.80	82	0.66	0.55
Sunday 20/01/02	103	5.58	167	1.82	2.23	143	0.87	-0.07
	104	5.79	104	1.62	1.55	158	0.89	1.02
	105	19.58	87	0.58	2.14	101	0.74	1.27
	106	19.82	190	3.14	0.70	85	0.70	0.42
Monday 21/01/02	107	8.70	178	2.08	0.64	98	0.92	0.91
	108	12.00	51	2.30	-0.06	62	0.65	1.30
	109	16.14	117	2.24	-1.70	103	0.84	0.97
	110	16.40	198	1.40	-1.07	101	0.86	0.83
	111	19.17	153	1.15	1.51	111	0.75	0.65
	112	23.47	212	1.96	0.21	119	0.51	0.39
	113	23.82	169	2.16	0.92	76	0.52	0.20
	114	24.82	106	1.30	0.24	111	0.62	0.70
Tuesday 22/01/02	115	3.75	102	0.56	1.49	175	0.01	1.30
	116	6.84	106	1.51	1.26	101	0.84	0.80
	117	8.21	152	1.74	0.10	88	0.79	1.93
	118	11.96	116	0.95	0.26	130	0.96	0.36
	119	12.80	60	2.50	1.99	81	1.33	-0.25
	120	20.55	141	1.18	0.62	256	0.54	0.43
	121	21.45	104	0.37	2.91	140	0.73	0.19
	122	21.69	68	1.50	0.93	263	0.68	-1.22
	123	24.72	144	1.44	1.12	85	0.72	0.23
Wednesday 23/01/02	124	5.10	183	1.66	0.59	111	0.84	0.50
	125	6.78	165	1.45	2.45	105	0.89	1.08
	126	11.46	245	2.17	0.27	58	0.37	1.00
	127	12.04	164	1.57	-1.65	83	0.97	0.65
	128	13.14	87	2.06	-0.68	102	1.04	1.35
	129	20.20	137	0.76	6.14	110	0.91	0.15
	130	21.94	226	1.60	2.13	98	0.63	-0.40
	131	23.30	96	2.01	-0.45	100	0.57	-0.10
Thursday 24/01/02	132	8.19	111	2.08	-1.47	73	1.35	1.05
	133	9.33	101	1.43	0.92	100	1.28	0.10
	134	12.85	97	3.32	0.20	54	0.73	1.04
	135	18.15	134	2.36	1.15	52	0.73	1.20
	136	19.86	142	2.00	1.79	130	1.00	0.83
	137	21.27	96	2.08	0.87	74	0.63	0.14
	138	23.76	101	1.43	0.36	136	0.50	-0.64
Friday 25/01/02	139	4.27	139	1.64	1.20	125	0.62	-0.08
	140	5.19	80	2.11	1.52	128	0.56	0.74
	141	7.45	153	2.08	-0.70	116	0.94	0.82
	142	21.44	105	1.97	1.37	124	0.63	0.93
Saturday 26/01/02	143	1.74	103	1.84	1.96	124	0.60	0.93

	144	4.03	90	2.00	1.01	110	0.72	0.32
	145	9.80	182	1.79	2.58	86	0.61	0.11
	146	16.34	95	2.28	1.02	183	0.87	0.87
	147	17.33	85	2.44	-0.90	108	0.68	0.85
	148	18.81	112	2.02	0.83	166	0.64	0.19
	149	21.68	51	2.07	0.99	175	0.61	0.25
	150	23.72	296	3.30	-1.70	179	0.67	0.01
Sunday 27/01/02	151	9.75	129	2.7	-0.88	155	0.55	0.27
	152	11.08	168	1.10	1.74	94	0.58	-0.60
	153	23.60	100	1.20	-0.58	133	0.58	0.05
	154	23.87	226	2.53	-0.14	200	0.77	0.21
Monday 28/01/02	156	5.07	81	1.77	1.82	129	0.70	-0.01
	157	7.34	127	1.50	1.53	89	1.07	1.19
	158	11.93	89	2.38	-0.74	115	0.95	1.45
	159	13.87	75	2.12	-1.30	115	0.90	-0.17
	160	18.92	170	1.84	1.03	166	0.88	-0.11
	161	21.43	176	1.62	2.75	101	0.63	0.64
	162	21.73	110	2.20	0.15	107	1.10	-0.48
	163	6.22	97	2.34	0.02	104	1.00	0.03
	164	10.04	102	2.0	1.90	189	0.59	1.50
	165	11.68	110	2.21	-0.03	146	0.95	0.62
	166	15.07	165	1.69	-0.58	268	0.68	0.14
	167	16.77	94	1.30	-1.04	193	1.17	-0.90
	168	19.71	102	1.81	0.85	157	1.26	1.15
	169	20.12	100	1.38	-0.12	106	0.69	0.66
	170	20.68	73	1.81	1.01	65	0.78	0.09
	171	21.39	106	1.76	0.46	100	0.86	-0.22
	172	21.65	89	0.94	0.18	104	0.40	-0.26
	173	23.70	101	1.09	0.86	117	0.80	0.02
Wednesday 30/01/02	174	5.53	134	0.60	1.58	223	1.18	-0.03
	175	12.91	279	2.72	-1.58	100	1.22	-0.23
	176	16.46	206	2.97	2.73	225	1.21	0.35
	177	18.73	78	1.11	0.69	96	0.88	-0.01
	178	21.40	127	1.25	0.52	121	0.85	0.88
	179	21.99	89	3.32	1.26	138	0.81	-0.55
Thursday 31/01/02	180	871	121	1.39	0.49	260	0.72	-0.72
	181	10.83	96	1.71	-0.02	77	1.21	0.58
	182	11.88	105	1.55	1.49	86	1.07	0.62
	183	13.70	101	1.29	-0.10	101	0.98	1.02
	184	17.57	147	1.49	-1.07	163	1.09	1.07

February

TOMELILLA V at 20 kV. Sunday 27/01/02 to Tuesday 19/02/02								
DATE	FILE	TIME	PLOAD			QLOAD		
			T_p	α_t	α_s	T_q	β_t	β_s
Friday 01/02/02	27	7.05	137	2.20	-0.34	126	1.35	0.04
	28	8.75	100	2.35	0.71	280	0.74	0.88
	29	12.85	399	2.99	1.00	219	0.55	0.92
Saturday 02/02/02	30	10.45	208	2.71	0.68	193	0.97	1.25
	31	21.95	158	2.37	1.15	291	0.68	0.48
	32	24.05	111	2.16	-0.25	216	0.61	0.19
Sunday 03/02/02	33	2.80	103	2.39	0.28	127	0.63	0.01
	34	9.80	55	1.95	0.00	175	0.50	0.24
	35	14.65	35	1.98	1.25	196	1.18	0.81
	36	22.65	256	2.41	0.00	196	1.18	0.81
Monday 04/02/02	37	3.95	23	2.39	1.20	29	0.56	0.20
	38	6.35	365	1.95	-0.21	107	1.35	0.82
	39	6.70	327	1.98	0.00	216	1.12	0.71
	40	10.70	91	2.41	-0.94	27	0.73	1.00
	41	14.75	96	3.58	0.17	106	2.08	1.08
	42	16.70	57	1.80	0.14	93	1.12	0.57
	43	20.90	53	1.20	1.21	91	0.70	0.79
Tuesday 05/02/02	44	6.80	97	2.76	0.00	95	1.23	0.85
	45	11.85	111	1.80	0.00	280	0.85	0.45
	46	12.75	113	1.64	-0.87	250	1.49	0.17
	47	16.05	81	1.20	0.00	90	1.19	0.08
	48	17.70	84	2.46	0.00	300	1.18	-0.85
	49	19.10	129	1.85	0.51	106	0.98	-0.16
Wednesday 06/02/02	50	3.20	96	1.99	0.32	58	0.67	0.40
	51	6.80	141	1.95	-0.07	163	1.12	0.44
	52	7.35	67	2.44	1.22	51	1.24	0.89
	53	9.85	125	2.16	-0.50	207	1.04	-0.35
	54	14.05	87	2.03	0.41	71	1.24	0.33
	55	17.65	44	1.22	0.08	105	0.88	0.73
Thursday 07/02/02	56	5.40	271	2.07	0.57	117	0.94	0.35
	57	15.25	168	1.42	2.07	197	0.94	0.08
	58	16.75	77	1.95	0.88	90	0.95	0.50
Friday 08/02/02	59	5.75	150	2.10	-3.64	104	0.96	-0.40
	60	12.65	72	2.80	1.63	114	0.82	0.22
	61	14.65	200	2.65	1.31	130	0.80	0.21
	62	24.45	70	1.77	0.50	184	0.40	-0.07
	63	24.70	189	1.89	0.33	176	0.74	0.00
Saturday 09/02/02	64	1.90	20	2.96	1.30	300	0.61	0.52
	65	8.00	43	2.82	1.51	281	0.50	-0.48
	66	17.00	98	3.15	1.08	301	1.06	-0.05
	67	22.85	83	1.80	1.98	205	0.75	-0.18
Sunday 10/02/02	68	4.30	172	2.33	0.20	211	0.53	1.04

	69	9.35	124	2.42	0.00	242	0.96	-0.30
Monday 11/02/02	70	9.90	131	2.35	-0.50	160	1.25	0.09
	71	11.75	296	1.54	0.82	23	1.30	0.48
	72	12.30	110	2.37	-0.58	172	0.82	-0.25
	73	23.80	35	3.60	0.48	112	0.85	-0.01
Tuesday 12/02/02	74	6.35	23	1.99	2.76	111	0.72	-0.24
	75	9.65	92	2.40	-0.54	283	0.70	0.83
	76	10.40	78	2.26	0.14	182	1.35	0.70
	77	14.40	209	1.21	0.00	308	1.03	0.91
	78	9.80	130	1.34	-1.31	160	0.96	0.21
	79	15.65	75	2.44	2.68	81	1.22	0.50
	80	18.80	94	1.99	0.06	126	0.95	0.29
Thursday 14/02/02	81	5.40	158	2.45	0.28	130	0.67	-0.20
	82	11.15	382	2.04	0.00	107	0.83	0.70
	83	16.25	240	2.05	0.00	117	0.677	0.11
	84	14.65	53	1.55	0.04	65	0.605	0.81
	85	23.35	292	1.61	0.00	117	0.39	-0.14
Saturday 16/02/02	86	7.60	118	2.32	1.75	108	0.76	0.72
	87	12.35	170	2.06	0.00	418	0.55	0.65
Sunday 17/02/02	88	12.35	56	2.06	1.82	30	0.45	0.36
	89	19.80	119	2.65	-0.35	125	0.84	-0.51
Monday 18/02/02	90	7.25	52	1.64	1.13	69	0.60	1.17
	91	18.55	254	2.55	0.70	52	0.97	0.51
	92	19.60	113	2.46	1.94	117	0.77	0.45
	93	23.40	137	1.61	1.31	158	0.70	-0.29

TOMELILLA V at 20 kV. Sunday 27/01/02 to Tuesday 19/02/02

DATE	FILE	TIME	PLOAD			QLOAD		
			T_p	α_t	α_s	T_q	β_t	β_s
Wednesday 20/02/02	94	5.00	121	1.72	1.24	273	0.43	1.67
	95	6.60	102	1.80	1.21	102	0.96	0.70
	96	7.35	174	2.75	-3.37	101	0.66	0.76
	97	8.28	100	1.84	0.26	55	0.54	1.15
	98	8.81	132	1.17	0.86	100	0.50	0.23
	99	11.59	70	1.22	2.27	145	0.51	1.47
	100	18.12	190	2.07	0.67	64	0.58	0.97
	101	18.70	100	1.45	1.49	144	0.78	0.38
	102	20.92	169	1.43	0.72	289	1.08	-0.11
Thursday 21/02/02	103	2.57	116	1.61	3.09	208	0.55	0.34
	104	4.99	60	2.82	1.50	155	0.97	0.54
	105	14.18	159	1.16	0.62	180	0.81	0.47
	106	18.24	111	1.69	0.59	102	0.58	0.64
	107	20.76	107	1.60	0.46	179	0.36	1.37
	108	21.31	99	1.93	0.55	141	1.13	-0.05
	109	21.86	136	1.53	0.76	101	0.45	0.45
Friday 22/02/02	110	7.27	130	1.63	3.43	233	0.65	3.45
	111	8.23	125	1.90	1.24	111	0.54	1.65

	112	15.94	92	1.31	2.57	75	0.69	0.97
	113	19.07	74	2.27	0.60	108	0.78	-0.08
	114	20.68	96	3.77	0.28	100	1.54	0.34
	115	24.26	100	2.60	0.05	133	0.51	0.28
Saturday 23/02/02	116	8.53	62	1.47	2.87	116	0.85	0.02
	117	8.84	136	2.56	-0.12	69	0.69	1.28
	118	10.19	168	1.83	0.76	142	0.43	0.91
	119	14.14	107	1.17	1.96	100	0.41	-0.36
	120	18.26	253	2.32	0.71	64	0.66	0.47
	121	20.17	67	1.36	0.68	91	0.81	0.12
	122	24.33	155	2.66	-0.76	101	0.80	0.75
	123	6.15	142	1.40	-1.50	143	0.60	0.16
	124	6.73	53	1.03	0.58	101	0.60	0.64
	125	9.40	60	2.64	0.86	68	0.52	0.74
	126	14.18	77	1.44	0.87	200	0.66	0.53
	127	17.89	138	2.39	-0.45	89	0.67	0.66
	128	21.83	72	1.59	2.78	101	0.53	0.13
	129	22.97	97	2.96	0.93	110	0.79	-0.79
Monday 25/02/02	130	2.08	99	1.13	-1.45	100	0.46	-0.38
	131	3.93	72	2.19	-0.42	71	0.59	0.56
	132	5.89	104	2.42	2.42	102	0.39	1.92
	133	6.92	179	2.23	0.94	111	0.98	0.56
	134	7.40	63	2.31	-0.15	101	0.60	0.40
	135	7.90	78	1.76	0.85	100	1.24	0.01
	136	10.99	101	2.88	1.12	139	1.15	0.37
	137	8.18	171	1.37	0.65	131	0.87	0.43
	138	20.37	108	1.98	0.52	102	0.79	0.78
	139	21.22	124	1.38	0.54	89	0.67	0.04
	140	21.83	95	2.21	-0.69	100	0.91	0.01
	141	23.35	192	2.37	0.44	101	0.90	0.93
Tuesday 26/02/02	142	5.94	158	2.98	-0.28	77	0.26	0.76
	143	6.36	78	2.07	1.45	97	0.95	-0.01
	144	6.73	86	1.14	1.18	66	0.44	0.78
	145	11.78	111	1.54	0.48	101	0.49	0.49
	146	13.14	80	2.96	-0.81	130	1.44	0.42
	147	15.37	277	1.12	-2.08	217	0.55	1.58
Wednesday 27/02/02	148	1.22	108	2.30	1.14	126	0.90	0.60
	149	5.93	100	2.06	0.41	100	0.68	-0.09
	150	6.60	267	1.63	0.92	122	0.87	0.10
	151	8.52	114	2.16	-0.28	102	0.85	1.70
	152	14.72	191	1.72	0.28	99	1.07	-0.85
	153	21.67	70	2.55	-0.20	120	0.44	1.60

April

TOMELILLA V at 20 kV. Monday 15/04/02 to Tuesday 30/04/02								
DATE	**FILE**	**TIME**	**PLOAD**			**QLOAD**		
			T_p	α_t	α_s	T_q	β_t	β_s
Monday 15/04/02	1	5.30	188	2.62	3.43	102	1.37	1.39
	2	10.14	247	1.15	0.13	100	0.80	-0.40
	3	10.70	96	0.16	0.07	104	0.91	-0.67
	4	17.13	104	2.75	3.90	222	0.36	2.35
	5	17.96	71	2.32	-2.30	101	0.82	0.34
	6	18.63	159	1.95	1.38	159	0.69	0.78
	7	18.92	77	1.86	0.48	193	0.98	0.36
Tuesday 16/04/02	8	11.14	129	0.59	2.65	95	0.97	0.24
	9	22.67	90	1.58	0.89	100	0.58	-0.09
	10	23.01	145	3.46	-2.75	95	0.54	1.66
Wednesday 17/04/02	11	5.01	164	2.40	-3.75	100	0.66	-0.23
	12	6.47	147	0.70	5.86	119	0.75	0.84
	13	7.09	64	1.71	2.66	155	0.66	0.75
	14	7.37	159	2.90	-3.78	192	0.84	1.63
	15	7.67	104	1.82	-0.39	111	0.95	0.82
	16	14.90	120	2.08	0.14	112	0.88	0.76
	17	18.11	96	1.59	-0.58	84	0.80	0.66
	18	18.73	233	0.59	3.82	224	0.43	1.00
Thursday 18/04/02	19	9.99	179	1.74	1.47	166	1.16	0.32
	20	11.95	239	1.94	0.47	101	0.92	1.00
	21	15.00	86	1.30	1.05	91	1.03	0.33
	22	16.08	251	1.31	1.42	185	0.79	0.03
	23	21.70	106	1.29	5.01	140	0.72	0.37
	24	22.05	111	1.52	1.43	131	0.64	0.38
	25	23.04	101	1.30	0.87	123	0.83	0.49
	26	6.10	78	1.30	0.07	284	0.53	1.11
	27	6.43	96	1.16	-0.30	77	0.91	0.40
	28	6.76	103	1.33	0.11	102	0.82	-0.72
	29	14.37	102	1.19	1.15	222	0.60	0.99
	30	16.18	156	1.40	0.80	64	0.70	1.10
	31	22.32	89	1.92	1.25	101	0.65	0.58
Saturday 20/04/02	32	6.75	262	2.10	0.76	132	0.81	0.61
	33	8.75	172	1.23	0.66	130	0.62	-0.28
	34	11.13	129	1.44	1.49	91	0.64	0.38
	35	14.30	70	1.77	0.35	101	0.78	0.38
	36	22.25	245	1.14	0.12	67	0.33	0.90
	37	14.03	91	1.39	-0.26	95	0.65	-0.80
Sunday 21/04/02	38	6.96	118	1.44	0.27	101	0.5	0.38
	39	13.05	57	1.46	0.91	96	0.64	-0.28
	40	15.60	200	2.19	0.66	126	0.59	0.10
	41	16.90	97	2.34	-0.29	160	0.70	0.17
	42	19.66	190	1.68	-0.38	217	0.62	0.79

	43	22.87	100	1.88	0.17	90	0.80	-0.05
Monday 22/04/02	44	5.09	140	1.95	1.04	101	0.62	0.64
	45	5.90	93	1.84	0.81	101	0.75	0.91
	46	6.30	78	2.05	1.20	80	0.80	-0.08
	47	8.03	140	1.90	0.99	287	0.72	1.93
	48	13.06	57	1.46	0.91	96	0.64	-0.28
	49	15.60	200	2.19	0.66	126	0.59	0.09
	50	16.93	97	2.34	-0.29	160	0.70	0.16
	51	19.66	190	1.68	-0.38	217	0.62	1.79
	52	22.09	195	1.15	0.78	101	0.70	0.53
	53	22.87	100	1.88	0.18	90	0.81	-0.06
Tuesday 23/04/02	54	5.09	140	1.95	1.04	101	0.62	0.64
	55	5.90	93	1.84	0.81	101	0.75	0.91
	56	6.30	78	2.05	1.19	80	0.80	-0.08
	57	8.03	140	1.90	0.99	287	0.72	1.90
	58	12.88	134	1.71	-1.50	183	0.93	1.82
	59	20.63	239	1.86	-1.18	122	0.96	0.51
	60	22.01	129	2.05	0.70	100	0.94	-0.06
Wednesday 24/04/02	61	4.88	216	1.37	1.57	174	0.60	0.17
	62	5.85	57	1.46	1.30	216	0.32	1.44
	63	9.57	52	1.37	0.96	195	0.69	0.90
	64	10.28	179	1.08	2.25	116	0.60	0.87
	65	10.92	112	1.84	1.80	100	0.59	-0.32
	66	11.13	104	1.25	0.80	100	0.30	0.05
	67	17.36	246	1.95	0.35	66	0.96	0.59
	68	18.41	132	1.15	1.70	237	0.86	1.20
	69	18.72	106	1.36	0.76	72	0.71	1.93
Thursday 25/04/02	70	11.58	107	1.49	-1.22	51	1.08	0.30
	71	13.02	140	1.19	1.50	102	0.84	0.57
	72	18.45	99	1.58	-0.43	113	1.00	0.87
	73	21.32	181	1.45	3.5	134	0.73	0.88
	74	23.67	126	1.70	6.21	92	1.38	1.44
Friday 26/04/02	75	6.97	156	2.19	0.47	117	1.24	0.55
	76	13.62	81	1.57	-0.68	283	0.90	0.28
	77	13.95	124	1.56	1.76	116	1.25	0.24
	78	22.60	200	1.78	2.36	90	0.48	-0.50
Saturday 27/04/02	79	1.00	181	2.58	0.19	113	0.89	-0.84
	80	7.00	89	2.15	-0.01	161	0.82	1.84
	81	11.17	278	0.56	3.61	200	0.80	0.80
	82	19.04	88	1.66	1.06	135	0.74	-0.01
	83	22.70	85	1.66	0.38	101	0.60	0.62
	84	22.74	117	1.82	0.79	103	0.71	0.67
Sunday 28/04/02	85	6.20	104	1.99	2.28	97	0.78	0.77
	86	21.80	133	1.62	0.92	100	0.87	-0.28
Monday 29/04/02	87	6.46	78	1.48	1.33	160	0.71	1.41
	88	6.77	86	1.53	-1.18	112	1.28	0.44
	89	8.09	84	1.64	-1.30	138	0.89	1.23
	90	12.57	121	2.15	-0.92	286	1.00	0.85
	91	15.60	264	2.44	0.24	102	1.10	0.76
	92	18.60	103	1.04	0.52	89	0.50	0.01
	93	22.59	205	1.15	4.68	159	0.74	0.26

Tuesday 30/04/02	94	6.74	156	2.77	-3.49	154	0.50	1.21
	95	16.44	142	1.99	-0.45	111	1.38	1.02
	96	18.68	114	2.31	1.00	130	0.96	1.30
	97	20.39	138	2.08	-0.90	120	0.88	0.21

May

TOMELILLA V at 20 kV. Wednesday 01/05/02 to Monday 13/05/02								
DATE	**FILE**	**TIME**	**PLOAD**			**QLOAD**		
			T_p	α_t	α_s	T_q	β_t	β_s
Wednesday 01/05/02	1	10.62	147	2.46	0.94	220	1.30	0.60
	2	12.36	54	1.63	0.27	101	0.78	0.47
	3	15.47	87	1.94	0.86	100	0.94	-0.02
	4	20.89	103	1.29	-0.31	117	0.63	0.11
	5	22.93	91	1.99	0.75	100	0.33	-0.18
	6	23.22	147	1.91	1.38	103	0.58	1.88
Thursday 02/05/02	7	5.91	79	1.30	-0.29	100	0.55	-0.09
	8	6.67	176	2.32	0.65	148	1.13	0.70
	9	12.03	136	1.38	-1.95	101	1.10	0.60
	10	13.94	145	1.96	2.97	113	1.13	0.98
	11	18.30	121	1.33	0.60	120	0.87	-0.09
	12	20.85	77	2.40	-1.46	100	0.94	-0.63
	13	21.58	95	2.09	2.13	148	1.00	-0.18
	14	22.58	102	1.43	1.81	89	0.85	0.18
Friday 03/05/02	15	4.12	111	1.55	1.46	194	0.67	0.16
	16	6.06	169	1.39	1.44	90	0.40	0.15
	17	6.30	103	2.08	2.26	122	1.37	0.97
	18	6.86	231	1.65	3.91	101	0.83	0.84
	19	7.15	81	1.04	0.49	119	0.86	0.63
	20	7.41	77	1.15	2.19	112	0.80	0.65
	21	11.60	141	1.67	0.69	111	1.54	1.21
	22	14.12	91	1.78	1.55	91	0.88	0.77
	23	16.55	126	1.24	1.03	111	0.53	0.48
	24	18.91	95	1.53	0.51	91	0.86	0.88
	25	20.28	62	1.70	1.63	230	0.55	0.98
Saturday 04/05/02	26	9.60	170	1.20	-0.80	100	0.60	-0.21
	27	16.98	174	1.00	-0.89	159	0.67	-0.26
	28	22.55	109	1.96	-0.95	183	0.65	0.46
Sunday 05/05/02	29	6.77	100	1.39	-0.17	154	0.70	0.73
	30	8.66	100	1.60	1.34	106	0.47	-0.07
	31	14.72	174	1.02	-0.80	150	0.50	-0.25
	32	21.46	104	2.93	-0.44	100	1.03	2.67
	33	22.82	65	2.82	-0.40	180	0.47	5.75
	34	23.74	186	1.95	-1.38	266	1.28	5.32
Monday 06/05/02	35	9.88	101	1.14	1.05	110	1.47	0.37
	36	10.39	100	0.58	0.03	140	1.04	1.47
	37	14.17	62	0.67	1.32	174	1.90	0.03

	38	22.55	259	0.69	3.30	94	0.98	0.04
Tuesday 07/05/02	39	11.93	64	1.75	1.25	150	1.23	0.68
	40	16.00	81	2.22	0.77	253	0.62	1.07
	41	17.98	227	2.63	0.01	124	1.50	0.91
	42	20.68	100	3.04	0.68	119	0.77	1.19
	43	22.15	181	1.99	0.85	215	0.76	1.26
	44	22.53	124	1.56	1.67	109	0.46	-1.09
Wednesday 08/05/02	45	6.00	140	1.30	1.97	100	0.45	0.18
	46	14.87	102	1.50	1.49	88	1.08	0.81
	47	16.21	91	1.34	1.60	147	1.23	1.03
	48	16.44	100	1.10	-0.17	88	0.74	0.30
	49	17.32	91	1.18	1.04	101	0.56	1.28
	50	19.66	112	1.69	1.33	104	0.73	0.75
	51	20.94	290	2.66	-1.92	102	1.22	1.26
	52	22.53	93	1.47	1.26	111	0.85	0.77
Thursday 09/05/02	53	6.74	125	1.57	-1.37	100	1.13	-1.04
	54	8.22	190	2.48	-5.08	101	0.87	0.66
	55	15.40	292	1.15	2.01	250	0.63	2.95
	56	16.62	178	4.06	-1.36	134	0.97	-0.31
	57	17.96	179	3.57	2.08	57	1.28	-0.01
	58	20.04	145	1.64	0.44	101	1.04	0.96
	59	20.22	219	2.56	-0.58	102	0.87	0.78
	60	20.91	152	4.26	0.78	68	0.42	1.30
Friday 10/05/02	61	6.17	84	1.60	0.18	266	1.05	2.33
	62	17.04	110	0.6	-1.77	188	0.65	-0.21
	63	18.62	174	1.80	0.90	112	0.72	0.95
Saturday 11/05/02	64	12.40	119	2.3	-2.66	18	0.74	0.28
	65	13.86	149	0.44	3.07	101	1.11	1.23
	66	14.75	100	2.48	-0.18	174	1.05	-3.21
	67	19.25	174	1.55	-0.2	172	0.68	0.27
	68	20.96	119	3.17	-0.88	100	0.34	-0.37
	69	22.50	151	1.67	0.51	123	0.84	0.46
	70	23.79	60	1.23	0.99	172	0.44	1.67
Sunday 12/05/02	71	4.84	115	1.02	-0.80	163	0.15	-1.58
	72	6.27	160	1.88	1.70	92	0.62	0.50
	73	9.37	203	1.61	0.31	115	0.80	0.89
	74	9.88	101	1.71	0.45	101	1.05	1.85
	75	10.50	233	1.23	2.60	130	0.78	1.55
	76	17.50	254	1.95	2.04	101	1.04	0.45
	77	17.90	101	2.95	1.17	99	1.42	-0.54
Monday 13/05/02	78	9.83	88	1.64	0.78	100	1.45	0.03
	79	12.90	129	2.57	-1.95	146	1.08	0.29
	80	20.95	99	1.05	-0.95	148	0.84	0.07
	81	21.29	121	1.26	0.76	116	0.58	0.22
	82	21.88	101	1.70	3.45	127	1.05	1.85
	83	22.91	105	0.78	3.45	53	0.77	0.88
	84	23.11	257	1.15	3.99	92	0.68	0.94
Tuesday 14/05/02	85	11.74	141	2.30	-1.25	273	1.09	0.63
	86	22.75	51	1.38	1.65	190	0.33	0.68
	87	24.80	71	2.14	1.80	267	0.64	1.39
Wednesday 15/05/02	88	6.46	87	1.95	-0.55	175	0.94	0.72

90	11.47	101	1.55	1.48	101	1.04	1.35
91	12.82	126	1.68	-0.44	103	0.93	2.14
92	18.76	107	1.43	-0.98	106	1.16	1.41
93	19.82	72	1.59	0.29	105	0.92	0.36
94	20.01	232	1.61	1.91	101	0.98	0.74
95	22.61	118	1.62	-0.13	119	0.60	-0.28
Thursday 16/05/02	96	5.90	114	1.03	0.33	65	1.20	0.97
	97	6.1	143	1.79	0.93	131	0.72	-0.38
	98	6.4	148	1.38	1.06	125	1.16	0.55
	99	15.80	58	1.63	0.99	100	1.61	0.26
	100	15.97	97	0.77	-0.38	117	1.91	0.75
	101	18.56	93	1.03	4.18	131	1.19	0.25
	102	19.70	158	2.74	-4.99	131	1.05	0.40
	103	20.71	116	1.79	0.58	101	0.79	0.46
	104	22.24	89	1.24	0.14	112	0.99	0.80
Friday 17/05/02	105	5.91	100	1.25	0.13	159	0.73	-0.49
	106	6.46	182	1.28	-0.68	257	0.85	1.91
	107	14.27	120	1.06	-0.47	173	1.06	1.37
	108	15.76	121	2.90	0.35	111	1.41	1.15
	109	18.66	104	1.60	2.47	131	0.85	1.25
	110	22.33	148	2.84	-0.22	121	1.24	1.04
	111	22.91	111	1.41	1.38	101	0.56	0.73
	112	23.70	52	1.10	-0.97	101	0.46	0.74
Saturday 18/05/02	113	11.70	63	1.86	0.74	100	0.80	0.00
	114	12.90	132	1.33	0.53	120	0.86	1.47
	115	19.30	99	1.43	3.12	103	0.62	1.09
Sunday 19/05/02	116	12.70	171	1.51	1.84	265	0.87	1.30
	117	17.80	60	2.15	-0.14	196	0.90	-0.61
	118	19.81	110	1.55	0.49	99	0.81	-0.44
	119	20.74	67	1.63	0.93	100	0.55	0.31
	120	21.29	12	2.18	2.39	101	0.82	-0.97
	121	22.39	89	1.73	1.01	285	0.72	0.56
	122	22.93	102	1.59	1.50	101	0.62	0.69
	123	23.69	104	2.08	2.94	185	1.34	-0.65
Monday 20/05/02	124	7.04	142	2.16	-2.44	196	1.40	0.62
	125	10.86	109	2.13	-0.88	101	0.79	1.50
	126	11.84	132	1.79	0.79	238	0.84	-1.38
	127	14.74	114	2.05	0.66	98	0.80	0.75
	128	20.70	119	1.30	-0.76	100	0.67	0.19
Tuesday 21/05/02	129	6.86	125	2.80	1.62	100	0.79	0.38
	130	10.15	85	1.18	0.32	206	0.80	1.43
	131	19.14	153	2.34	1.03	173	0.78	1.16
	132	19.33	95	1.51	-0.82	216	1.30	0.13
	133	20.93	107	1.54	-2.83	101	1.04	0.93
Wednesday 22/05/02	134	6.68	125	2.80	-1.60	100	1.30	0.19
	135	10.83	70	1.78	-0.40	101	0.96	0.87
	136	18.82	130	1.46	0.64	156	1.75	1.27
Thursday 23/05/02	137	11.95	85	1.78	0.86	254	1.27	3.17
	138	17.52	99	1.34	-0.85	97	1.18	-0.30
	139	18.88	113	1.46	-2.80	100	0.86	0.33
	140	20.93	107	1.54	-6.48	101	1.04	0.93

Friday 24/05/02	141	4.70	92	1.17	-1.30	99	1.06	-0.41
	142	8.30	101	1.03	0.92	101	0.88	0.87
	143	22.29	101	3.18	0.92	99	1.24	-0.99
	144	23.03	117	1.63	0.90	114	0.96	0.63
Saturday 25/05/02	145	4.84	112	1.77	1.95	118	1.38	-0.27
	146	6.40	107	1.35	-0.05	136	1.10	0.81
	147	6.68	73	0.95	0.00	90	0.95	0.35
	148	7.73	99	1.10	-0.49	102	0.89	0.18
	149	8.25	117	1.29	2.31	232	1.20	2.08
	150	13.49	188	1.52	-1.20	100	1.04	-0.03
	151	15.64	124	1.57	1.88	101	1.46	0.57
	152	18.36	92	1.58	1.17	57	0.83	0.35
	153	10.62	151	0.8	1.60	102	1.14	1.15
	154	12.72	104	1.61	2.77	97	0.45	-2.26
	156	7.04	151	0.91	1.25	100	0.83	0.12
	157	9.39	86	0.91	2.79	111	0.55	0.50
	158	17.19	58	1.55	1.03	154	0.42	1.72
	159	17.67	92	1.02	1.70	91	1.17	1.06
	160	19.23	89	1.54	0.52	100	0.91	0.14
	161	20.66	90	1.12	0.66	101	0.13	021
Sunday 26/05/02	162	10.46	145	1.47	3.14	226	0.87	1.88
	163	22.65	106	1.89	5.52	99	0.89	-0.22
Monday 27/05/02	164	5.61	180	1.52	2.94	165	0.81	1.82
	165	5.86	101	1.75	1.36	94	1.02	-1.21
	166	7.07	195	1.70	-0.07	218	0.83	3.14
	167	12.82	94	0.53	-0.84	166	1.68	-0.87
	168	13.11	80	0.99	1.04	205	1.45	-0.78
	169	16.88	59	1.63	0.52	99	1.13	-0.46
	170	17.84	98	0.70	-1.40	168	0.83	1.55
	171	20.77	125	1.28	1.06	91	0.70	0.72
	172	21.27	176	2.00	-5.27	100	0.79	-0.07
	173	22.27	83	1.64	1.11	129	0.87	0.11
	174	24.79	147	1.38	0.90	210	0.60	1.03
Tuesday 28/05/02	175	5.64	195	2.36	-1.00	61	0.69	0.32
	176	6.37	57	2.02	-1.23	73	1.31	-0.76
	177	7.33	104	1.49	2.49	188	1.33	0.31
	178	8.61	145	2.12	-2.14	119	1.36	0.66
	179	22.11	108	2.06	-0.68	220	1.08	1.68
Wednesday 29/05/02	180	8.09	89	1.00	0.51	158	0.69	1.15
	181	8.90	60	1.53	2.65	133	1.23	1.65
	182	20.60	229	2.02	-1.06	111	1.02	0.98
Thursday 30/05/02	183	6.35	104	1.53	5.15	101	1.07	0.67
	184	7.03	279	1.37	5.38	91	1.21	0.89
	185	10.70	148	1.61	4.56	132	1.60	1.32
	186	11.5	59	2.87	-0.23	58	1.20	-0.01
	187	12.36	80	0.59	1.49	91	1.29	1.20
	188	15.58	99	1.21	-0.92	101	0.78	0.79
	189	17.73	67	1.50	1.81	52	0.86	0.54
	190	19.53	281	1.75	8.23	234	1.08	2.43
	191	20.27	172	1.63	0.91	228	1.17	2.68
Friday 31/05/02	192	12.77	183	1.11	8.01	101	1.36	0.73

193	13.49	101	0.86	1.30	99	1.64	-0.44
194	15.64	141	0.16	0.34	100	1.54	-0.25
195	1640	269	1.35	4.76	291	0.78	2.25
196	18.4	166	1.90	2.44	238	1.03	0.17
197	18.68	101	1.35	1.57	151	0.65	1.17
198	20.39	80	1.46	1.07	100	0.79	0.10

June

TOMELILLA V at 20 kV. Wednesday 01/05/02 to Monday 13/05/02								
DATE	**FILE**	**TIME**	**PLOAD**			**QLOAD**		
			T_p	α_t	α_s	T_q	β_t	β_s
Saturday 1/06/02	1	9.65	80	1.59	-0.98	94	0.86	-1.25
	2	14.67	119	1.10	0.58	172	0.72	1.05
	3	20.44	115	1.07	0.56	101	0.66	0.76
	4	9.64	56	1.86	0.12	158	0.98	0.54
	5	18.52	54	0.68	2.58	133	0.58	0.30
	6	19.39	89	2.76	-0.52	100	0.71	0.04
Sunday 2/06/02	7	11.01	111	1.44	1.27	117	0.52	1.39
	8	19.65	101	1.25	0.93	55	0.30	0.71
	9	20.73	114	0.88	-1.05	99	0.71	-1.00
	10	10.42	189	1.87	3.81	59	1.06	1.33
	11	18.34	150	1.62	0.28	207	0.72	2.73
	12	19.64	104	1.66	1.88	102	1.23	1.80
	13	20.27	104	2.30	2.33	135	1.56	2.51
	14	20.41	117	0.48	0.07	111	1.05	0.71
Monday 3/06/02	15	9.56	290	3.33	-3.80	110	1.52	0.46
	16	17.05	72	2.04	1.52	100	1.35	-0.13
	17	19.60	122	1.33	0.36	100	0.98	0.00
	18	10.41	117	0.48	0.07	111	1.05	0.71
	19	12.64	90	1.12	0.02	91	1.29	0.39
	20	13.09	100	0.99	0.08	138	0.40	2.68
	21	17.58	70	0.75	1.16	100	0.79	-0.07
	22	18.41	231	1.62	-0.80	197	1.43	-2.27
	23	20.73	127	0.51	0.34	119	0.87	0.75
Tuesday 4/06/02	24	15.65	194	1.55	-1.69	112	1.20	1.04
	25	16.81	129	0.57	1.32	189	1.19	2.16
	26	17.78	58	0.43	4.09	97	1.24	-2.19
	27	18.06	134	1.75	-2.32	143	0.87	1.38
	28	18.60	212	1.12	0.88	100	1.68	0.42
	29	19.64	115	1.55	2.20	63	0.87	1.96
Wednesday 5/06/02	30	9.32	109	0.42	-2.08	100	1.55	0.21
	31	9.77	111	1.66	1.30	102	2.11	2.23
	32	10.64	99	0.40	-0.91	158	1.55	0.48
	33	18.02	57	0.85	-0.23	101	1.34	0.80
	34	19.35	200	1.51	2.83	75	1.32	0.64
Thursday 6/06/02	35	11.63	81	3.52	1.75	161	1.42	-1.78

	36	16.65	104	1.64	0.42	90	1.32	1.34
	37	11.14	81	1.80	-0.80	102	1.36	1.09
	38	17.83	138	0.39	-0.48	299	0.99	3.21
	39	18.57	86	1.23	-1.14	265	1.56	3.61
Friday 7/06/02	40	9.26	116	2.35	-0.05	288	1.65	2.30
	41	18.06	53	3.41	-0.44	132	0.70	0.84
	42	15.53	100	0.52	0.01	238	1.46	-4.64
	43	18.30	91	0.31	1.37	174	0.64	2.99
	44	18.97	132	2.87	-1.23	102	0.78	1.49
Saturday 8/06/02	45	9.64	107	0.98	4.36	93	0.84	0.15
	46	18.31	124	2.03	2.28	100	0.67	-0.45
	47	20.44	110	0.90	-0.01	113	0.69	0.93
Sunday 9/06/02	48	13.63	118	0.96	-0.13	128	0.64	1.76
	49	10.60	143	1.39	0.34	220	1.10	0.75
	50	18.04	83	1.49	1.87	121	0.93	0.37
	51	18.87	100	0.73	-0.03	130	0.72	0.26
	52	19.28	100	2.02	0.36	89	1.34	0.86
Monday 10/06/02	53	15.59	165	0.27	3.88	92	1.15	0.24
	54	16.61	77	1.33	-1.56	185	1.17	2.38
	55	17.65	68	0.84	2.88	141	1.15	0.24
	56	20.62	86	1.41	2.00	120	0.79	0.42
	57	22.18	93	0.76	1.60	57	1.04	2.15
	58	22.97	98	1.25	1.28	102	0.85	0.79
Tuesday 11/06/02	59	6.84	300	0.78	-2.00	101	1.35	0.47
	60	9.01	99	1.18	-0.70	96	1.23	-0.51
	61	13.68	107	3.07	2.48	203	1.51	0.88
	62	15.05	84	1.66	0.85	218	1.02	2.01
	63	16.40	199	2.11	-2.71	57	1.17	0.80
	64	17.85	100	0.71	-0.08	98	1.13	1.20
	65	18.62	51	0.84	1.92	94	1.21	-0.28
	66	19.61	99	1.50	-0.49	103	1.13	1.11
	67	22.18	119	2.40	1.02	61	0.79	1.34
	68	23.42	154	1.09	2.71	81	0.86	0.38
	69	24.85	266	1.97	-0.86	72	0.84	1.24
Wednesday 12/06/02	70	7.27	132	2.08	-0.09	123	1.15	1.67
	71	14.72	102	2.45	1.85	167	0.99	3.49
	72	15.44	188	0.50	2.89	118	1.99	0.74
	73	15.64	214	0.55	3.84	208	1.53	-0.76
Thursday 13/06/02	74	9.70	112	1.46	-0.51	108	1.87	1.28
	75	15.39	143	0.48	1.54	91	1.50	1.22
	76	15.64	99	0.24	0.16	138	1.31	2.33
	77	19.56	101	2.43	1.06	100	0.83	0.04
Friday 14/06/02	78	12.94	91	1.04	-1.35	212	1.63	0.25
	79	12.54	105	1.91	0.44	126	1.33	-0.32
	80	18.25	88	1.93	-2.93	102	0.70	1.76
	81	18.57	166	1.77	0.86	91	0.55	0.58
Saturday 15/06/02	82	13.31	262	2.41	0.37	103	1.03	3.62
	83	13.72	120	2.60	-1.48	94	0.58	0.11
	84	16.26	107	1.19	3.21	209	0.76	1.56
	85	13.63	92	2.12	-0.45	100	0.84	-0.04
	86	19.23	89	3.35	0.25	100	1.34	0.33

Sunday 16/06/02	87	13.55	105	1.46	1.19	133	1.43	-0.46
	88	10.31	102	0.82	1.40	222	0.89	3.72
	90	12.70	60	1.35	-0.50	100	0.49	0.12
	91	17.57	80	1.07	0.63	247	1.17	-2.59
	92	18.22	193	1.97	-0.09	163	1.26	0.84
	93	19.56	118	1.50	0.29	97	1.58	0.41
	94	20.15	118	1.15	1.55	149	1.49	1.83
Monday 17/06/02	95	18.07	92	1.41	0.31	96	1.12	0.21
	96	19.87	55	1.16	2.00	135	0.96	2.30
Tuesday 18/06/02	97	9.90	204	1.34	1.42	205	1.35	0.17
	98	11.60	97	1.66	-0.53	100	0.69	0.06
	99	14.37	112	1.58	0.92	141	1.14	0.38
	100	18.60	103	2.59	3.10	101	0.50	0.77
Wednesday 19/06/02	101	11.24	151	1.55	0.38	136	0.99	-0.47
	102	14.37	106	1.31	-0.41	61	0.99	0.81
	103	19.18	157	1.14	0.76	158	0.87	-0.60
Thursday 20/06/02	104	17.27	299	0.75	1.78	97	1.17	-0.24
	105	18.16	119	1.48	0.58	113	2.02	1.87
Friday 21/06/02	106	20.70	190	1.63	-0.86	231	1.30	2.70
Saturday 22/06/02	107	20.02	139	1.39	-3.11	99	1.04	-0.63
	108	22.49	287	1.17	0.45	125	0.72	0.13
Sunday 23/06/02	109	11.53	109	3.41	-3.81	143	0.90	-0.08
	110	12.56	70	1.44	-1.81	94	1.11	1.12
	111	17.16	138	3.30	-0.40	111	0.97	0.73
	112	19.02	130	1.44	-3.24	92	1.27	0.36
Monday 24/06/02	113	12.47	92	2.48	1.29	95	1.70	0.30
	114	16.84	107	2.26	2.45	146	1.61	0.64
	115	19.59	204	0.08	3.58	137	0.89	1.41
	116	20.76	109	0.76	0.08	100	0.78	0.18
	117	12.04	125	0.40	0.70	185	0.93	1.93
Tuesday 25/06/02	118	14.90	146	3.50	-0.70	100	1.41	0.19
	119	19.88	99	1.43	-0.06	156	0.62	1.89
	120	20.84	94	0.61	1.59	221	0.68	1.30
Wednesday 26/06/02	121	6.94	191	3.01	1.32	147	0.73	1.44
	122	9.90	142	1.42	2.07	52	0.74	0.44
	123	19.85	123	1.99	0.76	100	1.18	0.28
	124	22.46	145	1.47	3.14	226	0.87	1.88

Distribution of Outdoor Temperatures

The next two tables, table I.1 and I.2, include weekly and monthly temperatures respectively, absolute (max-min), and medium (max-min) under the period 9 July 2001 to 17 June 2002. The information has been

obtained from the website of the Danish Meteorological Institute, http://www.dmi.dk/vejr/index.html, and it corresponds to two different stations; Københavns Lufthavn (Copenhagen Airport), Dueodde (situated on Bornholm, the Danish island southeast of Ystad).

Weekly temperatures

Week	Place	Mean Temperature		Absolute Temperature	
		Minimum	Maximum	Minimum	Maximum
w. 28 09/7/01-16/7/01	Copenhagen Dueodde	13.3 14.5	20.8 20.0	11.2 12.6	23.5 21.9
w. 29 16/7/01-23/7/01	Copenhagen Dueodde	12.8 12.6	20.7 20.5	9.9 9.1	23.7 24.0
w. 30 23/7/01-30/7/01	Copenhagen Dueodde	15.5 13.6	24.8 25.7	13.4 11.6	27.1 26.9
w. 31 30/7/01-06/8/01	Copenhagen Dueodde	12.8 13.1	21.7 21.6	10.9 8.0	25.3 24.2
w. 32 06/8/01-13/8/01	Copenhagen Dueodde	12.5 12.6	19.5 20.0	10.8 8.8	20.9 21.1
w. 33 13/8/01-20/8/01	Copenhagen Dueodde	15.1 15.0	23.6 22.3	11.4 9.5	26.0 27.5
w. 34 20/8/01-27/8/01	Copenhagen Dueodde	14.7 16.4	22.6 22.9	12.2 14.5	25.1 25.0
w. 35 27/8/01-03/9/01	Copenhagen Dueodde	11.8 11.8	19.2 19.1	9.7 9.4	20.8 20.8
w. 36 03/9/01-10/9/01	Copenhagen Dueodde	10.5 10.9	17.4 17.2	8.6 8.1	20.2 19.8
w. 37 10/9/01-17/9/01	Copenhagen Dueodde	8.4 9.1	16.3 15.6	6.1 5.1	19.7 17.5
w. 38 17/9/01- 24/9/01	Copenhagen Dueodde	10.8 11.9	15.9 15.3	10.2 10.9	16.8 15.9
w. 39 24/9/01-01/10/01	Copenhagen Dueodde	8.7 8.8	12.9 13.4	6.1 5.3	14.4 15.1
w. 40 01/10/01-8/10/01	Copenhagen Dueodde	10.6 11.6	15.4 15.0	8.1 7.1	16.4 15.8
w. 41 08/10/01-5/10/01	Copenhagen Dueodde	10.0 11.4	15.5 15.0	7.8 11.1	16.7 15.9
w. 42 15/10/01-22/10/01	Copenhagen Dueodde	8.4 9.0	14.4 13.3	5.1 5.2	17.2 15.0
w. 43 22/10/01-29/10/01	Copenhagen Dueodde	7.9 7.6	11.1 10.7	6.2 4.9	12.9 12.3
w. 44 29/10/01-05/11/01	Copenhagen Dueodde	6.8 6.4	12.2 12.0	3.8 2.4	14.1 13.8
w. 45 05/11/01-12/11/01	Copenhagen Dueodde	1.9 2.8	7.5 7.2	-3.2 -2.0	10.4 9.4
w. 46 12/11/01-19/11/01	Copenhagen Dueodde	0.1 1.0	7.8 7.4	-3.6 -2.4	10.1 9.1

w. 47	Copenhagen	0.8	6.3	-2.2	8.9
19/11/01-26/11/01	Dueodde	1.2	6.3	-1.0	8.8
w. 48	Copenhagen	0.9	4.5	-1.4	5.9
26/11/01-03/12/01	Dueodde	1.0	4.3	-0.5	8.2
w. 49	Copenhagen	0.4	4.4	-3.3	6.8
03/12/01-10/12/01	Dueodde	2.0	4.7	-0.2	6.8
w. 50	Copenhagen	-0.7	3.7	-4.6	6.3
10/12/01-17/12/01	Dueodde	0.6	3.9	-4.4	5.9
w. 51	Copenhagen	-5.7	2.6	-11.6	5.8
17/12/01-24/12/01	Dueodde	-5.2	2.8	-11.4	5.5
w. 52	Copenhagen	-4.2	0.4	-12.2	4.2
24/12/01-31/12/01	Dueodde	-3.5	2.0	-10.9	4.2
w. 1	Copenhagen	-7.8	0.8	-12.3	5.0
31/12/01-07/1/02	Dueodde	-4.8	0.7	-12.3	4.5
w. 2	Copenhagen	-1.1	1.7	-4.6	3.8
07/1/02-14/1/02	Dueodde	0.4	3.0	-1.3	3.9
w. 3	Copenhagen	0.5	2.8	-1.3	6.8
14/1/02-21/1/02	Dueodde	0.3	2.5	-1.7	5.0
w. 4	Copenhagen	1.8	6.3	-1.2	7.9
21/1/02-28/1/02	Dueodde	2.0	5.7	-0.4	6.7
w. 5	Copenhagen	3.9	8.7	3.5	11.3
28/1/02-04/2/02	Dueodde	4.0	7.0	3.2	8.4
w. 6	Copenhagen	3.7	7.8	3.2	9.2
04/2/02-11/2/02	Dueodde	4.1	6.6	3.6	7.6
w. 7	Copenhagen	-0.5	5.9	-3.1	8.7
11/2/02-18/2/02	Dueodde	0.5	4.9	-2.0	7.4
w. 8	Copenhagen	-1.4	3.3	-3.2	6.0
18/2/02-25/2/02	Dueodde	-1.1	2.7	-5.7	3.8
w. 9	Copenhagen	-1.7	5.2	-6.3	8.2
25/2/02- 04/3/02	Dueodde	-0.9	4.5	-5.8	6.6
w. 10	Copenhagen	2.3	8.4	-0.8	10.7
04/3/02-11/3/02	Dueodde	2.8	5.8	1.9	6.8
w. 11	Copenhagen	0.9	6.7	-0.6	10.9
11/3/02-18/3/02	Dueodde	1.7	5.8	0.7	9.8
w. 12	Copenhagen	0.9	7.2	-4.2	9.5
18/3/02-25/3/02	Dueodde	1.5	5.6	-1.9	8.1
w. 13	Copenhagen	-1.3	9.7	-4.7	13.1
25/3/02-01/4/02	Dueodde	-0.9	7.1	-3.3	10.7
w. 14	Copenhagen	1.0	10.2	-1.7	14.5
01/04/02-08/4/02	Dueodde	0.1	8.0	-4.0	15.9
w. 15	Copenhagen	3.2	10.2	-2.1	12.3
01/04/02-08/4/02	Dueodde	3.3	8.0	-1.8	13.2
w. 16	Copenhagen	2.5	8.7	-0.5	17.1
08/04/02-15/4/02	Dueodde	2.3	6.3	-0.9	11.5
w. 17	Copenhagen	5.6	12.0	1.8	15.0
15/04/02-22/4/02	Dueodde	5.0	11.6	4.2	14.5
w. 18	Copenhagen	6.9	11.8	2.6	13.7
22/04/02-29/4/02	Dueodde	6.7	11.0	5.9	15.2
w. 19	Copenhagen	8.8	18.0	6.2	20.9
29/04/02-06/5/02	Dueodde	7.5	12.1	6.1	17.2
w. 20	Copenhagen	8.8	16.5	7.0	18.9
06/5/02-13/5/02	Dueodde	7.3	14.6	4.1	16.7

|					
w. 21	Copenhagen	10.0	18.5	7.2	22.6
13/5/02-20/5/02	Dueodde	10.4	15.8	7.7	19.7
w. 22	Copenhagen	9.9	18.3	7.4	23.0
20/5/02-27/5/02	Dueodde	9.0	16.2	7.0	20.5
w. 23	Copenhagen	13.3	21.4	12.2	23.5
27/5/02-03/6/02	Dueodde	12.6	17.6	9.6	19.4
w. 24	Copenhagen	11.5	19.3	10.2	21.8
03/6/02-10/6/02	Dueodde	12.2	17.3	9.2	19.5
w. 25	Copenhagen	13.7	21.8	11.8	24.8
10/6/02-17/6/02	Dueodde	13.6	19.8	10.2	23.1

Table I.1: Weekly outdoor temperature under the period July 2001 to June 2002 inclusive, measured at the two stations, Copenhagen and Dueodde.

Monthly temperatures

Month	**Place**	**Mean Temperature**		**Absolute Temperature**	
		Minimum	**Maximum**	**Minimum**	**Maximum**
July 2001	Copenhagen	14.2	22.8	9.8	28.1
	Dueodde	13.8	22.1	9.1	26.9
August 2001	Copenhagen	13.6	21.4	9.7	26.0
	Dueodde	13.8	21.3	8.0	27.5
September 2001	Copenhagen	9.7	15.8	6.1	20.6
	Dueodde	10.3	15.6	5.1	19.9
October 2001	Copenhagen	9.2	14.0	5.1	17.2
	Dueodde	9.8	13.5	4.9	15.9
November 2001	Copenhagen	1.4	7.3	-3.6	12.6
	Dueodde	2.0	7.2	-2.4	11.6
December 2001	Copenhagen	-2.6	2.7	-12.3	6.8
	Dueodde	-1.7	3.0	-12.3	6.8
January 2002	Copenhagen	-0.6	3.8	-10.3	8.4
	Dueodde	0.4	3.7	-12.0	7.8
February 2002	Copenhagen	0.9	6.1	-3.2	11.3
	Dueodde	1.6	5.0	-5.7	8.4
March 2002	Copenhagen	0.2	7.7	-6.3	13.1
	Dueodde	0.8	5.9	-5.8	10.7
April 2002	Copenhagen	3.3	10.3	-2.1	17.1
	Dueodde	3.0	8.6	-4.0	15.9
May 2002	Copenhagen	8.9	16.8	2.6	22.6
	Dueodde	8.3	13.9	4.1	19.7
June 2002	Copenhagen	12.4	20.3	10.2	24.8
	Dueodde	12.3	18.0	7.5	23.1

Table I.2: Monthly outdoor temperature under the period July 2001 to June 2002 inclusive, measured at the two stations, Copenhagen and Dueodde.

Figure I.1 shows the maximum, minimum and average monthly temperatures during the period July 2001-June 2002.
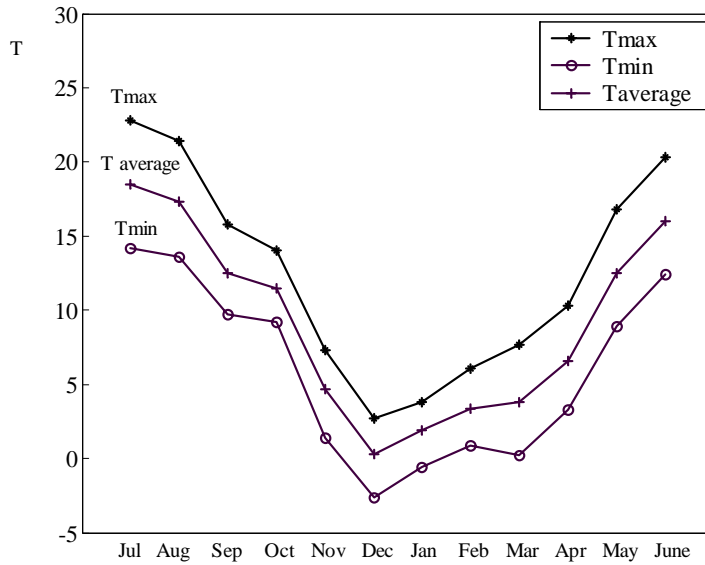
Figure I.1: Maximum, minimum and average monthly temperatures during July 2001-June 2002.

Appendix II

Equivalent Distribution System

A simplified scheme of the area of measurements in Tomelilla is shown in Figure II.1. It includes the distribution system from the 130 kV-level and downward. At the 130 kV bus, two three windings 100/100/40MVA, 130/50/20 kV tap changing transformers are connected in parallel. The tap changers, which are controlling the voltage at the 20 kV-level, are placed on the 130 kV windings.
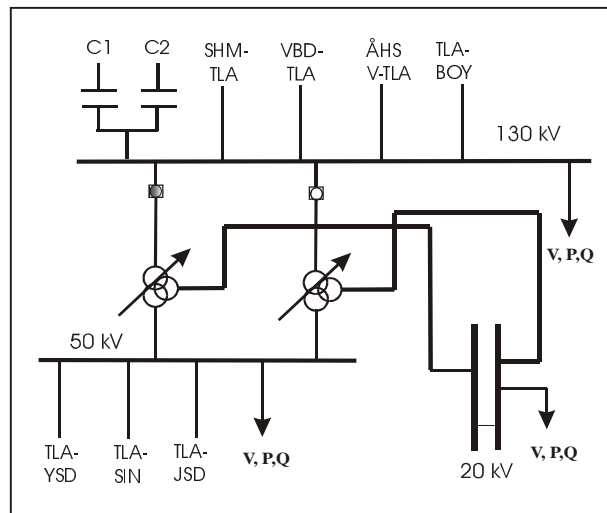

Figure II.1: Simplified test system at Tomelilla. Measurements of voltage, active and reactive power, are expressed in kV, MW and MVar respectively.

157

The equivalent circuit for each of the three-winding transformers is shown in Figure II.2.
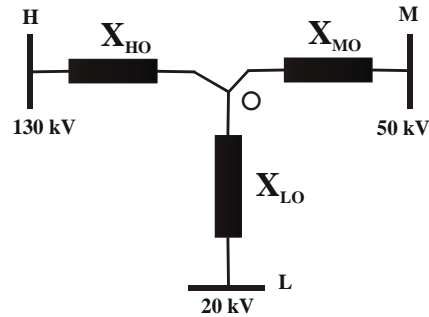
Figure II.2: Equivalent circuit of the three-winding transformer in Tomelilla. H, M and L name the high, medium and low voltage-side, respectively. X_{HO}, X_{MO} and X_{LO} are the equivalent transformer reactances for the high, medium and low voltage level.

As mentioned in Chapter 7, in order to check whether the reactive recovery really originates from the increase of reactive losses, the simplified distribution system shown in Figure II.3 has been used to determine those losses. The complete distribution system under the recording point at the 130 kV level has been modeled with a series reactance equal to the sum of both reactances at 130 and 20 kV. The measured values corresponding to 20 kV have been used to determine the value of the losses (Qlosses). Values in per-unit have been used for the voltages and respective reactances [Roos, 2002].
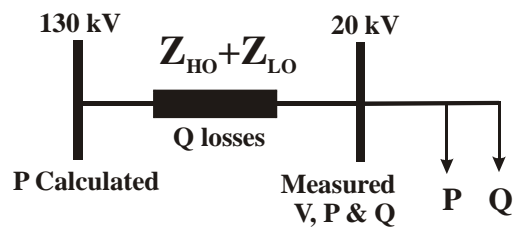
Figure II.3: Simplified distribution system from the 130 kV- level to the 20 kV- level for determining the reactive load losses.